UNIVERSITY OF CALIFORNIA
SANTA CRUZ

ECOLOGICAL CAUSES AND CONSEQUENCES OF SEA STAR WASTING SYNDROME ON THE PACIFIC COAST

A dissertation submitted in partial satisfaction
of the requirements for the degree of
DOCTOR OF PHILOSOPHY

in

ECOLOGY AND EVOLUTIONARY BIOLOGY

by

Monica M. Moritsch

September 2018

The Dissertation of Monica M. Moritsch is approved:

_____
Professor Peter T. Raimondi, chair

_____
Professor Mark H. Carr

_____
Professor Giacomo Berardi

_____
Professor Benjamin Miner

_____
Lori Kletzer
Vice Provost and Dean of Graduate Studies

Table of Contents

List of Tables

List of Figures

Abstract

Ecological causes and consequences of Sea Star Wasting Syndrome on the Pacific Coast

By

Monica M. Moritsch

Disease outbreaks are becoming more frequent as anthropogenic changes to ecosystem function stress species and create conditions favorable for pathogen infection. Marine outbreaks that were once locally constrained are re-emerging as large-scale epidemics with heightened mortality, decimating populations across multiple ocean basins. Effective prediction of future disease impacts requires a better understanding of their causes and consequences. In this dissertation, I explore the connections between environmental conditions, recovery of decimated host populations, and multispecies interactions to examine how a marine epidemic affects marine communities. I focus on a recent Sea Star Wasting Syndrome outbreak in rocky intertidal habitats along the Pacific coast of North America, with emphasis in Central California. Sea stars are an iconic intertidal species to many coastal visitors. Their absence has generated heightened public awareness of current challenges to ocean health, providing many opportunities for engagement in the process and outcomes of ecological research.

In my first chapter, I use data from long-term ecological monitoring to assess the recovery of sea star populations and predation pressure in the years immediately following the outbreak. I show that while sea star numbers are rebounding, these populations are made of smaller individuals that do consume the same amount of food. In my second chapter, I explore potential conditions associated with outbreak timing using data from citizen scientists and researchers combined. I identified associations between Sea Star Wasting Syndrome appearance, low tide exposure duration, proximity to other infected sites, and chlorophyll *a* concentration, though the relative importance of these factors varied across geographic regions of the coast. In my third chapter, I take advantage of a natural experiment created by the loss of predatory sea stars to measure the consequences of the outbreak on the intertidal community. I found that while mussels, the sea stars' primary prey, had increased their coverage, they had not displaced the species living below the mussel bed. At local field sites, mussel increases were positively correlated with mussel recruitment and not pre-outbreak sea star levels. However, a coast-wide scale, pre-outbreak sea star density was positively correlated with pre-outbreak sea star density. Finally, I conclude with key insights from this work. My dissertation provides evidence that sea star wasting does not have uniform causes or population-level and community-level consequences across coastal regions. I discuss the value of long-term ecological monitoring and citizen science as critical information sources in the process of evaluating disease impacts.

This body of work is dedicated to:

My grandmothers, Betty Chin and Marylin Ball,

who always supported my educational endeavors.

"It is advisable to look from the tide pool to the stars and then back to the tide pool again."

- John Steinbeck, *The Log from the Sea of Cortez*

Acknowledgements

Chapter 1 of this dissertation includes the following previously published material:

> Moritsch, M. M., and P. T. Raimondi. 2018. Reduction and recovery of keystone predation pressure after disease-related mass mortality. *Ecology and Evolution*: 8, 3952-3964. https://doi.org/10.1002/ece3.3953

The co-author listed in this publication directed and supervised the research which forms the basis for the dissertation. Reproduced with permission.

First, I owe so much to my advisor, Pete Raimondi, who encouraged me to pursue whatever opportunities were going to make me happy in my career. I am grateful that you always supported me in whatever project I wanted to accomplish and were there to answer my never-ending questions as I figured it out. I am also grateful to Mark Carr for helping my writing take shape and making the lab environment fun. Ben Miner and Giacomo Bernardi were also excellent committee members, and their broader-level feedback helped me identify how to make this work relevant to people who have no experience with sea stars.

The NSF Graduate Research Fellowship Program for providing my stipend support during the period of field observations and the Dr. Earl H. Myers and Ethel M. Myers Oceanographic and Marine Biology Trust for provided funds to conduct this research. Additional support came from the EEB Department and UCSC.

I give special thanks to the Partnership for Interdisciplinary Studies of Coastal Oceans and Multi-Agency Rocky Intertidal Network (PISCO/MARINe) partner

groups for continued monitoring of sea star and mussel populations and for so willingly sharing data: Sitka Sound Science Center, Padilla Bay National Estuarine Research Reserve, Olympic National Park, Olympic Coast National Marine Sanctuary, Redwoods National and State Park, Point Reyes National Seashore, Golden Gate National Recreation Area, University of California Los Angeles, California State University Fullerton, CalPoly Pomona, and Channel Islands National Park. All raw data for Pisaster ochraceus counts, sizes, and years are publicly available online in the PISCO/MARINe data repository: www.eeb.ucsc.edu/pacificrockyintertidal/contact/index.html. This collection of broad-scale data makes it possible to answer questions on so many more levels than would be possible starting from scratch at brand new field sites. I have always felt lucky to have access to this intertidal monitoring legacy and the wealth of knowledge.

PISCO was one of the major reasons that swayed me in favor of coming to UCSC. Beyond sharing data, they gave me field support, assistance with permitting, and advice on establishing sampling locations. Additionally, Melissa Miner and Rani Gaddam spend many hours managing the sea star wasting databases, which made data organization much easier. Nate Fletcher, Melissa Douglass, Laura Anderson, Christy Bell, Karah Ammann, Maya George, Rani Gaddam, Dave Lohse, and Rachael Williams, thank you for taking me along in the field with you, putting up with me as I struggled to be a morning person, and sharing your gear, truck space, and campsites. One day, I hope to know as much about the world as all of you.

Learning R in order to perform ecological modeling was a personal struggle. I thank Tim Tinker for extensive modeling and R assistance. The entirety of Chapter 2 would have happened much more slowly if not for all the help in class and out. I also thank A. Marm Kilpatrick for more R training and Steve Munch for modeling advice.

Furthermore, this work would not have been possible without thousands of citizen scientists visiting their local tidepools and sending us observations. When I talked to local people at the beach during field work, most people asked, "What can I do to help the dying sea stars?" While no intervention was necessary with *Pisaster ochraceus*, I admired their desire to help and wished I could respond with something more than "send us your pictures and locations" to fully harness that motivation for helping the world. It gives me hope that so many people will come together during an ecological crisis and do what they can to help. I was particularly touched when a packet of hard copy photos of wasting sea stars showed up in the mail, sent by a group of concerned residents of Lummi Island, Washington wanting to make sure that scientists got their observations.

Thanks to Dawn Hart for use for historical data, markers for field sites, and ideas. Thanks to B. Moritsch for providing transportation resources and help carrying heavy equipment over slippery rocks. I am grateful to S. Ayyagari, C. Cortez, J. Gomez, S. Deva, C. Seifert, D. Resnick, C. Aquino, K. Hershman, J. Valdez, J. Bickford, N. DiMartino, J. Sullivan, A. Moua, J. Sinn, L. Powers, L. Boswell, T. Kramer, E. Williams, L. Strope, E. Mulligan, C. Cortez, K. Stuhldreher, S. Magana, J. Valdez, A. Hunter, L. Zarri, C. Ray, C. Mann, G. Verutes, E. Salas, M. Ahmed, M.

Smith, P. Welsh, E. Firl, S. McCoy, E. Ford, K. Trueblood, Madeline M. Moritsch, and countless additional field helpers that braved the early mornings and cold winds to sample in the intertidal or sorted through sediment to count mussel recruits for hours on end. Madeline Moritsch and Kevin Trueblood, I owe you special thanks for keeping calm on that incredibly swelly day at Soberanes and still being so willing to come out in the field again after that.

During graduate school, I also managed to hold down a part time job as a geospatial analyst at Center for Ocean Solutions. Lisa Wedding made it possible by being extremely flexible and supportive. It never would have been possible without your encouragement and reassurance that a full field season was perfectly compatible with this job. Thank you for encouraging me to grow my GIS skills and giving me exciting, meaningful opportunities to do so. I learned a lot about what makes a great mentor from you.

The Raimondi-Carr labmates are amazing people. I felt like I had a large family of support around the lab. Carpooling to field sites or sharing supplies was always appreciated. In particular, I am grateful to Kate Melanson, Rachel Zuercher, and Kristin de Nesnerna, who provided a listening ear for all of the highs and lows of this long process.

Finally, my family has been incredibly supportive. My family was enthusiastic about my choice to go play in tidepools for six years while trying to become a marine biologist. Most of them helped me with field work at some point. To my parents, I cannot thank you enough for all that you have done to get me a solid education and

the means to even arrive in graduate school, let alone finish it. I also am grateful to my partner, Ed Ford. Thank you for reminding me to enjoy life, and for appreciating me being a nerd around you. Your encouragement through these years has meant the world to me.

Introduction

Broad context

The number of marine disease outbreaks has increased over the past few decades (Ward and Lafferty 2004, Scheibling and Lauzon-Guay 2010). Disease incidence is expected to continue rising in the near future, as climate change, habitat degradation, and global transport of hosts and pathogens create new conditions that favor pathogen spread (Harvell et al. 1999, Altizer et al. 2013, Burge et al. 2014). Epidemics, widespread disease outbreaks that kill or harm large proportions of a host's population, can have far-reaching effects on ecological communities. By causing severe declines of infected host populations, diseases modify species interactions and disrupt relationships between predator-prey pairs, competitors, and mutualists (Hatcher et al. 2006). Epidemics can even produce complex cascades of indirect effects throughout the community's interaction web (Selakovic et al. 2014).

Predicting the impact of diseases presents a multifaceted challenge that researchers must confront from several angles. First, population biology studies of infected taxa typically aim to quantify the losses and recovery dynamics within a single infected species (Fouchet et al. 2009, Froeschke and Von der Heyden 2014, Jousimo et al. 2014). These studies detect where diseases have had greatest impacts to host populations and which populations recover. This informs us of the spatial patterns of impact, identifying the areas critical for further investigation of conditions surrounding infections. Next, disease ecology research has traditionally focused on

host-pathogen-environment dynamics, seeking to identify ideal conditions for infection appearance and spread (Anderson and May 1991, Snow et al. 2004, Keesing et al. 2006, Piccinali et al. 2009). Environmental conditions define the optimal locations for epidemics by controlling the physiological performance of hosts and parasites (Lafferty and Kuris 1999). Lastly, community ecology has historically viewed disease as a special subset of predation due to pathogens' status as an antagonist of the host species. Impacts to community structure and biodiversity are predicted based on interaction strengths of the infected host with other species (Bascompte and Jordano 2007, Smith et al. 2009).

In the next three chapters, I apply all three approaches to understand how disease shapes rocky intertidal ecosystems. This narrow band between dry land and constant saltwater submergence is ideal for observing disease-driven changes because intertidal communities are compressed into a small physical space, making changes in host populations and species distributions apparent (Connell 1972b). Due to their accessibility and proximity to terrestrial habitats, rocky intertidal habitats also face many anthropogenic threats, including trampling, oil spills, shoreline development, and pollutant runoff (Rice et al. 1993, Thompson et al. 2002, de Nesnera 2016).

Starting in summer 2013, an epidemic of Sea Star Wasting Syndrome (SSWS, also referred to as Sea Star Wasting Disease) caused major declines of the keystone species *Pisaster ochraceus*, and affected over 20 other species on the Pacific coast (MARINe 2013). Infected individuals develop twisting arms and white lesions on their body. As these symptoms progress, individuals experience substantial tissue

decay and arm loss, often leading to death (Hewson et al. 2014, Fuess et al. 2015). Previous outbreaks on the Pacific coast occurred on smaller, regional scales (Eckert et al. 2000, Bates et al. 2009); the widespread geographic extent of the 2013-present outbreak from Alaska to San Diego is unprecedented (Miner et al. 2018). Populations in many locations were reduced by 90 to 99% (Miner et al. 2018). Sea stars serve as top predators in several marine ecosystems, and their near-absence could potentially cause drastic changes to prey populations (Paine 1966, 1969a, 1974a).

Many details about SSWS remain unknown. It is questionable whether SSWS technically meets the criteria necessary to be considered a true infectious disease (I. Hewson, *pers. comm.*), though for the purposes of this work, I will assume that SSWS is a disease. We currently do not know if SSWS is caused by single pathogen, a collection of pathogens, or is a complex organismal response to stress followed by secondary infection (Hewson et al. 2018). This hampers our ability to make mechanistic predictions about the impacts of future outbreaks. Instead, we must rely on patterns observed in past outbreaks and commonalities observed across infection sites in the current epidemic. Fortunately, the Pacific coast of North America has a strong history of long-term ecological monitoring with rich pre- and post-SSWS data for intertidal habitats. Researchers also took the initiative to establish a citizen science program to observe SSWS spread in progress. Members of the public visited tidepools to capture far more disease observations than would have been possible relying on research teams alone. These efforts provide a wealth of insight on the pre- and post-SSWS state of sea star populations, creating a data-rich system in which to

study how a marine epidemic affects intertidal communities.

Dissertation outline

In **Chapter 1,** I assess large-scale recovery patterns of sea star populations and sea star predation pressure relative to pre-SSWS levels. I estimate sea star numbers and biomass as a proportion of the long-term, pre-SSWS average to infer which biogeographic regions of the Pacific coast are regaining predation pressure and which are not. I show that despite sea star counts approaching pre-SSWS levels in some regions, biomass, and by extension predation pressure, was still far below the long-term mean. I also highlight differences in post-SSWS predation pressure between regions. I then discuss potential reasons for these discrepancies in recovery, including sea star recruitment and juvenile mortality. These results can improve predictions of which locations are most likely to experience community change due to reduced abundance of a keystone predator.

In **Chapter 2,** I use citizen science disease observations to explore potential environmental conditions associated with the SSWS outbreak. Using a survival analysis modeling framework, I estimate how natural and anthropogenic inputs shape the probability of SSWS infection both within regions and across the Pacific coast. At a coast-wide scale and within multiple regions, I identify that SSWS infection probability is negatively associated with distance from the nearest infected neighbor site and positively associated with duration of low tide exposure. Additionally, I show that chlorophyll *a* was positively associated with SSWS infection in multiple regions

but not on a coast-wide scale. No single factor could strongly explain infection probabilities in other regions. These results contradict previous hypotheses that warm water temperatures drive SSWS appearance, at least on a large spatial scale. Instead, they call attention to potential thermal stress during emersion.

In **Chapter 3,** I take advantage of a "natural experiment" to assess the consequences of SSWS for intertidal communities in the four years after the outbreak. In a six-site field study on the Central California coast, I examine whether mussel beds are expanding, whether mussels are growing larger, and whether the overall rocky intertidal community composition is changing in the near-absence of a keystone predator. I test whether changes in the extent of the mussel bed are associated with pre-SSWS sea star levels. I complement these small-scale detailed surveys with a large-scale multi-region assessment of how mussel cover relates to pre-SSWS sea star density based on long-term monitoring surveys. I provide evidence that mussel beds have moved down since the SSWS outbreak, likely due to a combination of juvenile mussel recruitment and adult mussel movement. Across all regions, but not within my Central California surveys, these changes were related to pre-SSWS sea star levels, underscoring how ecological processes differ across spatial scales. Mussel bed expansion did not eliminate low-zone intertidal communities, though it did reduce space available for these communities. These results add to a rich discussion on the importance of keystone predation to community composition.

Chapter 1: Reduction and recovery of keystone predation pressure after disease-related mass mortality

Moritsch, M. M., and P. T. Raimondi. 2018. Reduction and recovery of keystone predation pressure after disease-related mass mortality. *Ecology and Evolution*: 8, 3952-3964. https://doi.org/10.1002/ece3.3953

Received: 4 August 2017 | Revised: 8 February 2018 | Accepted: 11 February 2018

DOI: 10.1002/ece3.3953

ORIGINAL RESEARCH

WILEY Ecology and Evolution Open Access

Reduction and recovery of keystone predation pressure after disease-related mass mortality

Monica M. Moritsch | Peter T. Raimondi

Department of Ecology and Evolutionary Biology, University of California, Santa Cruz Long Marine Laboratory, Santa Cruz, CA, USA

Correspondence
Monica M. Moritsch, Department of Ecology and Evolutionary Biology, University of California, Santa Cruz Long Marine Laboratory, Santa Cruz, CA, USA.
Email: mmoritsc@ucsc.edu

Abstract

Disturbances such as disease can reshape communities through interruption of ecological interactions. Changes to population demographics alter how effectively a species performs its ecological role. While a population may recover in density, this may not translate to recovery of ecological function. In 2013, a sea star wasting syndrome outbreak caused mass mortality of the keystone predator *Pisaster ochraceus* on the North American Pacific coast. We analyzed sea star counts, biomass, size distributions, and recruitment from long-term intertidal monitoring sites from San Diego to Alaska to assess regional trends in sea star recovery following the outbreak. Recruitment, an indicator of population recovery, has been spatially patchy and varied within and among regions of the coast. Despite sea star counts approaching pre-disease numbers, sea star biomass, a measure of predation potential on the mussel *Mytilus californianus*, has remained low. This indicates that post-outbreak populations have not regained their full predation pressure. The regional variability in percent of recovering sites suggested differences in factors promoting sea star recovery between regions but did not show consistent patterns in postoutbreak recruitment on a coast-wide scale. These results shape predictions of where changes in community composition are likely to occur in years following the disease outbreak and provide insight into how populations of keystone species resume their ecological roles following mortality-inducing disturbances.

KEYWORDS

growth, keystone predator, *Pisaster ochraceus*, recruitment, sea star wasting disease, sea star wasting syndrome

1 | INTRODUCTION

Disturbance and mass mortalities can reshape the ability of affected populations to maintain their role within an ecosystem. Disturbances that remove individuals of species with large relative contributions to ecological functions often result in greater changes to community composition (Estes, Smith, & Palmisano, 1978; Lessios, 1988; Paine, 1966). For example, size-selective fishing of larger individuals from populations of predatory spiny lobster *Jasus edwardsii* and California sheephead *Semicossyphus pulcher* disproportionately decreases those populations' ability to control urchin grazing on kelp biomass, increasing the chance of overgrazing and transition of kelp forest to urchin barren (Hamilton & Caselle, 2015; Ling, Johnson, Frusher, & Ridgway, 2009). Demographic attributes such as size-dependent predation and ontogenetically influenced diet preferences can moderate recovery of ecological function. Younger, smaller individuals

typically do not consume the same biomass of prey as full-grown adults (Brodeur, 1991; Feder, 1956). This means that even when a population recovers to the same predisturbance number of individuals, it will not entirely resume its ecological role until more individuals reach adult size and restore predisturbance size structure (Bellwood, Hoey, & Hughes, 2012; Hamilton & Caselle, 2015). This is particularly true for species functioning as keystone predators, which play a large role in maintaining community composition relative to their abundance (Paine, 1966).

Diseases may act as natural disturbances that moderate the strength of affected populations' ecological interactions (Selakovic, de Ruiter, & Heesterbeek, 2014). Infected hosts can alter their prey consumption of a given species or become highly vulnerable prey for another species. In intertidal habitats, the marine snail *Littorina littorea* decreases its algal consumption when infected by trematodes, subsequently producing changes in intertidal macroalgal community composition (Wood et al., 2007). Behavioral shifts in infected terrestrial insects cause them to enter streams and encounter new predators (Ponton et al., 2011; Sato et al., 2012). In addition to food-web effects, diseases often cause age-specific mortality of the host, altering population demography, which in turn impacts the ecological function of the population (Groner et al., 2014). While dynamic cycles of infection and recovery in disease outbreaks are a common mechanism constraining host abundances, epidemics have the potential to cause mass mortalities in host populations beyond the fluctuations experienced in regular cycles because infections and deaths occur at much higher rates than recovery. Therefore, epidemics are expected to have greater ecological consequences (Anderson & May, 1991; Hughes, Deegan, & Wyda, 2002; Leighton, Boom, Bouland, Hartwick, & Smith, 1991; Lessios, 1988; Rockwood, 2006).

As global climate change increases temperatures and alters physical conditions within marine habitats, epizootic diseases and their associated mass mortalities are projected to increase in the coming decades (Baker-Austin et al., 2012; Burge et al., 2014; Harvell et al., 1999). Intensifying anthropogenic pressures on marine habitats will further contribute to stressful conditions that compromise host immune system activities (Harvell et al., 1999; Mydlarz, Jones, & Harvell, 2006). Altered species interaction strengths stemming from change in abundance or shifts in demographics can have cascading effects throughout the community, especially when the affected host plays a role of major ecological importance such as a keystone, dominant, or foundational species (Hughes et al., 2002; Menge, 1995; Smith, Behrens, & Sax, 2009). As such, understanding the recovery dynamics of infected species is critical to predicting potential changes to the broader community.

Beginning in summer 2013 and continuing through 2014, an epidemic of sea star wasting syndrome (SSWS; Figure 1) caused major declines in multiple species of echinoderms on the Pacific coast of North America (Hewson et al., 2014; MARINe 2013). The high disease prevalence of the epidemic subsided after 2014, but SSWS was still present in sea star populations at lower prevalence (<20% of sea stars with symptoms) as of 2016 (Figure S3). In rocky intertidal habitats, the ochre star *Pisaster ochraceus* (Brandt) was one of the most

FIGURE 1 *Pisaster ochraceus* with sea star wasting syndrome symptoms. The body can appear deflated. White lesions appear on the body wall, followed by tissue decay, arm loss, and death

dramatically reduced species. Some sites experienced nearly 100% mortality, but considerable spatial variability in mortality patterns was present over larger spatial scales of tens and hundreds of kilometers (Eisenlord et al., 2016; Menge et al., 2016). Levels of recruitment two orders of magnitude higher than average followed in the 1–2 years after mass mortality, shifting *P. ochraceus* size structure toward smaller individuals (Menge et al., 2016).

Pisaster ochraceus is recognized as a keystone predator in intertidal habitats because of its ability to reduce the abundance and constrain spatial distributions of the California mussel *Mytilus californianus*, a competitive dominant species (Paine, 1966, 1974). Larger sea stars have the physical strength to consume larger mussels and eat more mussel meat than smaller individuals (Feder, 1956; McClintock & Robnett, 1986; Robles, Desharnais, Garza, Donahue, & Martinez, 2009). While a superabundance of newly settled sea stars exerts substantial predation pressure on mussel recruits (Menge et al., 2016), reduced abundance of adults and demographic shifts to smaller *P. ochraceus* reduce overall predation pressure on *M. californianus* (Menge & Menge, 1974; Robles et al., 2009). Experimental sea star removals in many locations on the Pacific coast have demonstrated that when *P. ochraceus* abundances are severely reduced for a sufficiently long duration, *M. californianus* increase in percent cover (Paine, 1966, 1974; Robles et al., 2009). This expansion of the mussel bed decreases the number of other species on the primary substrate, while it creates more habitat for infaunal and epibiont species (Lafferty & Suchanek, 2016; Suchanek, 1986). Conversely, experimental additions of *P. ochraceus* result in the elimination of larger mussels, a reduction in overall mussel cover, and greater cover of other prey species over time (Robles et al., 2009).

Speed of recovery for sea star populations depends on the magnitude of recruitment and postsettlement mortality, which influences the number of new individuals available to replace those that died (Lessios, 1988; Miner, Altstatt, Raimondi, & Minchinton, 2006). However, assessment of whether a population has returned

to historic levels of predation pressure must also incorporate growth rates of sea stars because predation pressure is more related to collective predator biomass than predator abundance. *P. ochraceus* requires three to five years to reach terminal adult size given abundant food availability (Feder, 1970; Pilkerton et al., 2016). As population recovery of *P. ochraceus* progresses, overall predation pressure will show a lagged response as individuals gradually increase in biomass.

Here, we focus specifically on geographic differences in the recovery process, as this improves our understanding of where we may expect community changes and where to direct future intertidal monitoring efforts. We assessed spatial patterns in which populations have begun recovery based on recruitment of *P. ochraceus*. We characterized the spatiotemporal trends in recovery of predation pressure on mussel populations using abundance, biomass, and size structure through comparisons of post-SSWS populations to long-term observations preceding the wasting event. We discuss the importance of recruitment and postsettlement mortality as potential contributors to the differential recovery patterns that we observed.

2 | MATERIALS AND METHODS

We characterize the recovery process using multiple metrics. Recruitment, indicated by sea stars arriving that are too young to have experienced the outbreak, is a marker of postdisease reproduction. While recruitment pulses occurred in some locations during the peak of the outbreak, it is possible that large numbers of those recruits died before reaching maturity due to juveniles' high SSWS mortality. Those that survived would contribute to recovery, but ultimately true recovery and persistence of the population require successful reproduction and recruitment after the outbreak. From an ecological perspective, recovery requires the return of the population's function within the community in addition to replacement of lost individuals. Sea star biomass serves as a proxy of predation pressure on the mussel bed due to its correlation with prey size and mass of soft tissue consumption (Feder, 1956; Robles et al., 2009). Finally, comparison of pre-SWSS and post-SSWS size distributions over several years allows us to evaluate trajectory of ecological recovery by whether it is regaining larger individuals that contribute disproportionately to predation pressure.

2.1 | Sea star surveys

The Partnership for Interdisciplinary Studies (PISCO) and the Multi-Agency Rocky Intertidal Network (MARINe) monitor long-term abundances and sizes of *P. ochraceus* on the Pacific Coast from Southern California to Alaska. To capture trends in populations of intertidal species across a large geographic range, a network of data collection groups coordinates methods for counting and measuring species. The authors were part of the PISCO survey team. The first year of surveys varies between sites, but data are generally available for at least the past decade. Individual sites are surveyed in the same season(s) annually, although because of geographical differences in the timing of suitable tides, not all regions are surveyed in the same season. California sites are generally surveyed in the spring and fall, while sites to the north are surveyed in the summer. Sites containing sea star plots were nonrandomly selected for optimal sea star habitat and logistic feasibility of sampling. Monitoring sites had stable rocky surfaces, low to moderate scour by sand and gravel, and moderate wave protection for safe low tide sampling (MARINe 2008). Our goal was to compare sea star recovery trends in similar habitat types across regions rather than to examine sea star recovery patterns in all habitats where sea stars could survive. To assess geographic trends within and among regions, we designated nine regions as follows (abbreviations in parentheses): Southeast Alaska (AK), Washington Olympic Coast (WA Olympic Coast), Washington Salish Sea (WA Salish Sea), Oregon (OR), North California (CA North), North Central California (CA North Central), Central California (CA Central), California Channel Islands (CA Channel Islands), and South California (CA South). The extent of these regions (Table S1) corresponds to major units in marine management by state governments. These regional designations are consistently used all in PISCO/MARINe surveys.

We used PISCO/MARINe data from spring and summer 2015, 2016, and 2017 (post-SSWS) and from 1989 to 2012 (pre-SSWS) for *P. ochraceus* counts and sizes. We did not use fall data from these 3 years because fall 2017 sampling was still in progress at the time of this writing. We excluded data from 2013 and 2014 because the inconsistent timing and monitoring of the disease outbreak between regions during this period prevented definitive designations of sites as preoutbreak or postoutbreak. Count and size data availability for 2015–2017 for each site are summarized in Tables S1–S3. These surveys counted visible sea stars within permanently marked nonstandard polygons (plots) of ideal *P. ochraceus* habitat: middle and low intertidal zones, some containing deep crevices, overhangs, or vertically protruding rock. Each site had three sea star survey plots. Surveyors used flashlights to examine crevices and overhangs to improve visibility, and surveyors moved around the plot to inspect all safely accessible places where a sea star could hide. Despite these steps to improve visibility, it is possible that these rock structures obscured detection of some *P. ochraceus*. A plot's rock structure remained consistent over time, so searchable area of a plot was comparable between years. Due to nonstandardized plot areas, sea star counts from these surveys are able to identify trends but are not able to perform direct site-to-site comparison in terms of raw abundances or biomass. With a ruler, the surveyor physically measured the radius (center of body to arm tip) of the longest visible arm of all sea stars in the plot. Each arm measurement was rounded to the nearest 10 mm with the exception of sea stars ≤7 mm, which were binned as 5 mm (MARINe 2008). This smallest size category is often difficult to see in visual field surveys and is likely consistently underrepresented in counts across all years. Sea star counts for all years were maintained in the PISCO/MARINe database. All raw data for *Pisaster ochraceus* counts, sizes, and years are publicly available online at www.eeb.ucsc.edu/pacificrockyintertidal/contact/index.html.

2.2 | Estimation of sea star arrival dates and sites in recovery

We considered the arrival of offspring of survivors the first step in the recovery process. Given the severe mortality from SSWS and the low postoutbreak reproduction in some regions, we defined a site as being "in recovery" if juvenile *P. ochraceus* that were offspring from the spawning of survivors of the initial SSWS mass mortality were present. This definition excluded sites that had not experienced recruitment success since the outbreak. To differentiate offspring of survivors from juveniles that were already alive during the outbreak, we estimated the date of arrival of post-SSWS recruits at each site. Mass mortalities within a region took place over a few weeks to several months since the first regional observation of SSWS. Most population declines occurred by 4–6 months after the first SSWS observations in the region (Menge et al., 2016). We considered sea stars to have made it through the mass mortality period if they were alive 8 months (240 days) after the first observation of SSWS in their respective regions. This includes a two-month buffer to be conservative in classifying sea stars as survivors. We designated this eight-month benchmark as the earliest time of reproduction by SSWS survivors. We assumed that recruits from these survivors would arrive after a 70-day pelagic larval duration period (Strathmann, 1978), setting the earliest defined date of arrival of new recruits at 310 days after the first observation of SSWS in the region.

Pisaster ochraceus broadcast spawn and larvae remain in the water column for several weeks (George, 1999; Strathmann, 1978). This definition of the earliest post-SSWS arrival date would underestimate offspring from disease survivors that spawned before the end of the mass mortality period, making it a conservative estimate of post-SSWS sea star numbers. Gene flow is generally high along the open coast with little genetic structure (Frontana-Uribe, de la Rosa-Vélez, Enríquez-Paredes, Ladah, & Sanvicente-Añorve, 2008; Harley, Pankey, Wares, Grosberg, & Wonham, 2006; Stickle, Foltz, Katoh, & Nguyen, 1992). However, it is possible for sea star populations in embayments and sounds to exhibit higher levels of genetic structure (Keever et al., 2009; Sewell & Watson, 1993). While we did not expect high levels of self-recruitment, the timing of SSWS mass mortalities was generally similar over the distance scales which larvae would typically travel. Because of our conservative designation of what counted as the offspring of survivors, this method of back-calculation is robust to within-region variations in the timing of outbreaks.

We used site-specific growth rate (Table S4) and 2015–2017 sizes of sea stars to back-calculate arrival date. We assumed growth rate was linear until sea stars reached adult sizes (Pilkerton et al., 2016; Sewell & Watson, 1993), although this is a simplification of field growth rates, which can vary with food availability (Feder, 1970). All sea stars calculated to arrive at the site after the earliest (post-SSWS) arrival date were considered to have originated after the SSWS outbreak. Sites with individuals arriving post-SSWS were considered "in recovery". Sites with 0% of their individuals arriving post-SSWS were considered "not in recovery" at the time of surveys.

2.3 | Influence of SSWS on the *Pisaster ochraceus* reproductive cycle

Pisaster ochraceus invest in gonadal growth in September through March and usually spawn in April through June under normal conditions (Mauzey, 1966; Pearse & Eernisse, 1982; Sanford & Menge, 2007). This species has a long pelagic larval duration of 5–32 weeks, after which larvae settle in the intertidal and metamorphose into juveniles (George, 1999; Strathmann, 1978). The new recruits are generally detectable by the following spring (Sewell & Watson, 1993). Had the epidemic not occurred, we likely would have observed stronger seasonal constraints in when larvae arrived. However, in Central California, we observed *P. ochraceus* spawning during the mass mortality period in fall 2013 and winter 2014. Spawning activity was prevalent at high enough levels to include the appearance of spawning stars on SSWS identification guides for citizen science data collection efforts during this period (MARINe 2014). With this disruption in seasonality of the reproductive cycle, we did not apply seasonal constraints to the possible arrival times of recruits.

2.4 | Degrees of recovery of predation pressure

We considered replenishment of abundance and predation pressure the next steps in recovery. We used sea star biomass as a proxy for predation pressure. Any sites that did not have historical size data were excluded from calculation of size distribution or biomass but still used in analysis of counts (Eel Point and West Cove in CA Channel Islands).

We used PISCO/MARINe sea star survey data from 1989 to 2012 to calculate the pre-SSWS long-term means for abundance, biomass, and size distribution. We defined a site's degree of ecological recovery in two ways: (1) individuals present; and (2) biomass present in the plots as a proportion of the site's pre-SSWS mean. We standardized abundance and biomass to the pre-SSWS mean because nonstandard plot sizes prevented meaningful among-site comparisons of absolute numbers.

From the measured arm length, we calculated sea star biomass by performing a linear regression between log-transformed radius (mm) and log-transformed mass (g) based on data from the reserve at Hopkins Marine Station by Feder (1956) and our own measurements of 58 individuals from the Central California region:

$$\ln(\text{biomass}) = 2.34723 \times \ln(\text{radius}) - 5.50262$$

To calculate a site's relative predation pressure, we summed the biomass of all individuals present in the site's plots in a given year and divided it by the site's pre-SSWS mean biomass. The relationship between biomass and predation pressure is simplified for our purposes. Under natural densities, larger *P. ochraceus* tend to consume longer mussels, though the relationship between sea star biomass and mussel meat consumed is not thoroughly explored (Robles et al., 2009). The summation of biomass for all individuals at a site also assumes that biomass

is the only factor controlling predation pressure and does not account for spatial patterns of predation by large and small individuals. Larger sea stars can eat more meat, but they more frequently stay in pools or in the low intertidal, where they may not eat as many mussels (Fly, Monaco, Pincebourde, & Tullis, 2012; Petes, Mouchka, Milston-Clements, Momoda, & Menge, 2008). However, large sea stars can move >3 m during high tide and will aggregate on dense patches of mussel recruits, so they still exert some control over the lower limit of the mussel bed (Robles, Sherwood-Stephens, & Alvarado, 1995). Small sea stars have a more varied diet, but they also consume small mussels that contribute heavily to mussel bed expansion (Feder, 1959; Menge & Menge, 1974). Despite these limitations as a proxy for absolute predation pressure, biomass combined with size distribution can characterize how predation at a site compares to the preoutbreak state.

If sea star populations had a stable size distribution, we would expect that an increase in the proportion of pre-SSWS count would result in an equal increase in the proportion of pre-SSWS biomass. However, with shifts in size distributions resulting from the disease outbreak, numerical gains are not necessarily coupled with proportionate gains in biomass. To examine how relative biomass changes with relative counts, we calculated change in proportion of pre-SSWS mean counts (% pre-SSWS $\text{count}_{\text{time 2}}$ − % pre-SSWS $\text{count}_{\text{time 1}}$) and proportion of pre-SSWS mean biomass (% pre-SSWS $\text{biomass}_{\text{time 2}}$ − % pre-SSWS $\text{biomass}_{\text{time 1}}$) for each

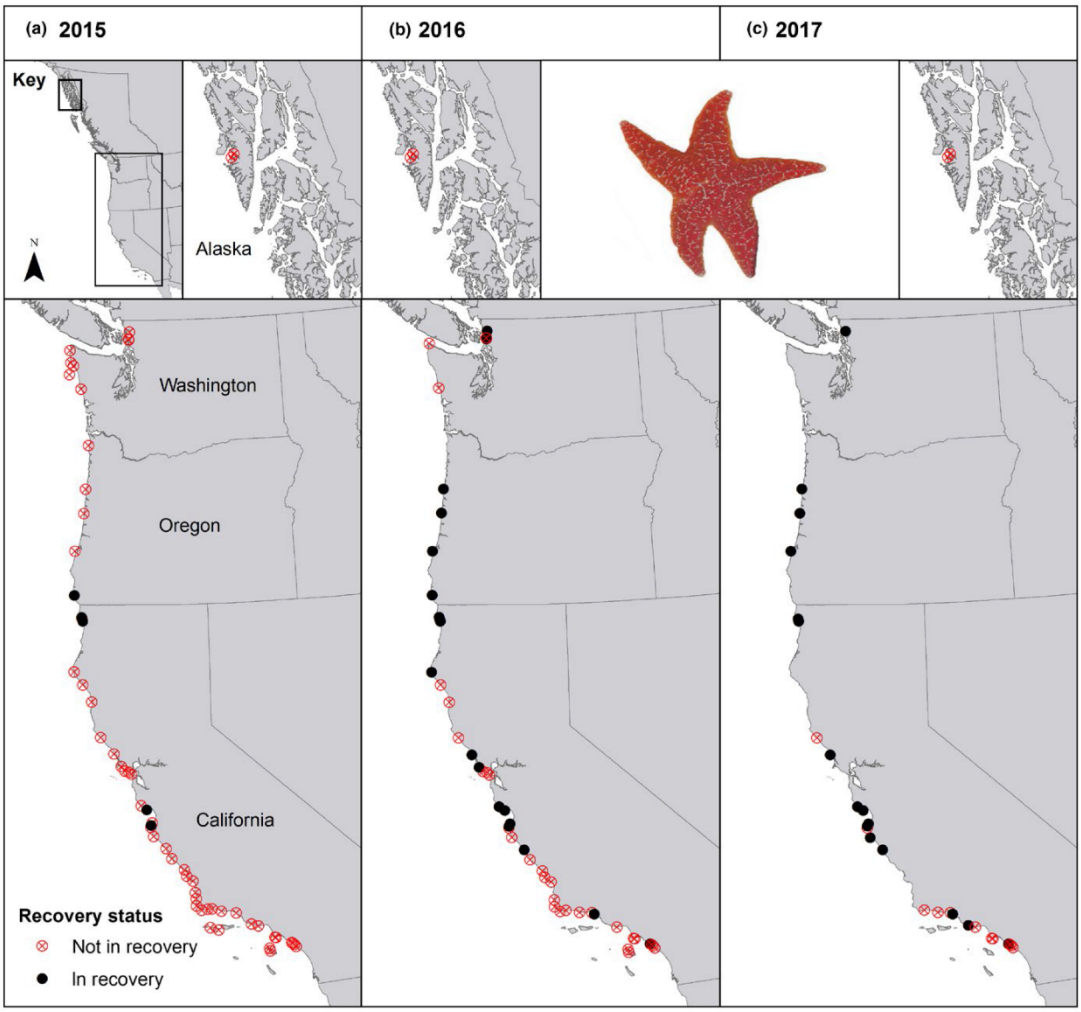

FIGURE 2 Map of sites that have begun population recovery in (a) 2015, (b) 2016, and (c) 2017. Closed black circles represent sites with post-SSWS-born *Pisaster ochraceus* present. Open red circles with an "x" represent sites with no post-SSWS-born *P. ochraceus* present

site between 2015 and 2016 (n = 60) and between 2016 and 2017 (n = 33). We also performed this calculation on changes in consecutive years of proportion of count and biomass (n = 268) at each site with pre-SSWS data. We determined the relationship between count change and biomass change using linear regression for each region and each year-to-year period separately. If the slope of the regression was less than the slope of the regression for that of pre-SSWS count and biomass changes, gains in relative count resulted in less gains than expected to relative biomass, and therefore less gains to the recovery of pre-SSWS predation pressure. We excluded regions that had fewer than four sites sampled in consecutive post-SSWS years due to low sample size in change of count and biomass (Table S3).

Comparing preoutbreak and postoutbreak size distributions gives an indication of demographic changes. To determine whether size distributions were approaching or diverging from the pre-SSWS distributions, we compared 2015 (n = 49), 2016 (n = 44), and 2017 (n = 22) size distributions to the long-term average size distributions at each site using a Kolmogorov–Smirnov test (hereafter "K–S test"). For each site, the K–S tests generated a D statistic, a measure of difference between the long-term focal year distributions. We averaged the D statistic for all sites in a region in each year to assess

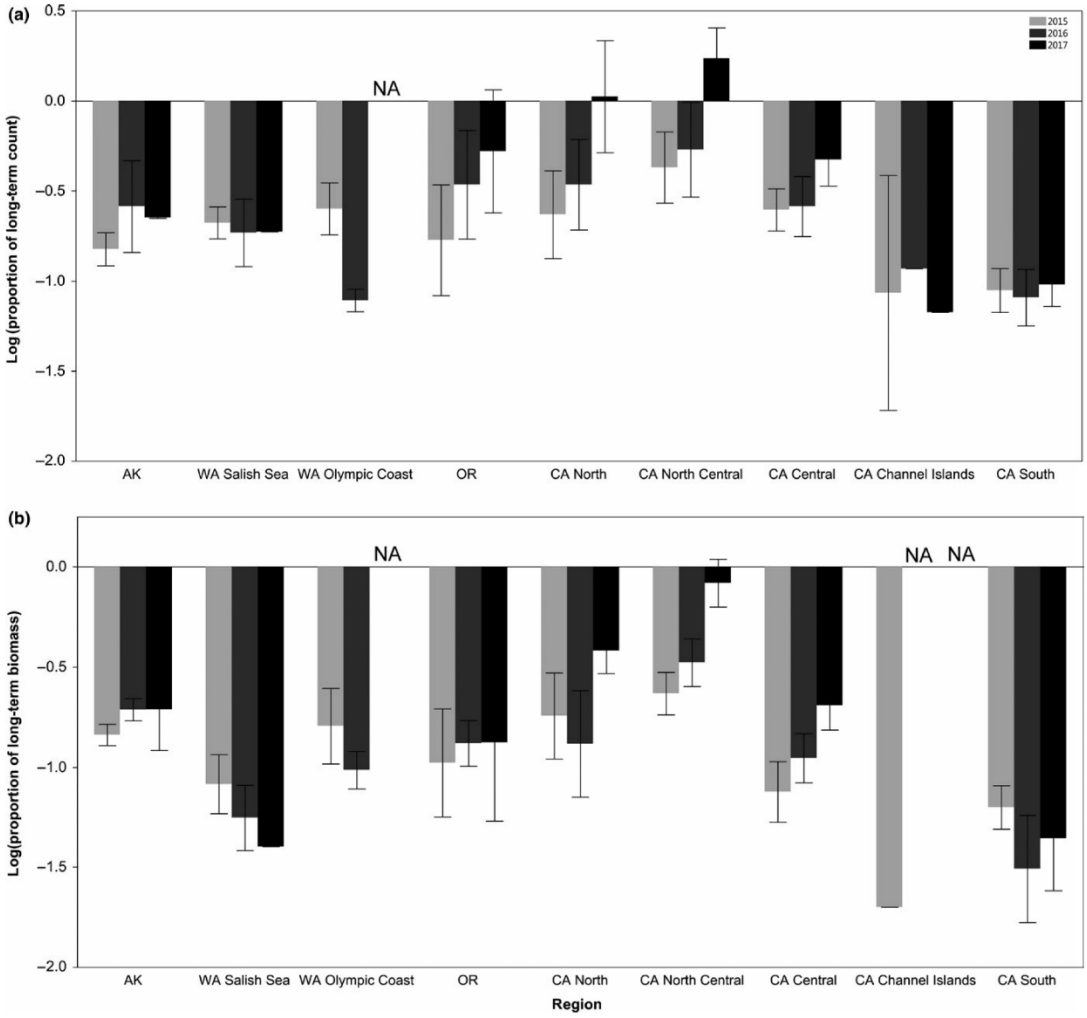

FIGURE 3 Regional means of (a) log-transformed counts and (b) log-transformed biomass of *Pisaster ochraceus* as the proportion of each site's pre-SSWS mean. Light gray bars represent 2015, medium gray bars represent 2016, and black bars represent 2017. Error bars denote standard error. Sites sampled each year are described in Tables S1 and S3. In 2016 and 2017, all sites sampled in the CA Channel Islands region had either no pre-SSWS size data or had counts of 0 individuals, preventing calculation of mean biomass

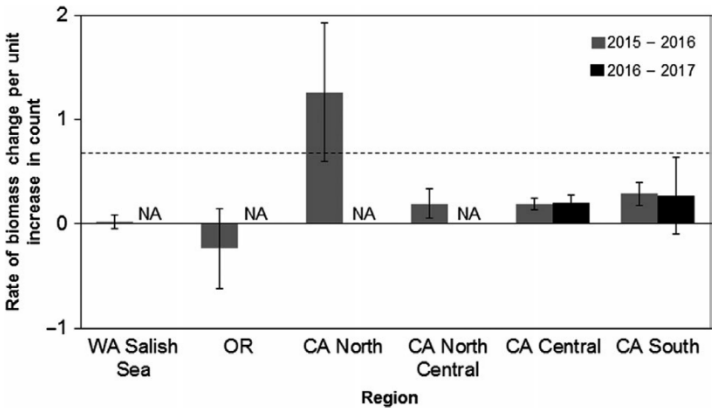

FIGURE 4 Rate of change in relative biomass per unit increase in relative counts. The height of the bar represents the slope of the linear regression between change in proportion of pre-SSWS count and change in proportion of pre-SSWS biomass between two consecutive years. Only regions with enough sites ($n \geq 4$) in consecutive years are shown. Dashed reference line at $y = 0.67$ represents the average slope of the linear regression between change in proportion of count and biomass at sites from 1989 to 2012

geographic trends in size distributions (number of sites per region are detailed in Table S2). Linear regressions were performed in JMP Pro 13. All other statistics were performed in R 3.2.2.

3 | RESULTS

3.1 | Geographic patterns of population recovery

In 2015, few sites coast-wide were in recovery, defined by the presence of individuals with a post-SSWS arrival date. Oregon, North California, and Central California were the only regions with recovering sites that year (Figure 2a). We detected post-SSWS recruits starting in 2016 in Washington Salish Sea, North Central California, and South California. Recovering sites clustered spatially in North and Central California (Figure 2b). In 2017, the percentage of sites in recovery continued to increase in all regions that had recovering sites the previous year (Figure 2c). In contrast, we did not observe post-SSWS individuals in Southeast Alaska, the Washington Olympic Coast, or the Channel Islands in any of the years sampled (Figure 2a–c). Across all regions, we observed five sites (8%) in recovery in 2015, 19 sites (37%) in 2016, and 16 sites (55%) in our partial year of sampling in 2017.

3.2 | Geographic patterns of recovery of predation pressure

We observed regional differences in the degree of recovery of sea star abundances as well as biomass, our proxy for predation pressure. Oregon, North California, and North Central California had counts approaching or exceeding their pre-SSWS averages by 2017. From 2015 to 2017, number of individuals increased in these three regions and Central California (Figure 3a). Mean abundance remained approximately the same or declined in Southeast Alaska, Washington Salish Sea, Washington Olympic Coast, the California Channel Islands, and South California over the same time period. These regions had 30% or less of their pre-SSWS abundances. The Channel Islands and South California had particularly low abundances of 0%–10% of pre-SSWS averages. The gains in sea star counts were not matched by the same gains in sea star biomass, and by extension, predation pressure was still far below its pre-SSWS state for most sites in 2017. All regions except for North Central California had below 40% of their respective long-term biomass in 2015–2017 (Figure 3b). In years where size and biomass data were available, Southern California and the Channel Islands had near-zero biomass.

Gains in relative count were not reflected in equal gains in relative biomass between years. Relative biomass increased at an average of 0.28 ($SE = 0.19$) times the rate that relative count increased between 2015 and 2016 and increased at 0.23 ($SE = 0.03$) times the rate between 2016 and 2017 (Figure 4). This is below the 0.67 ($SE = 0.02$) rate of increase in relative biomass and count that would be expected based on year-to-year changes in count and biomass during the pre-SSWS period. A region could even lose biomass while increasing count if the new individuals were small and mortality was primarily of large individuals. This occurred at some sites in Oregon between 2015 and 2016 and is reflected in the negative relationship between count and biomass for this region (Figure 4).

3.3 | Shifts in size distribution

For sites in recovery (postoutbreak recruits present), smaller individuals comprised a greater proportion of total *P. ochraceus* than large individuals, producing post-SSWS size and biomass distributions shifted toward smaller body sizes (≤45 mm in radius; Figure 5c,d), whereas in pre-SSWS distributions, medium and large individuals (≥75 mm) represented the greatest segment of a site's sea stars (Figure 5a,b). Pre-SSWS populations had multiple normal distributions of individuals reflecting each past recruitment event. Pre-SSWS biomass resembled a normal distribution across the size classes (Figure 5b). Sites not in recovery either had somewhat left-shifted distributions of size and biomass (Figure 5c,d) or highly irregular size distributions shaped by the site's few remaining individuals (Figure 5e,f). These irregular distributions had many

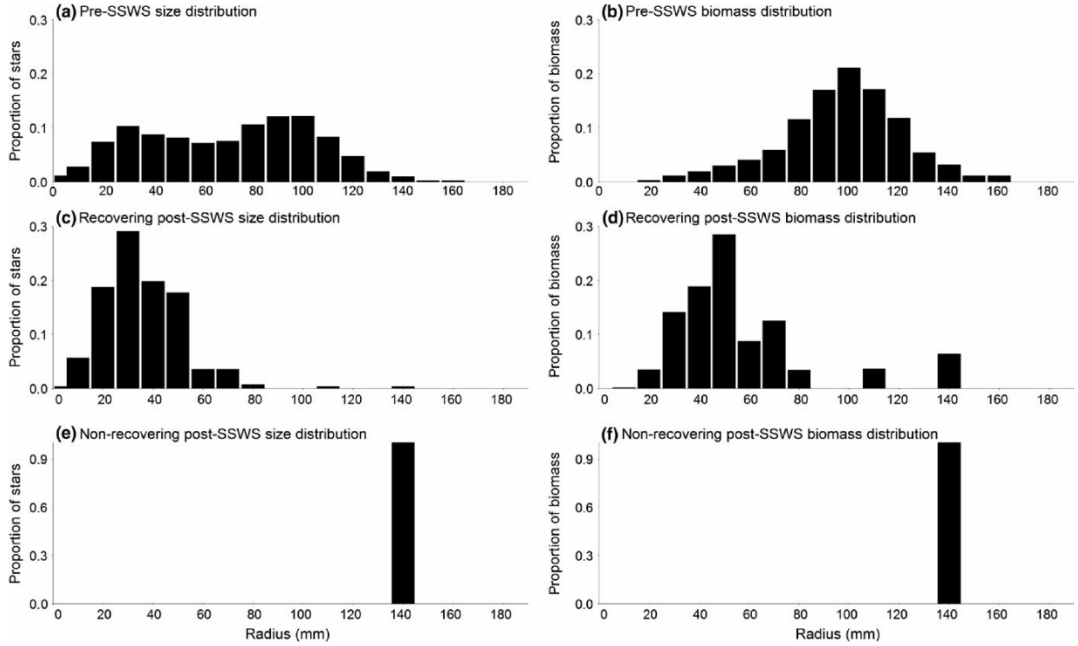

FIGURE 5 Example size distributions of *Pisaster ochraceus*. (a) Pre-SSWS sizes are more uniformly distributed throughout the observed size range with increases reflecting strong recruitment years. (b) Pre-SSWS biomass distributions resemble a normal distribution centered on large sizes. (c) Distribution of sea stars is shifted toward small individuals at recovering sites with high recruitment. (d) Biomass at recovering sites is still concentrated in small to medium individuals. At nonrecovering sites (e), both size and (f) biomass distributions were irregular, shaped by a low number of sea stars (<10) remaining survivors in survey plots. Data for (a, b) from Mill Creek 2017, Monterey County, CA. Data for (c, d) from Mill Creek pre-SSWS. Data for (e, f) from Coal Oil Point 2017, Santa Barbara County, CA

absent size classes, and relative abundances between present size classes were highly variable. Only three sites (Damnation Creek, CA North; Andrew Molera, CA Central; and Government Point, CA South) had size and biomass distributions resembling their respective pre-SSWS distributions by 2017. Distributions in Southern California and the Channel Islands were nearly all irregular, while all other regions had a mix of sites with left-shifted or irregular distributions.

We observed regional differences in directional change in size distribution. From 2015 to 2017, size distributions shifted closer to the pre-SSWS distribution (represented by decreasing *D*-values of K–S test) in North California, North Central California, and Central California. Size distributions shifted further away from the pre-SSWS distribution (represented by increasing *D*-values) in all other regions (Figure 6). Magnitude of these shifts was not uniform across all sites in a region. In Washington Salish Sea, Oregon, and all California regions, we observed within-region variability in the direction and magnitude of shifts in size distributions. Washington Olympic Coast and Southeast Alaska experienced only shifts away from the pre-SSWS distribution, although both regions had substantial variation within them, indicated by large standard errors (Figure 6).

4 | DISCUSSION

4.1 | Factors influencing regional trends in recovery

Despite site-level differences, recovery of *Pisaster ochraceus* populations and their predation potential has begun at regional levels in Washington Salish Sea, Oregon, and for the majority of the California coast north of Point Conception. Individuals produced during and after the outbreak have brought abundances to levels approaching or even exceeding their long-term averages, but predation pressure in terms of biomass is still at <40% of pre-SSWS levels at most sites outside of North Central California.

The regional variability in percent of recovering sites does not indicate a single explanatory factor for drivers of sea star recruitment. Because increases in relative count yielded less than 0.67:1 changes in relative biomass (Figure 4), it suggests that abundances alone are a poor metric of ecological interaction strengths of sea stars of different sizes. Even if the populations grow to their pre-SSWS numbers of individuals, the shift in size structure to domination by smaller sea stars (Figure 5c,d) constitutes a reduction in predation pressure due to lower biomass of juveniles. The regional differences in time elapsed since the mass mortality period influenced time available to

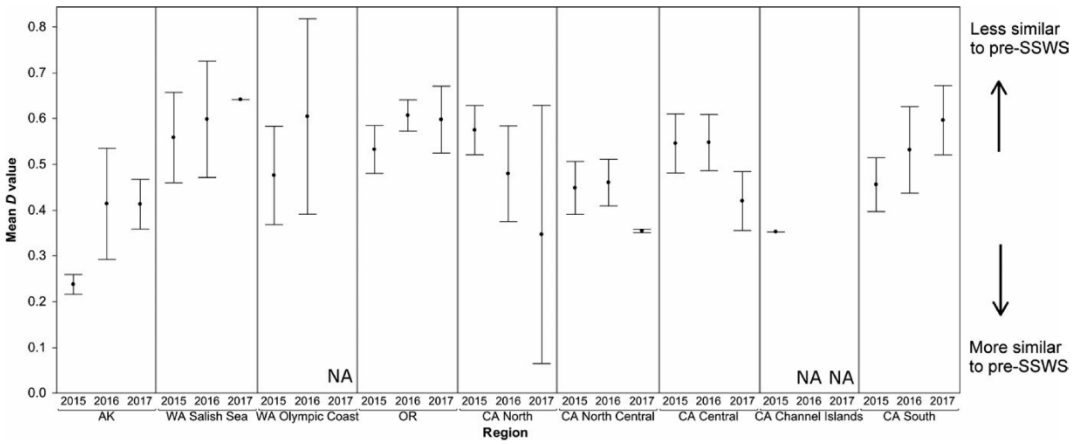

FIGURE 6 Regional mean similarity of *Pisaster ochraceus* size structure to the long-term pre-SSWS (1989–2012) mean size structure. Point heights represent the average *D* statistic of the K–S test (i.e., difference between current and pre-SSWS distributions) for all sites in a region from 2015 to 2017. Error bars denote standard error. A single line for error bars indicates that only one site in that region had size data that year. The WA Olympic Coast region had no size data in 2017. The CA Channel Islands had no size data in 2016 and 2017

detect recovery in these initial postoutbreak years. Mass mortality began in Central California and Washington's Puget Sound area in Fall 2013, while SSWS did not have substantial impacts on the Oregon coast until Summer 2014, at least 9 months later (MARINe 2013; Menge et al., 2016). Assuming the mass mortality period's duration was similar between regions, the time available for postoutbreak reproduction differs by the same amount, potentially giving Central California and the Washington Olympic Coast an earlier start on recovering. In addition, the severity of SSWS mortality varied dramatically between regions. Central and Southern California experienced mortalities of over 95% at many of their sites, while the Oregon coast experienced mortalities closer to 70% (Menge et al., 2016). Washington Salish Sea and Puget Sound experienced a 67% decline in sea star populations, with zero *P. ochraceus* found at some monitoring sites (Eisenlord et al., 2016). These regions have the most information on severity of mortality, while in other regions, less is known about SSWS mortality. The disjunct nature of SSWS appearance combined with the variation in mortality likely contributes to the lack of temporal coherence in spatial patterns of sea star recovery. Our results are also restricted to rocky intertidal sites. Recovery patterns may differ when including sea star populations from a broader suite of sea star habitats, particularly in Alaska and Washington Salish Sea where intertidal habitats are not fully represented by our limited number of sampling sites in these regions (C. M. Miner, personal communication). Additionally, Washington Olympic Coast and the Channel Islands did not have available data in 2017.

Post-disease regional variations in the magnitude of recruitment may contribute to the geographical variation in the number of sites "in recovery." At a regional level, North California and Oregon experienced extremely high numbers of sea star recruits in 2015 (Menge et al., 2016). It is likely this high recruitment was in part responsible for the high percentage of recovering sites in these regions (Figure 2b,c). PISCO sea star surveys in spring 2014 showed high numbers of juvenile sea stars (<25 mm) in the Monterey Bay area of Central California, but a relatively small percentage of them were detected in the next largest size class the following spring (Figure S2), suggesting that small individuals did not survive in large numbers until 2015 or later. It is possible that the first wave of recruits (<15 mm) experienced high mortality from residual SSWS, particularly in the warm temperatures of late summer and early fall. Central California's recruit survival in 2014 appears low and unlikely to contribute substantially to population or biomass increases, potentially negating the temporal head start from earlier outbreak onset. Many of the 2014 recruits were spawned during the outbreak period, late summer through winter of 2013. PISCO surveys in spring 2015 showed a substantially lower number of recruits, but numbers in medium size classes began to increase in 2016, suggesting they survived to contribute to predation pressure (Figure S2b). These recruits did not arrive postoutbreak and did not technically provide an indication of recovery, as recovery depends on successful reproduction and recruitment after the disease subsides.

Lack of recruitment combined with high adult mortality likely contributed to the lack of recovery and the extremely low sea star density and biomass in Southern California (Figure 2d,g,h). Marine invertebrates exhibit major breaks in magnitude and timing of recruitment at Point Conception, Cape Mendocino, and Cape Blanco (Broitman et al., 2008), due at least in part to oceanographic patterns. Based on these studies, the geographic break in sea star recruitment could be due to the absence of larval transport originating further north. After previous SSWS outbreaks, sites in Southern California and the Channel Islands took nearly a decade to return to

preoutbreak *P. ochraceus* densities. It is possible this area will require a similar amount of time to fully recover after the latest outbreak (Blanchette, Richards, Engle, Broitman, & Gaines, 2005).

The variation in sites in recovery within regions (Figure 2) suggests that local factors exert influence on recovery dynamics. Both adult *P. ochraceus* density and recruitment of juveniles often vary by orders of magnitude between sites separated by only a few kilometers (Hart, 2010; Sewell & Watson, 1993). As more time passes after the outbreak, differences in recovery may become more pronounced within and among regions, making influence of local scale dynamics, severity of mortality, and recruitment better defined.

Recruits rarely come from the site where they were spawned due to the long pelagic larval duration, although biogeographic barriers reduce larval transport between regions (Strathmann, 1978). While we cannot ascertain precisely where recruits originated, their source is likely within the same region. Recruits cross regional biogeographic boundaries in sufficient quantities to maintain gene flow (Frontana-Uribe et al., 2008), but high recruitment across a gene flow barrier without high recruitment in the adjacent region would be unlikely. These geographic patterns of recovery have not aligned with those of other species of Pacific coast sea stars, suggesting that initial post-SSWS recruitment patterns have been species-specific (Montecino-Latorre et al., 2016).

In another example of disease influencing intertidal community structure, rates of recruitment appear to have a substantial influence on rates of species recovery and subsequent community shifts. Changes in intertidal community structure have been documented after outbreaks of withering syndrome in black abalone *Haliotis cracherodii*. Abalone graze on attached and drifting macroalgae in the lower intertidal and subtidal zones (Scheibling, 1994). Grazing action by adults promotes a covering of bare rock or coralline algae, which helps cue settlement of larval abalone. After withering syndrome caused mass mortalities of black abalone in Southern California, grazing action was reduced and the dominant cover shifted to sessile invertebrates and sea urchins. These substrates are unfavorable for recruitment of abalone and other invertebrates, increasing the barriers to recovery of abalone populations and their grazing pressure (Miner et al., 2006). Extremely low recruitment was considered one of the major factors for limited black abalone recovery and sustained changes in low intertidal communities (Miner et al., 2006; Raimondi, Wilson, Ambrose, Engle, & Minchinton, 2002).

4.2 | Implications of SSWS recovery dynamics for rocky intertidal communities

If the new juveniles survive to adulthood, the shift in *P. ochraceus* size structure and reduction in predation pressure are only temporary. However, the likelihood of changes to intertidal communities is sensitive to the duration of reduced predation pressure, even if those reductions are temporary (Pfister, Paine, & Wootton, 2016). *P. ochraceus* removal experiments of varying durations have demonstrated that below a certain threshold in mussel size, community change is reversible. Hart's (2010) three-year removal of sea stars produced moderate downward shifts in *Mytilus californianus* lower boundaries, which were reversed 3 years after sea star predation returned. In contrast, Paine (1966, 1974, and 1976) removed *P. ochraceus* for 5 years. During this time, the mussel bed boundary moved substantially lower and many mussels grew beyond the size at which *P. ochraceus* could consume them. This resulted in longer-term increases in mussel cover and change in intertidal species composition. Regional-level and site-level context influence the strength of *P. ochraceus* predation as well. Geographic variation in the growth rates of both sea stars and mussels also influences the amount of time that community changes remain reversible (Kroeker et al., 2016; Phillips, 2007; Sanford, 2002). Wave exposure, local variation in recruitment of mussel species such as *M. californianus*, and frequency of disturbances that disrupt mussel beds will all shape the long-term impact of temporary sea star reductions on the community (Menge, Berlow, Blanchette, Navarrete, & Yamada, 1994; Phillips, 2007; Sousa, 1984). It is more difficult to predict changes to predation pressure in communities where mussels do not occupy a significant portion of the rocky substrate, as *P. ochraceus* will eat a diversity of sessile and mobile invertebrate species in the absence of their preferred mussel prey (Feder, 1956; Landenberger, 1968; Mauzey, Birkeland, & Dayton, 1968).

These results provide insight into how populations of a keystone species are recovering following disturbance events such as disease. Postoutbreak sea star recruitment, survival of adults, and local factors controlling prey dynamics shape the level of predation pressure that those populations exert in the early years following a mass mortality. We predict that sites and regions that take longer to complete the recovery process will likely experience greater changes in community composition following the outbreak. Understanding regional and local differences in postmortality demographics is a first step in predicting where communities are likely to change before enough time has elapsed to observe those shifts. These insights could be used to inform site choices in existing monitoring efforts to document intertidal communities throughout the recovery process. As the occurrence of epidemics is expected to rise, emphasis on the geographic patterns and dynamics of recovering host populations will become increasingly important to assessing how diseases shape communities.

ACKNOWLEDGMENTS

The authors thank PISCO/MARINe partner groups for continued monitoring of sea star populations and supplying data: Sitka Sound Science Center, Padilla Bay National Estuarine Research Reserve, Olympic National Park, Olympic Coast National Marine Sanctuary, Redwoods National and State Park, Point Reyes National Seashore, Golden Gate National Recreation Area, University of California Los Angeles, California State University Fullerton, CalPoly Pomona, Channel Islands National Park, PISCO, and MARINe. MMM is grateful to M. H. Carr, B. Miner, and G. Bernardi for feedback in shaping this work. MMM also thanks K. Melanson for draft feedback and C. Cortez, S. Ayyagari, E. Salas, the Summer 2016 UCSC Marine

Ecology Class, along with many other volunteers for field assistance. All raw data for *Pisaster ochraceus* counts, sizes, and years are publicly available online at www.eeb.ucsc.edu/pacificrockyintertidal/contact/index.html.

CONFLICT OF INTEREST

The authors have no conflict of interests to declare.

AUTHOR CONTRIBUTIONS

MMM designed study, assisted with collection of data, performed analysis, and wrote the manuscript. PTR guided study design, guided analysis, and provided substantial feedback.

ORCID

Monica M. Moritsch http://orcid.org/0000-0002-3890-1264

REFERENCES

Anderson, R. M., & May, R. M. (1991). A framework for discussion the population biology of infectious diseases. In R. M. Anderson, & R. M. May (Eds.), *Infectious diseases of humans: Dynamics and control* (pp. 13–23). Oxford, UK: Oxford University Press.

Baker-Austin, C., Trinanes, J. A., Taylor, N. G. H., Hartnell, R., Siitonen, A., & Martinez-Urtaza, J. (2012). Emerging *Vibrio* risk at high latitudes in response to ocean warming. *Nature Climate Change*, *3*, 73–77.

Bellwood, D. R., Hoey, A. S., & Hughes, T. P. (2012). Human activity selectively impacts the ecosystem roles of parrotfishes on coral reefs. *Proceedings of the Royal Society B-Biological Sciences*, *279*, 1621–1629. https://doi.org/10.1098/rspb.2011.1906

Blanchette, C. A., Richards, D. V., Engle, J. M., Broitman, B. R., & Gaines, S. D. (2005). Regime shifts, community change and population booms of keystone predators at the Channel Islands. *Proceedings of the sixth California Islands Symposium*, *6*, 1–10.

Brodeur, R. D. (1991). Ontogenetic variations in the type and size of prey consumed by juvenile coho, *Oncorhynchus kisutch*, and chinook, *O. tshawytscha*, salmon. *Environmental Biology of Fishes*, *30*, 303–315. https://doi.org/10.1007/BF02028846

Broitman, B. R., Blanchette, C. A., Menge, B. A., Lubchenco, J., Krenz, C., Foley, M., … Gaines, S. D. (2008). Spatial and temporal patterns of invertebrate recruitment along the west coast of the United States. *Ecological Monographs*, *78*, 403–421. https://doi.org/10.1890/06-1805.1

Burge, C. A., Eakin, C. M., Friedman, C. S., Froelich, B., Hershberger, P. K., Hofmann, E. E., … Ford, S. E. (2014). Climate change influences on marine infectious diseases: Implications for management and society. *Annual review of marine science*, *6*, 249–277. https://doi.org/10.1146/annurev-marine-010213-135029

Eisenlord, M. E., Groner, M. L., Yoshioka, R. M., Elliott, J., Maynard, J., Fradkin, S., … Harvell, C. D. (2016). Ochre star mortality during the 2014 wasting disease epizootic: Role of population size structure and temperature. *Philosophical transactions of the Royal Society of London. Series B, Biological sciences*, *5*, 371.

Estes, J. A., Smith, N. S., & Palmisano, J. F. (1978). Sea otter predation and community organization in the western Aleutian Islands, Alaska. *Ecology*, *59*, 822–833. https://doi.org/10.2307/1938786

Feder, H. M. (1956). *Natural history studies on the starfish Pisaster ochraceus (Brandt, 1835) in Monterey Bay area*. PhD thesis, Department of Biological Studies, Stanford University, Stanford, CA.

Feder, H. M. (1959). The food of the starfish, *Pisaster Ochraceus* along the California coast. *Ecology*, *40*, 721–724. https://doi.org/10.2307/1929828

Feder, H. M. (1970). Growth and predation by the ochre sea star, *Pisaster ochraceus* (Brandt), in Monterey Bay, California. *Ophelia*, *8*, 165–185.

Fly, E. K., Monaco, C. J., Pincebourde, S., & Tullis, A. (2012). The influence of intertidal location and temperature on the metabolic cost of emersion in *Pisaster ochraceus*. *Journal of Experimental Marine Biology and Ecology*, *422–423*, 20–28. https://doi.org/10.1016/j.jembe.2012.04.007

Frontana-Uribe, S., de la Rosa-Vélez, J., Enríquez-Paredes, L., Ladah, L. B., & Sanvicente-Añorve, L. (2008). Lack of genetic evidence for the subspeciation of *Pisaster ochraceus* (Echinodermata: Asteroidea) in the north-eastern Pacific Ocean. *Journal of the Marine Biological Association of the United Kingdom*, *88*, 395–400.

George, S. B. (1999). Egg quality, larval growth and phenotypic plasticity in a forcipulate seastar. *Journal of Experimental Marine Biology and Ecology*, *237*, 203–224. https://doi.org/10.1016/S0022-0981(98)00205-6

Groner, M. L., Burge, C. A., Couch, C. S., Kim, C. J., Siegmund, G. F., Singhal, S., … Wyllie-Echeverria, S. (2014). Host demography influences the prevalence and severity of eelgrass wasting disease. *Diseases of Aquatic Organisms*, *108*, 165–175. https://doi.org/10.3354/dao02709

Hamilton, S. L., & Caselle, J. E. (2015). Exploitation and recovery of a sea urchin predator has implications for the resilience of southern California kelp forests. *Proceedings of the Royal Society of London B: Biological Sciences*, *282*, 20141817.

Harley, C. D. G., Pankey, M. S., Wares, J. P., Grosberg, R. K., & Wonham, M. J. (2006). Color polymorphism and genetic structure in the sea star *Pisaster ochraceus*. *Biological Bulletin*, *211*, 248–262. https://doi.org/10.2307/4134547

Hart, D. M. (2010). *Generality and consequences of keystone predation in rocky intertidal habitats of central California*. PhD thesis, Department of Ecology and Evolutionary Biology, University of California, Santa Cruz, CA.

Harvell, C. D., Kim, K., Burkholder, J. M., Colwell, R. R., Epstein, P. R., Grimes, D. J., … Porter, J. W. (1999). Emerging marine diseases–Climate links and anthropogenic factors. *Science*, *285*, 1505–1510. https://doi.org/10.1126/science.285.5433.1505

Hewson, I., Button, J. B., Gudenkauf, B. M., Miner, B., Newton, A. L., Gaydos, J. K., … Fradkin, S. (2014). Densovirus associated with sea-star wasting disease and mass mortality. *Proceedings of the National Academy of Sciences of the United States of America*, *48*, 17278–17283. https://doi.org/10.1073/pnas.1416625111

Hughes, J., Deegan, L., & Wyda, J. (2002). The effects of eelgrass habitat loss on estuarine fish communities of southern New England. *Estuaries*, *25*, 235–249. https://doi.org/10.1007/BF02691311

Keever, C. C., Sunday, J., Puritz, J. B., Addison, J. A., Toonen, R. J., Grosberg, R. K., & Hart, M. W. (2009). Discordant distribution of populations and genetic variation in a sea star with high dispersal potential. *Evolution*, *63*, 3214–3227. https://doi.org/10.1111/j.1558-5646.2009.00801.x

Kroeker, K. J., Sanford, E., Rose, J. M., Blanchette, C. A., Chan, F., Chavez, F. P., … McManus, M. A. (2016). Interacting environmental mosaics drive geographic variation in mussel performance and predation vulnerability. *Ecology Letters*, *19*, 771–779. https://doi.org/10.1111/ele.12613

Lafferty, K. D., & Suchanek, T. H. (2016). Revisiting Paine's 1966 sea star removal experiment, the most-cited empirical article in the *American Naturalist*. *American Naturalist*, *188*, 365–378. https://doi.org/10.1086/688045

Landenberger, D. E. (1968). Studies on selective feeding in the Pacific starfish *Pisaster* in southern California. *Ecology, 49*, 1062–1075. https://doi.org/10.2307/1934490

Leighton, B., Boom, J., Bouland, C., Hartwick, E., & Smith, M. (1991). Castration and mortality in *Pisaster ochraceus* parasitized by *Orchitophyra stellarum* (Ciliophora). *Diseases of Aquatic Organisms, 10*, 71–73. https://doi.org/10.3354/dao010071

Lessios, H. A. (1988). Mass mortality of *Diadema antillarum* in the Caribbean: What have we learned? *Annual Review of Ecology and Systematics, 19*, 371–393. https://doi.org/10.1146/annurev.es.19.110188.002103

Ling, S. D., Johnson, C. R., Frusher, S. D., & Ridgway, K. R. (2009). Overfishing reduces resilience of kelp beds to climate-driven catastrophic phase shift. *Proceedings of the National Academy of Sciences of the United States of America, 106*, 22341–22345. https://doi.org/10.1073/pnas.0907529106

MARINe (2008). *Unified monitoring protocols for the multi-agency Rocky Intertidal Network*. 1–84.

MARINe (2013). *Unprecedented sea star mass mortality along the west coast of North America due to wasting syndrome*. Press Release, 1–3

Multi-Agency Rocky Intertidal Network (MARINe). (2014). *Pisaster ochracues symptoms guide. Sea Star Wasting Syndr.* Retrieved from https://www.eeb.ucsc.edu/pacificrockyintertidal/data-products/sea-star-wasting/#id-guides

Mauzey, K. P. (1966). Feeding behaviour and reproductive cycles in *Pisaster ochraceus*. *Biological Bulletin, 131*, 127–144. https://doi.org/10.2307/1539653

Mauzey, K., Birkeland, C., & Dayton, P. (1968). Feeding behavior of asteroids and escape responses of their prey in the Puget Sound region. *Ecology, 49*, 603–619. https://doi.org/10.2307/1935526

McClintock, J. B., & Robnett, T. J. (1986). Size selective predation by the asteroid *Pisaster ochraceus* on the bivalve *Mytilus californianus*: A cost-benefit analysis. *Marine Ecology, 7*, 321–332. https://doi.org/10.1111/j.1439-0485.1986.tb00167.x

Menge, B. A. (1995). Indirect effects in marine Rocky Intertidal interaction webs: Patterns and importance. *Ecological Monographs, 65*, 21–74. https://doi.org/10.2307/2937158

Menge, B. A., Berlow, E. L., Blanchette, C. A., Navarrete, S. A., & Yamada, B. (1994). The keystone species concept: Variation in interaction strength in a Rocky Intertidal Habitat. *Ecological Monographs, 64*, 249–286. https://doi.org/10.2307/2937163

Menge, B. A., Cerny-Chipman, E. B., Johnson, A., Sullivan, J., Gravem, S., & Chan, F. (2016). Sea star wasting disease in the keystone predator *Pisaster ochraceus* in Oregon: Insights into differential population impacts, recovery, predation rate, and temperature effects from long-term research. *PLoS ONE, 11*, e0153994. https://doi.org/10.1371/journal.pone.0153994

Menge, J. L., & Menge, B. A. (1974). Role of resource allocation, aggression and spatial heterogeneity in coexistence of two competing intertidal starfish. *Ecological Monographs, 44*, 189–209. https://doi.org/10.2307/1942311

Miner, C. M., Altstatt, J. M., Raimondi, P. T., & Minchinton, T. E. (2006). Recruitment failure and shifts in community structure following mass mortality limit recovery prospects of black abalone. *Marine Ecology Progress Series, 327*, 107–117. https://doi.org/10.3354/meps327107

Montecino-Latorre, D., Eisenlord, M. E., Turner, M., Yoshioka, R., Harvell, C. D., Pattengill-Semmens, C. V., ... Gaydos, J. K. (2016). Devastating transboundary impacts of sea star wasting disease on subtidal asteroids. *PLoS ONE, 11*, e0163190. https://doi.org/10.1371/journal.pone.0163190

Mydlarz, L. D., Jones, L. E., & Harvell, C. D. (2006). Innate immunity, environmental and disease ecology of marine and freshwater invertebrates. *Annual Review of Ecology Evolution and Systematics, 37*, 251–288. https://doi.org/10.1146/annurev.ecolsys.37.091305.110103

Paine, R. T. (1966). Food web complexity and species diversity. *The American Naturalist, 100*, 65–75. https://doi.org/10.1086/282400

Paine, R. T. (1974). Intertidal community structure. Experimental studies on the relationship between a dominant competitor and its principal predator. *Oecologia, 15*, 93–120. https://doi.org/10.1007/BF00345739

Pearse, J. S., & Eernisse, D. J. (1982). Photoperiodic regulation of gametogenesis and gonadal growth in the sea star *Pisaster ochraceus*. *Marine Biology, 67*, 121–125. https://doi.org/10.1007/BF00401277

Petes, L. E., Mouchka, M. E., Milston-Clements, R. H., Momoda, T. S., & Menge, B. A. (2008). Effects of environmental stress on intertidal mussels and their sea star predators. *Oecologia, 156*, 671–680. https://doi.org/10.1007/s00442-008-1018-x

Pfister, C. A., Paine, R. T., & Wootton, J. T. (2016). The iconic keystone predator has a pathogen. *Frontiers in Ecology and the Environment, 14*, 285–286. https://doi.org/10.1002/fee.1292

Phillips, N. E. (2007). A spatial gradient in the potential reproductive output of the sea mussel *Mytilus californianus*. *Marine Biology, 151*, 1543–1550. https://doi.org/10.1007/s00227-006-0592-x

Pilkerton, A., Apple, J., Kohnert, C., Bohlmann, H., & Burnett, N., (2016). *Investigating patterns in the growth dynamics of Pacific northwest sea stars, E. troschelii and P. ochraceus*. Proceedings of the Pacific Estuarine Research Society, 39th Annual Meeting. Brackendale, BC.

Ponton, F., Otálora-Luna, F., Lefevre, T., Guerin, P. M., Lebarbenchon, C., Duneau, D., ... Thomas, F. (2011). Water-seeking behavior in worm-infected crickets and reversibility of parasitic manipulation. *Behavioral Ecology, 22*, 392–400. https://doi.org/10.1093/beheco/arq215

Raimondi, P. T., Wilson, C. M., Ambrose, R. F., Engle, J. M., & Minchinton, T. E. (2002). Continued declines of black abalone along the coast of California: Are mass mortalities related to El Niño events? *Marine Ecology Progress Series, 242*, 143–152. https://doi.org/10.3354/meps242143

Robles, C. D., Desharnais, R. A., Garza, C., Donahue, M. J., & Martinez, C. A. (2009). Complex equilibria in the maintenance of boundaries: Experiments with mussel beds. *Ecology, 90*, 985–995. https://doi.org/10.1890/08-0919.1

Robles, C. D., Sherwood-Stephens, R., & Alvarado, M. (1995). Responses of a key intertidal predator to varying recruitment of its prey. *Ecology, 76*, 565–579. https://doi.org/10.2307/1941214

Rockwood, L. L. (2006). Host-parasite interactions. In L. L. Rockwood (Ed.), *Introduction to population ecology* (pp. 221–235). Malden, MA: Blackwell Publishing.

Sanford, E. (2002). Water temperature, predation, and the neglected role of physiological rate effects in rocky intertidal communities. *Integrative and Comparative Biology, 42*, 881–891. https://doi.org/10.1093/icb/42.4.881

Sanford, E., & Menge, B. A. (2007). Reproductive output and consistency of source populations in the sea star *Pisaster ochraceus*. *Marine Ecology Progress Series, 349*, 1–12. https://doi.org/10.3354/meps07166

Sato, T., Egusa, T., Fukushima, K., Oda, T., Ohte, N., Tokuchi, N., ... Lafferty, K. D. (2012). Nematomorph parasites indirectly alter the food web and ecosystem function of streams through behavioural manipulation of their cricket hosts. *Ecology Letters, 15*, 786–793. https://doi.org/10.1111/j.1461-0248.2012.01798.x

Scheibling, R. E. (1994). Molluscan grazing and macroalgal zonation on a rocky intertidal platform at Perth, Western-Australia. *Australian Journal of Ecology, 19*, 141–149.

Selakovic, S., de Ruiter, P. C., & Heesterbeek, H. (2014). Infectious disease agents mediate interaction in food webs and ecosystems. *Proceedings of the Royal Society of London B: Biological Sciences, 281*, 20132709. https://doi.org/10.1098/rspb.2013.2709

Sewell, M., & Watson, J. (1993). A "source" for asteroid larvae?: Recruitment of *Pisaster ochraceus*, *Pycnopodia helianthoides* and

Dermasterias imbricata in Nootka Sound, British Columbia. *Marine Biology*, *117*, 387–398.

Smith, K. F., Behrens, M. D., & Sax, D. F. (2009). Local scale effects of disease on biodiversity. *EcoHealth*, *6*, 287–295. https://doi.org/10.1007/s10393-009-0254-9

Sousa, W. P. (1984). Intertidal mosaics: Patch size, propagule availability, and spatially variable patterns of succession. *Ecology*, *65*, 1918–1935. https://doi.org/10.2307/1937789

Stickle, W. B., Foltz, D. W., Katoh, M., & Nguyen, H. L. (1992). Genetic structure and mode of reproduction in five species of sea stars (Echinodermata: Asteroidea) from the Alaskan coast. *Canadian Journal of Zoology*, *70*, 1723–1728. https://doi.org/10.1139/z92-239

Strathmann, R. (1978). Length of pelagic period in echinoderms with feeding larvae from the Northeast Pacific. *Journal of Experimental Marine Biology and Ecology*, *34*, 23–27. https://doi.org/10.1016/0022-0981(78)90054-0

Suchanek, T. (1986). Mussels and their role in structuring rocky shore communities. In P. G. Moore, & R. Seed (Eds.), *Ecology of Rocky coasts* (pp. 70–96). New York, NY: Columbia University Press.

Wood, C. L., Byers, J. E., Cottingham, K. L., Altman, I., Donahue, M. J., & Blakeslee, A. M. H. (2007). Parasites alter community structure. *Proceedings of the National Academy of Sciences of the United States of America*, *104*, 9335–9339. https://doi.org/10.1073/pnas.0700062104

SUPPORTING INFORMATION

Additional Supporting Information may be found online in the supporting information tab for this article.

How to cite this article: Moritsch MM, Raimondi PT. Reduction and recovery of keystone predation pressure after disease-related mass mortality. *Ecol Evol*. 2018;8:3952–3964. https://doi.org/10.1002/ece3.3953

Chapter 2: Environmental contributors to timing of Sea Star Wasting Syndrome appearance in North America

Abstract

Predicting and responding to epidemics requires detailed understanding of the conditions promoting their emergence. For disease outbreaks to escalate from background levels of mortality to widespread high-mortality epidemics, susceptible hosts and appropriate conditions for the pathogen must coincide in the space and time. Since summer 2013, an epidemic of Sea Star Wasting Syndrome (SSWS) has been documented in intertidal and subtidal echinoderm species over most of the Pacific coast and some of the Atlantic coast of North America. Previous outbreaks, as well as the most recent one, have reduced intertidal and subtidal sea star populations to near-absence in many locations. It is currently unclear what conditions induced the epidemic. To identify factors associated with SSWS emergence, we combined intertidal sea star health surveys, citizen scientist disease reports, and data on natural physical stressors or anthropogenic disturbances at infected and non-infected sites. We modeled potential relationships between environmental variables, anthropogenic variables, and the risk of SSWS occurrence using a Cox Proportional Hazards Model. On a coast-wide scale, the leading models suggested that probability of SSWS infection is negatively associated with distance (positively associated with proximity) to the nearest infected neighbor site and positively associated with hours of afternoon low tide exposure. At a regional scale, these same variables were associated with

SSWS infection in the Salish Sea and the California Channel Islands. In contrast, chlorophyll *a* concentration was positively associated with SSWS in Central California and negatively associated with SSWS in the Channel Islands. While these factors might not necessarily cause SSWS, they might identify conditions that increase host susceptibility by inducing physiological stress, increasing proximity to pathogen reservoirs, or providing conditions that favor growth and reproduction of the underlying pathogen. Understanding the factors associated with SSWS will allow us to predict where this epidemic and its ecological consequences are most likely to occur.

Introduction

Diseases are a major cause biodiversity decline and disruption of ecological function (Hughes 1994, Harvell et al. 1999, Smith et al. 2006, Selakovic et al. 2014). Predicting when and where epidemics might happen is fundamental to disease management, yet we have a poor understanding of how large-scale disease outbreaks emerge (Groner et al. 2016). To improve our ability to predict and prevent epidemics, we need to investigate the causes of disease and conditions promoting outbreaks (Harvell et al. 1999, Rogers and Randolph 2003, Groner et al. 2016). Infectious diseases require three factors to be able to spread: a pathogen, a susceptible host, and environmental conditions beneficial to pathogen invasion and reproduction (Snieszko 1974). Many marine pathogens are continually present in marine environments at sufficient levels to cause disease, yet host populations experience variable levels of

disease prevalence and severity through time. These dynamics are in part related to changes in optimal conditions for host and pathogen health (Altizer et al. 2013). Natural physical conditions and anthropogenic activities influence host physiology and their susceptibility to illness. Stressful external environments frequently reduce host immune functions (Meentemeyer et al. 2004, Gálvez et al. 2011, Chen et al. 2012). Simultaneously, these conditions impact pathogen physiology and their abilities to invade hosts and reproduce (Anderson 1987, Altizer et al. 2013). Changes in conditions can also shift a host's relationship with mutualistic or amensalistic microfauna from positive or neutral to pathogenic (Thompson 2005, Bourne et al. 2009). Understanding the relationships between environmental conditions, human activities, and host susceptibility is critical to prediction of epidemics.

Sea star wasting syndrome (SSWS) has affected over 20 species of sea stars in North American waters along the Pacific coast (Hewson et al. 2014), Atlantic coast (DelSesto 2015, Bucci et al. 2017), and Gulf of California (Dungan et al. 1982). Starting in Summer 2013, the SSWS epidemic caused major declines of the keystone species *Pisaster ochraceus* and many other sea star species (Eisenlord et al. 2016, Montecino et al. 2016, Moritsch and Raimondi 2018, Rogers et al. 2018). The widespread geographic extent of the current outbreak from Alaska to San Diego on the Pacific coast and places along the Atlantic coast is largest documented outbreak of this disease (DelSesto 2015, Miner et al. 2018). SSWS outbreaks in *P. ochraceus* have occurred on regional scales several times in the last century (Eckert et al. 2000, Bates et al. 2009). Given this history and the broad range of host species, it is likely

that the causal pathogen(s) have been present in the environment for decades (Hewson et al. 2014). This implies that the conditions that host organisms experience, rather than mere presence of the pathogen, determines when major outbreaks occur.

Temperature has been implicated as a major factor controlling the onset and severity of disease outbreaks in both marine and terrestrial environments (Meentemeyer et al. 2004, Boyett et al. 2007, Bruno et al. 2007, Kilpatrick et al. 2008). As temperature rises, many bacterial pathogens experience increased growth rates, and many marine hosts experience greater levels of physiological stress, which compromises immune system activities (Snieszko 1974, Harvell et al. 1999, Fly et al. 2012, Schade et al. 2014). Connections between disease prevalence and temperature have been observed in several echinoderm diseases, including balding urchin disease and paramoebiasis (Scheibling and Stephenson 1984, Jellett and Scheibling 1988, Clemente et al. 2014). Depending on the temperature of the air and access to thermal refuges, low tide exposures can expose organisms to another form of thermal stress and desiccation stress (Petes et al. 2008, Monaco et al. 2015). Toxins from harmful algal blooms accumulated in shellfish then ingested as food also weaken echinoderms' abilities to resist hydrodynamic stress (Ferrer et al. 2015).

Human population density and coastal development might also influence transmission dynamics and host immunity. Entangled fishing gear and debris provide surfaces for increased microbial colonization, and injuries from these items create an entryway for microbes to circumvent external defenses against invasion (Lamb et al. 2016, 2018). Wastewater discharges into the marine environment potentially

influence infection by supplying nutrients that increase already-present marine pathogens and bacteria involved in secondary infections to harmful levels (Thompson et al. 2002, Miller et al. 2010). Even if the disease agent is not directly linked to human activities, larger human populations create more stress for coastal ecosystems through a wide variety of pollution and contaminants, disturbance, increased coastal visitation, and habitat modification (Snieszko 1974, Sindermann 1993, Thompson et al. 2002, Smith and Murray 2005).

Complicating efforts to find consistent patterns in disease causes, the onset of symptoms might occur after a substantial temporal lag following a chronic or acute stressor (Powell et al. 1992, Caldwell et al. 2016). Potential for long lag times and buildup of stressors highlights the importance of using time series of environmental conditions in addition to short-term measurements near the dates of disease emergence. Furthermore, multiple stressors often interact additively or synergistically, elevating physiological challenges beyond what is tolerable of each stressor individually (Snieszko 1974, Thompson et al. 2002, Remily and Richardson 2006, Smith et al. 2009).

The most recent SSWS outbreak appearance jumped between non-adjacent regions of the coast. Sea stars with symptoms were first observed in June 2013 in Washington state and then in Central California within weeks. Assuming that symptoms were detected as they appeared, the epidemic progressed over the course of a year to Southern California, Oregon, and then the Salish Sea (Fuess et al. 2015, Eisenlord et al. 2016, Menge et al. 2016, Miner et al. 2018). This disjunct progression

also suggests that the pathogen was present in multiple regions of the coast before the outbreak. Epidemic levels of infection might have been triggered by different mechanisms on separate occasions, though this does not rule out the possibility of a single trigger mechanism acting at different times. It is also possible the pathogen spread to all regions before visually detectable SSWS symptoms appeared (Hewson et al. 2018), suggesting that stressors triggered symptom onset as opposed to the infection itself.

In past SSWS outbreaks, areas with warmer water experienced higher disease prevalence and symptom severity, both in laboratory experiments (Bates et al. 2009, Staehli et al. 2009) and in field observations (Dungan et al. 1982, Eckert et al. 2000). Small-scale observations suggest that rapid increases in SSWS prevalence and severity occurred during periods of anomalously high temperatures in some regions of the coast, while in other regions, the outbreak preceded warm seawater temperatures (Eisenlord et al. 2016, Menge et al. 2016, Miner et al. 2018). Host population density is commonly correlated with disease outbreaks (Anderson and May 1991), yet Miner et al. (2018) observed no correlation with density and relative magnitude of population declines from SSWS in *P. ochraceus*. Lower than average rainfalls have also been proposed as a driver of SSWS via increased concentration of terrestrial contaminant outflow during rare rain events, though this is still a speculative hypothesis (Hewson et al. 2018). No other environmental drivers have currently been proposed as obvious triggers for SSWS.

As marine diseases are expected to increase under global climate change, identifying the drivers of infection will improve abilities to successfully predict and manage epidemics. Here we explore potential relationships between SSWS infection and potentially related environmental conditions leading up to the time of infection. It is essential to highlight factors that warrant further investigation as contributors to SSWS emergence and to rule out hypotheses around factors where no association with SSWS is found. As very few studies have examined the abiotic and biotic conditions surrounding SSWS outbreaks outside of a lab setting (Bates et al. 2009, Kohl et al. 2016), these insights are central to understanding the mechanisms that increase infection rates, the conditions that led to the emergence of the recent epidemic, and what conditions might increase the likelihood of future outbreaks.

Methods

We used a survival analysis modeling approach to explore the relationship between environmental or anthropogenic conditions at a site and the time to SSWS appearance. Survival analysis, also known as time-to-event analysis, estimates the probability (or "hazard") of a discrete event occurring during any given time interval. This probability is a function of conditions present leading up to the event (Heisey 2009a). We used this approach to estimate how well different conditions predicted the time at which any given site switched from "no SSWS observed" to "SSWS present." The conditions that better explain the probability of SSWS appearance are more likely to be associated with the outbreak of disease. While this modeling method

cannot discern which factors are causes of disease, this approach allows integration of spatially and temporally disjunct observations of disease emergence and conditions present at the time over thousands of kilometers of coastline.

SSWS observations and timing of appearance

Opportunistic SSWS presence/absence observations were collected through a combination of site surveys by intertidal monitoring groups, citizen science groups, and recreational tidepoolers and divers submitting standardized tracking logs and photos to the Partnership of Interdisciplinary Studies of Coastal Oceans (PISCO) consortium for observation vetting (PISCO 2014a). If any individual sea star of any species was found with the disease at that site, SSWS was considered "present" at that site for that date and all later dates regardless of whether a subsequent observation noted no sea stars with symptoms. We assumed that all sites experienced a similar lag between the true onset of SSWS and the earliest observation of SSWS presence. For the purposes of this analysis, we used observations made between January 2014 and January 2015. This was the period of peak citizen science observation, as SSWS was receiving a high volume of media attention during this time. We did not use observations from late 2013 because PISCO did not announce they were seeking observations until November of 2013. After January of 2015, SSWS had reached most areas of the Pacific coast (Miner et al. 2018, Moritsch and Raimondi 2018). We did not have sufficient observations from the Atlantic coast, so this area was excluded from analysis.

PISCO received over 1,200 observations of sea stars across multiple species during the citizen science monitoring period. Of these, 650 observations were for sea stars that were attached to the substrate. We did not use observations of dead individuals that had drifted ashore because we could not verify where they had lived before. Once a single infected sea star was observed at a site, that site was defined as "infected" and could never revert to a definition of "healthy," even if only healthy sea stars were observed on future site visits. These revisited sites often had very few remaining individuals to count, indicating high mortality between the observation of infection and revisit date. Because our goal was to investigate conditions surrounding the time of infection, we had to discard 345 observations at sites where the first observation made was of infected sea stars, as these observations gave us no information on when infection occurred. After applying these criteria, we were left with sites that were never infected over the study period and sites that had at least one healthy observation followed by infection. Observations at the same site on different days counted as separate observations because the conditions changed between observation dates. We also excluded observations of SSWS presence at sites where the time between an initial "SSWS absent" observation exceeded 30 weeks because of increased uncertainty over the potential time surrounding infection. This yielded a total of 284 usable observations ($n_{healthy} = 228$ and $n_{infected} = 56$).

Because the spatially disjunct progression of the SSWS outbreak allows the possibility of multiple instances of development into an epidemic, assessing the host-pathogen-environment relationship on a regional scale allowed us to identify possible

contributing factors that would not appear important when assessing the coast over larger spatial and temporal range. We also searched for these relationships on the scale of the whole coast. We used all 284 observations in modeling on a coast-wide scale from British Columbia, Canada (49.757 ^{o}N) to Baja California, Mexico (31.281 ^{o}N). We tested whether regions behaved differently from the whole-coast model for the same variables by comparing the value of Akaike Information Criterion (AIC) in models with and without the regional effect term (Table A2.2). We then compared models of these variables within each geographic region (Table 2.1) to evaluate which conditions were most associated with the risk of SSWS infection at that scale and whether these conditions differed between regions. All observations from Baja California were of healthy *P. ochraceus*. Because there we had no infection observations within this region, we were unable to analyze Baja at a regional scale, though these sites are still included in coast-wide scale analysis.

Conditions surrounding SSWS appearance

To generate data on site-specific conditions on the date of emergence, we calculated the distance of SSWS observation locations from the following features: wastewater outfalls, major North American ports, shipping paths, and densely populated coastlines. We used Ocean Health Index data (Halpern et al. 2008, 2009) and land use/land cover data to assess relative degree of coastal habitat disturbance (Table A2.1). For each week, we estimated the minimum over-water distance between each site and any infected site (not restricted to the 284 observations we

focused on for the hazard model). This did not account for the influence currents on transport of waterborne pathogenic units, but given how little is known about the pathogen or infection etiology, such an approach was beyond the scope of this study. Using remote sensing data, we calculated the weekly average chlorophyll *a* concentration and average daily hours of daytime low tide exposure. *In situ* intertidal temperature loggers at 76 sites provided daily mean temperatures. For every week in 2013 through 2015, we calculated the difference (^{o}C) between the weekly mean temperature and the 80th percentile weekly mean temperature (T_{80}) observed at a given site during that week of the year. Degree Heating Weeks (DHW), the sum of a site's weekly degrees above T_{80} in the 12-week period before a sea star health observation, provided an estimate of accumulated thermal stress leading up to the observation. Only degrees above T_{80} (positive) were included in DHW. Details and sources for spatial processing of environmental and anthropogenic variables are provided in Table A2.1. We used ArcGIS 10.4 for all spatial processing. Pre-outbreak *P. ochraceus* population density was not correlated with the degree of mortality within a population (Miner et al. 2018), so we did not include it as a variable in our model.

To account for covariation between variables of similar type (e.g., pollution-related, population related), we used Principle Component Analysis (PCA) (JMP Pro 13) to form composite variables for use in the model. Excessive missing values reduce the number of sites with Principal Component predictor values. Given the large number of variables we considered, no site had data for all variables at the time

of observation. Because of this limitation, we performed PCA separately on variables of the same category; we used a separate PCA for static pollution-related variables, static human population-related variables, and time-series environmental variables. All variables were appropriately transformed prior to PCA to meet assumptions of normality (Table A2.1). This generated three composite Principle Components: one related to distance from dense populations and two related to disturbance to coastal waters or adjacent watershed (Table 2.2). Due to the dynamic nature of chlorophyll *a*, DHWs, low tide exposure hours, and distance from infected sites, we were unable to perform PCA on these variables and instead tested for collinearity of variables week by week. Low tide exposure was colinear with latitude more than 20% of weeks, preventing them from being used in the same predictive model. We standardized all variables using their z-score, the difference from the mean divided by the standard deviation ($z = (x - \bar{x})/SD$) for their use in the hazard model. Time (weeks) was represented as a fraction k from 0 to 1 where k = (weeks between given observation and Jan 1, 2013)/(weeks between final observation and Jan 1, 2013). Missing data points were assumed to be equal to the mean so they would contribute a mean risk instead of no risk to the total risk of infection. In regional models, all variables were rescaled to the mean values of that region instead of the mean for the whole coast.

Risk of infection modeling

We searched for correlations between these environmental variables and the risk of SSWS infection occurring at an observation site during any given week. We then selected for the most explanatory models using AIC values.

We grouped SSWS observations into weekly time bins for the purpose of modeling discrete time periods. January 1, 2013 served as time t_0, as all sites were free of detectable SSWS symptoms at this writing. If any individual sea star of any species was found with the disease at that site, SSWS was considered "present" at that site for that date and all later dates regardless of whether a subsequent observation noted no sea stars with symptoms. We assumed that a site's earliest observation date of SSWS presence was a proxy for date of emergence. If all stars found at a site showed no symptoms of SSWS at the time observation, SSWS was considered "absent" for 12 weeks after the observation or until symptoms were observed. After the 12-week period, the site was considered unobserved with no data until rechecked for signs of disease.

For our survival analysis model, we used a discrete-time maximum likelihood Cox proportional hazards model (Table 2.4, Equations 2.1-2.2) (Cox 1972) to analyze the relationship between site conditions and the probability of SSWS presence. The Cox proportional hazards model is commonly used in epidemiology to estimate time-to-illness or time-to-death for individuals that experience specified conditions (Kumar and Klefsjo 1994, Heisey 2009a). This model uses a Unit Cumulative Hazard (UCH) function to calculate the probability of SSWS status changing from absent (y = 1) to

present ($y = 0$) during an infinitely short time period as a function of several independent variables. This is the complement of the survival probability, or the probability that a site remains SSWS-free over the same period of time (Heisey 2009b). The hazards model assumes that the event probability is constant over time and that external factors additively influence that probability without synergistic interactions (Crichton 2002). Synergistic interactions are common in disease occurrence, but to avoid overfitting, we limited our model to additive effects due to the already high number of variables potentially contributing to SSWS.

We modeled all additive combinations of 1 variable through 7 variables (i.e., all variables individually, all 2-variable combinations, all 3-variable combinations, etc.) (Table 2.3, Table 2.4). Latitude and low tide exposure hours were colinear, so no model included both terms at once, though individual model combinations could contain either term. *In situ* temperature data was only available for sites in WA Outer Coast, Oregon, and all mainland California regions. WA Outer Coast only had 4 sites with temperature data, which was insufficient for detecting relationships with SSWS appearance. We did not include any model combinations using temperature for the Salish Sea, WA Outer Coast, and CA Channel Islands.

For every combination of variables, we constructed a unique function (the UCH function) to estimate the weekly probability of infection at each site using the WINBUGS approach outlined by (Heisey 2009b). The UCH value for every week was multiplied over the entire observation period to calculate the overall probability of a site becoming infected during this time, the sum of hazards (SH) (Equation 2.2).

We used the R built-in function “optim” to find the parameters for the UCH function that would result in the lowest error between the predicted probability of infection and actual SSWS infection status. We compared the fit of each model to the existing data using residual sum of squares (Equation 2.3) and AIC values (Equation 2.4) (Heisey 2009b). The best fitting model(s) informed us as to which site conditions are important in predicting the time of SSWS appearance and warrant further research in discerning potential causative relationships. To assess the predictive accuracy of each model, we calculated the area under the receiver-operating curve (ROC), a common measure of a model’s specificity vs sensitivity, scaled from 0 to 1. All model evaluations, optimizations, and AIC calculations were performed in R version 3.4.1 (R Core Team 2017). ROC calculations were performed in JMP Pro 13.

Our sea star observations have limitations in their ability to discern the timing of the disease outbreak. We assumed that the first date of SSWS observation was the date that it appeared, and that if it was truly present at the site, it was observed (i.e., no false negatives). SSWS takes 1 to 2 weeks to appear after exposure to infected individuals, and the time to symptom visibility varies with local conditions and age of the sea star (Hewson et al. 2014, Eisenlord et al. 2016, Kohl et al. 2016). It is also possible that the disease developed between the first and second visits to a site. While *in situ* and remote sensing allow near-continuous monitoring of coastal physical conditions, it was not feasible to observe all sites at the 1-week time interval needed to discern the absolute timing of the infection. Despite these limitations, the recent SSWS outbreak was an extremely well-documented marine disease for a

noncommercial species due to rapid communication to a broad network of researchers as well as with the public (Miner et al. 2018). The sea star observations across thousands of kilometers and multiple seasons carry high statistical power that is not normally reached in epidemics of this spatial scale.

Equation 1: Generic Unit Cumulative Hazard Function for a given site *j* at the number of weeks *k* from the observation start time (UCH). *gamma0, alpha,* and *a* represent constants in the model. UCH is constrained to values between 0 and 1. A generic "input variable" is shown. Specific input variables are described in Table 2.3. More variables are added to the UCH function as desired.

$$UCH[j,k] = e^{(sum(b + alpha*k + a* input\_variable1 + \ldots))}$$

Equation 2: Cumulative hazard probability at a given site *j* from observation start time *obs_start* to observation end time *obs_end* (sum of hazards, SH). For observations of SSWS "absent", y = 1 (the sea stars "survived" the observation period). For observations of SSWS "present", y = 0 (the sea stars "die").

$$SH[j] = e^{(-1*(1-product(1-UCH[j,obs\_start[j]:max(1,obs\_end[j]-1)])))}$$

Equation 3: Residual sum of squares (RSS)

$$RSS = sum\ ((1-y[j])-SH[j])^2$$

Equation 4: AIC value

$$AIC = N_{observations} * \log(RSS / N_{observations}) + 2 * N_{parameters}$$

Results

Whole-coast disease patterns indicate association between coastal disturbance and SSWS appearance

At the scale of the North American west coast, duration of daily afternoon low tide exposure and the distance from the nearest infected site (Fig. 2.1, Fig. 2.2) received the strongest support as being associated with risk of SSWS infection (AIC = -545.72, Table 2.5). This model had high predictive accuracy (ROC = 0.88). The second-best model contained time and distance from nearest infected site as the only variables, and it predicted infection outcomes with similar accuracy (ΔAIC = 0.69, ROC = 0.88). Though no single model had clear support, the models with the lowest AIC values (ΔAIC < 2) all contained these two variables (Table 2.5). Risk of infection was negatively associated with distance from the nearest infected site (positively associated with proximity to the nearest infected site) (Fig. 2.1a, 2.2a). Infection risk began to decrease when the nearest site was 25 to 50 km away (Fig. A2.1).

Risk of infection was positively associated with low tide exposure hours (Fig. 2.1b, 2.2b), though this relationship was not as pronounced (Fig. 2.2). While latitude and low tide exposure were often autocorrelated, we did not observe strong correlations with latitude when it was modeled alone or in combination with variables

other than low tide exposure hours (Table 2.5). The null model, which tested the relationship of disease risk and time elapsed since the start of the outbreak and no other variables, was the worst-performing model, and its predictive accuracy was only slightly higher than random (ΔAIC = 74.22, ROC = 0.63). This indicates that adding any of the variables that we examined in this study improved predictions of SSWS infection probability.

Water temperature stress, represented by degree heating weeks, was found in two of the top performing models (ΔAIC = 1.05 and 1.99, ROC = 0.88 and 0.88), though it was always accompanied by distance from nearest infected site or low tide exposure. Thermal stress by itself was not in the 20 best models (ΔAIC = 3.82, ROC = 0.57), and support for the inclusion of DHWs in the SSWS risk model increased when it was combined with additional variables.

Regional level disease patterns indicate association between low tide exposure and distance from nearest infected site and SSWS appearance

Model performance improved slightly when regional coefficients were included (ΔAIC = -4.91 ± 3.00 SD), indicating regional differences in factors associated with SSWS. In the Salish Sea, distance from the nearest infected site was negatively correlated with outbreaks of SSWS. (AIC = -237.44, ROC = 0.88). This region had 7 models that performed similarly (ΔAIC ≤ 2, ROC > 0.84), and all of them contained this term and one of the other variables. Similarly, in the California Channel Islands, the leading model contained time and distance from nearest infected

site (AIC = -81.33, ROC > 0.99). Out of 10 similarly performing models (ΔAIC = 2), 6 had distance from nearest infected site coupled with another variable. Additionally, 5 of the models in this group indicated a negative association with chlorophyll *a* and disease outbreak (Fig. 2.3a) paired with one other variable. In Central California, the best-performing model showed a positive association chlorophyll *a* and distance from the nearest infected site (AIC = -49.55, ROC = 0.91). An additional 5 models in this region received similar support (ΔAIC = 2, ROC > 0.90), all of which contained these two variables. There was a positive relationship between probability of SSWS, chlorophyll *a*, and infection risk in this region (Table 2.5, Fig. 2.3b). The relationship of afternoon low tide exposure and distance from nearest infected site with infection risk followed the same patterns in these regions as they did on the whole-coast scale (Fig. 2.4).

Washington Outer Coast, Oregon, Northern California, and Southern California all had >10 models that offered similar support (ΔAIC ≤ 2, Table 2.5). These models used some combination of all variables (except for temperature in Washington Outer Coast, where temperature was not tested), indicating no strong relationship with any one variable and risk of SSWS infection.

While we only had sufficient temperature data to examine its potential relationship to disease in four of our eight geographic regions, we did not observe strong support for association of SSWS appearance and thermal stress. Risk of infection based on only elapsed weeks since the first appearance (the null model) was never in the 20 best-performing models in any region. It had low support in the Salish

Sea, Oregon, Central California, Southern California, and the Channel Islands (ΔAIC > 5). The time-only model received moderate support in Washington Outer Coast and Northern California (ΔAIC < 5), regions where no variables received strong support. Predictive accuracy was low (ROC < 0.75) in all regions except for Oregon (ROC = 0.85) and Northern California (ROC = 0.82).

Discussion

Negative anomaly in distance from the nearest infected site and positive anomaly in low tide exposure emerged as the variables most commonly associated with risk of SSWS infection at a whole-coast scale and in some regions (Table 2.5). It is possible that patterns in the Salish Sea had a strong influence on the whole-coast model due to the large number of observations in this region relative to other regions as of the coast. However, some regional-level models also identified distance from infected site and low tide exposure as important, indicating that these factors are associated with SSWS both inside and outside of the Salish Sea. The negative relationship with distance from infected sites (positive correlation with proximity) aligns with expectations based on disease ecology. Because SSWS is likely waterborne (Hewson et al. 2014, 2018), proximity to other infected areas increases opportunities for transfer of infectious particles. Proximity to sources of the disease are commonly incorporated in epidemiological models as a proxy for the probability of transmission between individuals or spatially distinct populations, particularly

when transmission does not require direct contact (Anderson and May 1991, Jousimo et al. 2014).

Afternoon low tide emersion can expose animals to strong sunlight and ultraviolet rays during the hottest period of the day, increasing thermal stress independent of water temperature anomalies (Petes et al. 2008). Strong winds during emersion also increase desiccation risk (Monaco et al. 2015). *Pisaster ochraceus* reduce their exposure to high emersion temperatures by hiding in crevices or remaining in tide pools (Fly et al. 2012, Monaco et al. 2015). However, access to thermal refuges depends on site geomorphology and size of refuge areas relative to sea star body size. Sea stars unable to find refuge during stressful air temperatures experience heat shock stress, increased respiration, reduced relative thermal performance, and mortality (Petes et al. 2008, Monaco et al. 2014, 2016), which could weaken their immune response.

Chlorophyll *a* was the only variable to receive strong support on a regional scale that was not supported at the whole-coast scale. It appeared frequently in the strongest models from Central California and the Channel Islands, but the sign of the relationship differed between regions. Bacterial and viral abundance increase with chlorophyll concentrations, increasing load of potential pathogens (Bird and Kalff 1984). Algal blooms, characterized by periods of high chlorophyll concentrations, periodically bathe organisms in toxins for weeks or months at a time (Schulien et al. 2017). Algal bloom-associated neurotoxins, such as saxotoxin and domoic acid, accumulate in the tissues the mussel *Mytilus californianus*, the main prey of *Pisaster*

ochraceus (Ferrer et al. 2015, Ohman et al. 2016, Peacock et al. 2018). Even after a harmful algal bloom ends, some toxins might take several months to clear out of mussel tissues, prolonging effects of a bloom event on sea star food supply (Gibble et al. 2016). Harmful algal blooms on the California coast have been implicated in regional mortalities of both molluscs and echinoderms, though mortality rates vary among species (De Wit et al. 2014, Jurgens et al. 2015). In contrast, periods of anomalously low chlorophyll have also been associated with *Vibrio spp.* outbreaks (Vezzulli et al. 2010).

The lack of clear associations between SSWS infection and external conditions in Washington Outer Coast, Oregon, Northern California, and Southern California suggest that regional triggers for the outbreak are complicated and not easily explained by a few variables. The disjunct nature of SSWS appearance between these regions also supports the notion that regional dynamics mattered to the timing of the outbreak. It is possible that detection of associations would be improved if sample sizes were larger, as the regions with the smallest sample sizes also had no support for a single factor (Table 2.1, 2.5). Alternatively, this pattern aligns with the interpretation of SSWS as a suite of multiple diseases with similar symptoms (Hewson et al. 2018). If this outbreak is truly a product of multiple diseases, then each component pathogen might respond to different environmental factors or be aggravated by stressors unique to the region. This pattern also supports the idea that SSWS might not be pathogen-driven. Instead, region-specific stressors could trigger a common set of symptoms (I. Hewson, *pers. comm.*).

We observed little support for water temperature stress as a contributor to risk of SSWS infection at whole-coast or regional spatial scales. Despite laboratory evidence of temperature's role in speeding up SSWS onset symptom progression (Eisenlord et al. 2016, Kohl et al. 2016), we did not demonstrate a correlation between temperature and appearance of disease in a field setting. This aligns with observations from other regional and large-scale studies of the SSWS outbreak (Menge et al. 2016, Miner et al. 2018). Associations between SSWS emergence and warm water anomalies also vary by species (Hewson et al. 2018). It is still possible that the outbreak followed temperature anomalies on a sub-regional scale or in regions where we did not have temperature data, such as the Salish Sea (Eisenlord et al. 2016). The lack of *in situ* temperature data in some regions of the coast might have influenced our coast-wide assessment of the overall role of water temperature in SSWS outbreaks. Acute pulses of thermal stress rather than chronic thermal stress might be more strongly associated with the onset of disease, but cumulative measures of temperature stress over several months have served as successful predictors for disease outbreaks in other marine invertebrates (Caldwell et al. 2016).

Limitations of SSWS observations

Our estimation of the week of the outbreak depended on the assumption that we could observe the disease very soon after a site became infected. We were unable to use many of the initially reported sea star observations because they did not contain insights as to the timing of infection. Though we had a large number of observations,

we did not have observers at every site every week. We assumed that symptoms were detectable once an SSWS infection established at a site. However, symptoms typically appear one to two weeks after exposure (DelSesto 2015, Kohl et al. 2016), so a site with a subclinical infection at the time of observation could present a false negative. Given the widespread geographic extent of this disease and the speed of its onset in some regions, this outbreak was extremely well-documented (Miner et al. 2018). If we are unable to discern outbreak time with this dataset, then it raises the question of how often such large-scale events can be evaluated. This study provides support for using the observational citizen science and monitoring network approach employed here for future assessments of epizootics.

Our study meets several of the criteria for successful disease surveillance and management (Groner et al. 2016). First, *Pisaster ochraceus* populations of the North American Pacific Coast were regularly monitored for over a decade by the Multi-Agency Rocky Intertidal Network (MARINe, www.pacificrockyintertidal.org) and additional research partners. This provided opportunities for early detection and established baseline sea star population counts for pre- and post-disease comparison (Miner et al. 2018). Monitoring sites were deliberately placed to give sufficient representation of the diverse geography and ecology of the coast's different geographic regions. When the disease was first observed, monitoring protocols were quickly adapted to take data on the disease, and these protocols were disseminated throughout MARINe research groups. Next, the public was also rapidly informed of

how they could contribute to SSWS monitoring. This increased disease observation capacity, resulting in the large dataset utilized in this model (PISCO 2014b).

Other potential factors contributing to SSWS onset

Despite our exploration of many factors commonly associated with marine disease, there are other potential contributory anthropogenic and natural inputs that we did not test. For example, contaminants beyond those produced by algae might be present in sea star food supply, causing physiological stress when consumed (Sindermann 1993). Human-produced organic pollutants such as pesticides and polycholorinated bisphenols also accumulate in prey tissues (Suchanek 1994). These chemicals act as endocrine disruptors in humans, though effects on sea stars are far less explored. Data for these and other contaminants in the food web (Center for Coastal Monitoring and National Ocean Service 2014) were not available at the resolution required for this spatially explicit modeling approach at the time of this study.

Our model did not account for geographic differences in sea star genetics, microbiome composition, or genetic x environment effects. Pre- and post-outbreak frequency differences alleles and haplotypes in North Central California *P. ochraceus* populations raise the possibility that some of these genes played a role in SSWS survival and resistance (Schiebelhut et al. 2018). However, it is unclear how frequencies of potential resistance alleles differ geographically (Pankey and Wares 2009, Wares and Schiebelhut 2015). Microbiomes of both infected and asymptomatic

sea stars are highly variable between individual sea stars or sites within the same region (Gudenkauf and Hewson 2015). Similar variation exists in transcriptional changes during the immune response (Fuess et al. 2015), which might contribute to the chance of individuals surviving long enough to be observed in disease monitoring surveys. More replication of microbiome and transcriptomic responses to SSWS exposure challenges under different conditions is needed to assess patterns across multiple regions.

Additionally, associations between disease presence and candidate SSWS viruses vary by species. The relative populations of the various sea star species with high and low pathogen loads within a site could influence transmission dynamics (Wood and Lafferty 2013). Interspecific infection between sea star species occurs easily, though the relative frequency of transfer between different species and competency of species as reservoirs for the pathogen are still largely unknown (DelSesto 2015). Candidate viruses have been found in asymptomatic stars, suggesting that infections can remain subclinical unless the right conditions inside or outside of the host induce symptoms (Hewson et al. 2014, 2018). Hewson et al. (2018) suggest the disease is caused by multiple pathogens or conditions across its range and across species. The lack of model support for a single or a few explanatory factors in multiple regions aligns with this multi-pathogen explanation.

We caution against the interpretation that any of these relationships imply causality. More experimental and observational data are necessary before it can be determined which natural and anthropogenic factors impact activity of the pathogen.

However, the relationships we have identified can provide a focal point for future SSWS research about specific mechanisms of infection. Understanding which environmental and anthropogenic factors contribute to this disease is critical to predicting future SSWS outbreaks. Predicting and responding to these outbreaks is particularly important for species that have large ecological impact, such as *Pisaster ochraceus* and *Pycnopodia helianthoides*. This version of the Cox Proportional Hazard model could also be adapted to explore other marine diseases on multiple spatial scales.

Disease occurrence is increasing as anthropogenic pressures on the marine environment rise (Harvell et al. 1999). Detecting the spatial and temporal occurrences of outbreaks is critical to understanding the conditions that trigger them. Continued monitoring is necessary to identify conditions conferring refuge or resistance to infection (Friedman et al. 2014) and to detecting population- or ecosystem-level consequences (Blanchette et al. 2005, Miner et al. 2018). This underscores the need for long-term ecological monitoring programs for making large-scale disease studies possible (Groner et al. 2016, Hughes et al. 2017).

Tables

Table 2.1. Description of the geographic regions, their boundaries, and observations within each region.

Region Name	Region Boundaries	N observations
Washington Outer Coast	All outer coast shores of British Columbia, Canada and Washington state, USA	25
Salish Sea	Sound- or strait-enclosed areas between southern British Columbia and northern Washington including the Salish Sea, Strait of Georgia, Strait of Juan de Fuca, and Puget Sound	125
Oregon	All areas of the Oregon coast, between the Washington-Oregon border and the Oregon-California border	27
Northern California	From the Oregon-California border to Point Arena	14
Central California	From Point Arena to Point Conception	26
Southern California	Mainland coast from Point Conception to the US-Mexico border	29
California Channel Islands	Island coasts offshore of Southern California	41
Baja California	From the US-Mexico border to the Baja California-Baja California Sur border	6

Table 2.2a. Population-related variables loading with each principal component, PC eigenvalues, and variance explained. No PCA input variables were non-loading. For details on geospatial processing of inputs, see Table A1.

PC Name	Eigenvalue	Variance explained	Loading variables
Population PC1	2.1349	53.4%	Distance from major shipping lanes Distance from ports Distance from wastewater outfalls Distance from dense human population areas

Table 2.2b. Disturbance- and pollution-related variables loading with each principal component, PC eigenvalues, and variance explained. No PCA input variables were non-loading. For details on geospatial processing of inputs, see Table A1.

PC Name	Eigenvalue	Variance explained	Loading variables
Disturbance PC1	3.9834	56.9%	Mean coastal watershed disturbance index Percent of watershed area developed Percent of watershed area used for pasture Percent of watershed area disturbed Ocean Health Index disturbance and pollution metric
Disturbance PC2	1.4594	20.8%	Percent of watershed area used for agriculture Percent of watershed area used for mineral extraction (oil, gas, or mining)

Table 2.3. Description of individual variables in the model. Details on data inputs, data sources, and geospatial processing of these variables are provided in Table A2.1.

Variable	Type of variable	Description
Time	Epidemiological	Weeks since January 1, 2013 (pre-SSWS starting point)
Population PC1	Anthropogenic	Distance from major population centers and associated point source pollution
Disturbance PC1	Anthropogenic	Disturbance of coastal waters and adjacent coastal watershed
Disturbance PC2	Anthropogenic	Intensive disturbance of coastal watershed
Low tide exposure time	Environmental	Average monthly hours of water levels below 0.0 m MLLW
Degree heating weeks (DHW)	Environmental	Number of weeks in a 12-week window above the 80^{th} percentile daily mean temperature recorded at a site for a given week of the year
Chlorophyll *a* (chl a)	Environmental	Remotely sensed surface chlorophyll (mg/m^3)
Latitude	Epidemiological	Latitude of site
Distance from nearest infected site	Epidemiological	Distance from a site to the nearest site with a "SSWS present" observation one week prior to the date of observation

Table 2.4. Instantaneous hazard probability functions (Unit Cumulative Hazard, UCH) at site *j*, and week of observation *k*. Each function, *f*, was evaluated in the expression $UCH_{j,k} = \exp(f(j,k))$. Individual variables are listed as the terms for time as a linear function (*alpha*k + model term + b*). *b* is a constant included in every model. Latitude and low tide exposure hours covaried and were never included in the same model. All remaining possible combinations of the individual variables were modeled but are not listed for brevity. When regions had insufficient *in situ* temperature data, excluded all model combinations with DHWs, yielding 96 possible combinations for those regions.

Model No.	**Function, *f*, used for UCH expression**
1	Time + b, linear (null model)
2	Time + Population PC_j + b
3	Time + Disturbance $PC1_j$ + b
4	Time + Disturbance $PC2_j$ + b
5	Time + low tide $hours_{j,k}$ + b
6	Time + $DHW_{j,k}$ + b
7	Time + $chla_{j,k}$ + b
8	Time + Latitude of $site_j$ + b
9	Time + Distance from nearest infected $site_{j,k}$ + b
10	Time + Population PC_j + Disturbance $PC1_j$ + Disturbance $PC2_j$ + low tide $hours_{j,k}$ + $DHWs_{j,k}$ + chl $a_{j,k}$ + nearest infected $site_{j,k}$ + b
11	Time + Population PC_j + Disturbance $PC1_j$ + Disturbance $PC2_j$ + $latitude_j$ + $DHWs_{j,k}$ + chl $a_{j,k}$ + nearest infected $site_{j,k}$ + b
12-38	Time + 2-variable combinations + b
39-88	Time + 3-variable combinations + b
89-143	Time + 4-variable combinations + b
144-179	Time + 5-variable combinations + b
180-192	Time + 6-variable combinations + b

Table 2.5. Top three candidate models for each region sorted by AIC values. We include all models with ΔAIC ≤ 2 or the results for the three models with the lowest AIC value if ΔAIC > 2. Parameter values (coefficients) for the terms are included. Parameter values correspond to contribution to the probability of survival (1 - probability of infection) in any given one-week interval.

Terms in UCH function	AIC value	Δ AIC	Relative log likelihood	constant (b)	time coefficient	a1	a2	a3	a4
Whole Coast									
time + b + a1*low tide + a2*distance from infected	-545.72	0.00	1.00	-0.24	-1.41	-0.29	0.49		
time + b + distance from infected	-545.04	0.69	0.71	-0.55	-1.23	0.34			
time + b + a1*low tide + a2*DHWs + a3*distance from infected	-544.67	1.05	0.59	-0.64	-0.48	-0.31	-0.36	0.52	
time + b + a1*DisturbancePC1 + a2*low tide + a3*distance from infected	-543.87	1.85	0.40	-0.22	-1.44	0.03	-0.29	0.51	
time + b + a1*PopulationPC + a2*low tide + a3*distance from infected	-543.80	1.93	0.38	-0.24	-1.40	-0.03	-0.30	0.50	
time + b + a1*DisturbancePC2 + a2*low tide + a3*distance from infected	-543.78	1.94	0.38	-0.18	-1.52	-0.03	-0.30	0.50	
time + b + a1*low tide + a2*chl + a3*distance from infected	-543.76	1.96	0.38	-0.21	-1.48	-0.30	0.04	0.49	
time + b + a1*DHWs + a2*distance from infected	-543.73	1.99	0.37	-0.84	-0.54	-0.30	0.37		
Salish Sea									
time + b + distance from infected	-237.44	0.00	1.00	0.58	-2.91	0.67			
time + b + a1*low tide + a2*distance from infected	-236.16	1.28	0.53	0.73	-2.88	-0.21	0.76		
time + b + a1*DisturbancePC1 + a2*distance from infected	-235.69	1.75	0.42	0.91	-3.38	0.08	0.83		

Table 2.5. continued

time + b + a1*DisturbancePC2 + a2*distance from infected	-235.46	1.98	0.37	0.64	-3.02	-0.04	0.69	
time + b + a1*lat + a2*distance from infected	-235.45	2.00	0.37	0.55	-2.88	0.01	0.65	
time + b + a1*chl + a2*distance from infected	-235.44	2.00	0.37	0.59	-2.95	0.01	0.67	
time + b + a1*PopulationPC + a2*distance from infected	-235.44	2.00	0.37	0.59	-2.92	0.01	0.67	
WA Outer Coast								
time + b + a1*DisturbancePC1 + a2*lat	-29.30	0.00	1.00	3204.2	-3900.0	-2600.9	-1363.8	
time + b + a1*DisturbancePC2 + a2*lat	-29.30	0.00	1.00	3270.7	-3952.1	2842.7	-1410.8	
time + b + a1*low tide + a2*chl	-29.30	0.00	1.00	704.5	-662.59	466.50	335.54	
time + b + a1*PopulationPC + a2*DisturbancePC1 + a3*lat	-27.30	2.00	0.37	9465.2	-7007.6	10074	-39047	-7043.2
time + b + a1*PopulationPC + a2*low tide + a3*chl	-27.30	2.00	0.37	322.5	-423.59	60.87	195.53	167.95
time + b + a1*PopulationPC + a2*low tide + a3*distance from infected	-27.30	2.00	0.37	5077.3	-5943.5	2605.1	5551.00	88.00
time + b + a1*PopulationPC + a2*lat + a3*distance from infected	-27.30	2.00	0.37	22454	-19167	-5657.1	-7251.4	2387.0
time + b + a1*DisturbancePC1 + a2*DisturbancePC2 + a3*low tide	-27.30	2.00	0.37	4180.0	-3116.3	-28463.0	-36496	4549.1
time + b + a1*DisturbancePC1 + a2*DisturbancePC2 + a3*lat	-27.30	2.00	0.37	4268.5	-4921.9	-3437.4	79.78	-1897.95
time + b + a1*DisturbancePC1 + a2*low tide + a3*chl	-27.30	2.00	0.37	1521.6	-2031.9	-216.50	723.33	729.26
time + b + a1*DisturbancePC1 + a2*chl + a3*lat	-27.30	2.00	0.37	4003.3	-4624.1	-3648.4	-83.29	-1793.72
time + b + a1*DisturbancePC1 + a2*lat + a3*distance from infected	-27.30	2.00	0.37	5395.9	-6500.5	-3964.9	-2272.30	34.65

Table 2.5. continued

time + b + a1*DisturbancePC2 + a2*low tide + a3*chl	-27.30	2.00	0.37	4767.2	-3094.6	926.98	3645.28	2206.16	
time + b + a1*DisturbancePC2 + a2*lat + a3*distance from infected	-27.30	2.00	0.37	15754	-18291	13930	-6904.87	114.28	
time + b + a1*low tide + a2*chl + a3*distance from infected	-27.30	2.00	0.37	2910.3	-2922.2	1364.6	890.73	339.37	
time + b + a1*PopulationPC + a2*DisturbancePC2 + a3*lat	-27.30	2.00	0.37	706.52	-824.39	44.77	812.25	-323.97	
Oregon									
time + b + a1*PopulationPC + a2*DisturbancePC1 + a3*distance from infected	-50.79	0.00	1.00	7715.88	-24765	7190.93	11685.76	2627.56	
time + b + a1*PopulationPC + a2*low tide + a3*distance from infected	-50.79	0.00	1.00	-167.31	118.56	183.94	-304.85	243.06	
time + b + a1*low tide + a2*DHWs + a3*distance from infected	-50.79	0.00	1.00	31.28	51.31	-116.87	75.05	109.13	
time + b + a1*PopulationPC + a2*chl	-49.23	1.55	0.46	3858.9	-5308.2	-917.31	2758.3		
time + b + a1*low tide + a2*chl	-49.23	1.55	0.46	243.99	-608.87	-91.77	-53.62		
time + b + a1*PopulationPC + a2*DisturbancePC1 + a3*DisturbancePC2+ a4* low tide	-48.79	2.00	0.37	1754.7	-10289	1853.94	1615.5	2292.6	-1597.8
time + b + a1*PopulationPC + a2*DisturbancePC1 + a3*DisturbancePC2+ a4* distance from infected	-48.79	2.00	0.37	6604.8	-17577	5175.67	9815.1	-2021.2	2245.6
time + b + a1*PopulationPC + a2*DisturbancePC1 + a3*low tide+ a4* distance from infected	-48.79	2.00	0.37	-76.46	-118.58	159.64	138.90	-157.58	92.14
time + b + a1*PopulationPC + a2*DisturbancePC1 + a3*chl+ a4* distance from infected	-48.79	2.00	0.37	3990.8	-9216.7	1694.87	3236.8	387.73	763.04

Table 2.5. continued

time + b + a1*PopulationPC + a2*DisturbancePC1 + a3*lat+ a4* distance from infected	-48.79	2.00	0.37	11276	-27039	11722.8	27875.4	-2595.4	4719.8
time + b + a1*PopulationPC + a2*DisturbancePC2 + a3*low tide+ a4* chl	-48.79	2.00	0.37	2874.4	-9657.9	503.34	-255.41	-1567.4	-101.22
time + b + a1*PopulationPC + a2*DisturbancePC2 + a3*low tide+ a4* distance from infected	-48.79	2.00	0.37	-115.77	-45.31	154.15	-2.19	-156.37	119.90
time + b + a1*PopulationPC + a2*DisturbancePC2 + a3*chl+ a4* distance from infected	-48.79	2.00	0.37	569.84	-5557.9	1279.8	2689.0	463.31	185.98
time + b + a1*PopulationPC + a2*low tide + a3*DHWs+ a4* distance from infected	-48.79	2.00	0.37	-14.51	-80.58	66.80	-202.70	98.30	132.24
time + b + a1*PopulationPC + a2*chl + a3*lat+ a4* distance from infected	-48.79	2.00	0.37	1751.9	-5994.6	847.61	379.22	324.44	294.10
time + b + a1*DisturbancePC1 + a2*low tide + a3*DHWs+ a4* distance from infected	-48.79	2.00	0.37	37.37	-81.73	-164.80	-123.22	41.45	114.53
time + b + a1*DisturbancePC1 + a2*DHWs + a3*chl+ a4* distance from infected	-48.79	2.00	0.37	7014.0	7977.9	14336.8	2061.1	1430.8	5019.1
time + b + a1*DisturbancePC2 + a2*low tide + a3*DHWs+ a4* distance from infected	-48.79	2.00	0.37	-225.29	949.00	-286.84	-672.62	120.35	463.61
time + b + a1*low tide + a2*DHWs + a3*chl+ a4* distance from infected	-48.79	2.00	0.37	62.70	-120.43	-124.25	47.95	-34.21	97.58
CA North									
time + b +pollutantPC1	-22.17	0.00	1.00	772.63	-1205.38	345.34			
time + b +latitude	-20.56	1.61	0.45	0.75	-5.21	-0.58			
time + b + distance from infected	-20.51	1.67	0.43	0.98	-3.01	1.73			
time + b + a1*PopulationPC + a2*DisturbancePC1	-20.17	2.00	0.37	411.92	-2423.01	909.39	2532.31		

Table 2.5. continued

time + b + a1*PopulationPC + a2*low tide	-20.17	2.00	0.37	557.36	-247.46	-168.89	21.10
time + b + a1*PopulationPC + a2*DHWs	-20.17	2.00	0.37	640.29	-186.95	-209.31	-76.48
time + b + a1*PopulationPC + a2*lat	-20.17	2.00	0.37	1003.4	-734.49	-233.15	-60.36
time + b + a1*PopulationPC + a2*distance from infected	-20.17	2.00	0.37	1171.0	-898.46	-284.14	-6.55
time + b + a1*DisturbancePC1 + a2*DisturbancePC2	-20.17	2.00	0.37	3.16	-3359.9	1136.87	4944.37
time + b + a1*DisturbancePC1 + a2*low tide	-20.17	2.00	0.37	1338.38	-1000.92	1227.24	59.63
time + b + a1*DisturbancePC1 + a2*DHWs	-20.17	2.00	0.37	70.70	-27.57	118.43	-48.04
time + b + a1*DisturbancePC1 + a2*chl	-20.17	2.00	0.37	-2.39	-4.93	2.93	-48.06
time + b + a1*DisturbancePC1 + a2*lat	-20.17	2.00	0.37	578.81	-837.03	266.51	-23.57
time + b + a1*DisturbancePC1 + a2*distance from infected	-20.17	2.00	0.37	273.24	-463.01	167.65	-50.53
time + b + a1*DisturbancePC2 + a2*low tide	-20.17	2.00	0.37	-1458.64	-310.71	3353.42	55.51
time + b + a1*DisturbancePC2 + a2*DHWs	-20.17	2.00	0.37	-11325.46	1939.52	22034.18	-809.05
time + b + a1*DisturbancePC2 + a2*lat	-20.17	2.00	0.37	-9604.11	-5336.90	25810.06	-579.69
time + b + a1*DisturbancePC2 + a2*distance from infected	-20.17	2.00	0.37	-4408.81	-1027.27	10154.18	-115.72
time + b + a1*low tide + a2*DHWs	-20.17	2.00	0.37	5861.51	-12856.72	334.75	1504.35
time + b + a1*low tide + a2*chl	-20.17	2.00	0.37	-6.24	-3.34	32.75	-36.62
time + b + a1*low tide + a2*distance from infected	-20.17	2.00	0.37	83.62	172.66	135.59	281.94
time + b + a1*DHWs + a2*chl	-20.17	2.00	0.37	-18.24	27.48	-10.09	-56.88
time + b + a1*DHWs + a2*distance from infected	-20.17	2.00	0.37	-814.60	1997.84	-241.80	189.16
time + b + a1*chl + a2*lat	-20.17	2.00	0.37	-5.40	-6.81	-41.05	-10.12
time + b + a1*chl + a2*distance from infected	-20.17	2.00	0.37	2.43	16.91	-41.97	20.53

Table 2.5. continued

time + b + a1*lat + a2*distance from infected	-20.17	2.00	0.37	1270.24	-1327.24	-135.81	752.59	
CA Central								
time + b + a1*chl + a2*distance from infected	-49.55	0.00	1.00	2458.78	-4146.21	-1221.86	873.25	
time + b + a1*PopulationPC + a2*chl + a3*distance from infected	-47.55	2.00	0.37	3606.62	-4941.49	115.63	-568.30	1258.12
time + b + a1*DisturbancePC1 + a2*chl + a3*distance from infected	-47.55	2.00	0.37	6610.18	-4584.28	-2459.71	-1677.45	1386.02
time + b + a1*DisturbancePC2 + a2*chl + a3*distance from infected	-47.55	2.00	0.37	2778.39	-1590.79	-821.66	-458.22	364.29
time + b + a1*DHWs + a2*chl + a3*distance from infected	-47.55	2.00	0.37	1282.46	-670.05	-790.13	-895.44	1082.33
time + b + a1*chl + a2*lat + a3*distance from infected	-47.55	2.00	0.37	2070.22	-2957.12	-385.73	-62.23	759.76
CA South								
time + b +chl	-51.11	0.00	1.00	-116.82	401.38	93.47		
time + b +PopulationPC1	-50.20	0.91	0.63	-2.16	0.20	-1.12		
time + b +DHW over T80 in 12 weeks	-49.68	1.43	0.49	-2.85	3.03	-0.62		
time + b +latitude	-49.45	1.66	0.44	-0.91	-1.12	-0.12		
time + b + a1*PopulationPC + a2*DHWs	-49.43	1.68	0.43	-10.82	17.75	-1.89	-2.45	
time + b + distance from infected	-49.37	1.73	0.42	-0.86	-1.13	0.07		
time + b + low tide exposure hours	-49.37	1.73	0.42	-0.92	-1.06	-0.08		
time + b + a1*DHWs + a2*lat	-49.25	1.86	0.40	-20.24	41.48	-6.64	-2.38	
time + b + a1*PopulationPC + a2*chl	-49.11	2.00	0.37	-86.62	292.05	0.15	80.15	
time + b + a1*DisturbancePC1 + a2*chl	-49.11	2.00	0.37	-269.40	898.84	3.01	151.90	
time + b + a1*low tide + a2*chl	-49.11	2.00	0.37	107.82	-214.76	108.56	290.47	

Table 2.5. continued

time + b + a1*DHWs + a2*chl	-49.11	2.00	0.37	59.66	121.95	60.86	163.04
time + b + a1*chl + a2*lat	-49.11	2.00	0.37	29.29	317.04	761.69	23.25
CA Channel Islands							
time + b + distance from infected	-81.33	0.00	1.00	314.35	-263.46	197.99	
time + b + a1*PopulationPC + a2*chl	-79.33	2.00	0.37	199.55	-148.54	-87.27	231.73
time + b + a1*PopulationPC + a2*distance from infected	-79.33	2.00	0.37	1411.92	-1326.44	-267.47	777.87
time + b + a1*DisturbancePC1 + a2*chl	-79.33	2.00	0.37	-58.99	68.72	-34.33	150.72
time + b + a1*DisturbancePC1 + a2*distance from infected	-79.33	2.00	0.37	62.78	-36.39	-16.86	100.40
time + b + a1*DisturbancePC2 + a2*chl	-79.33	2.00	0.37	-31.49	9.96	-894.23	175.10
time + b + a1*DisturbancePC2 + a2*distance from infected	-79.33	2.00	0.37	1721.42	6586.35	-4743.83	3894.47
time + b + a1*low tide + a2*distance from infected	-79.33	2.00	0.37	51.06	-3.10	-6.53	54.30
time + b + a1*chl + a2*lat	-79.33	2.00	0.37	117.05	63.28	356.68	152.01
time + b + a1*chl + a2*distance from infected	-79.33	2.00	0.37	99.82	-32.65	24.19	70.96
time + b + a1*lat + a2*distance from infected	-79.33	2.00	0.37	387.87	-211.90	-50.43	247.28

1

Figures

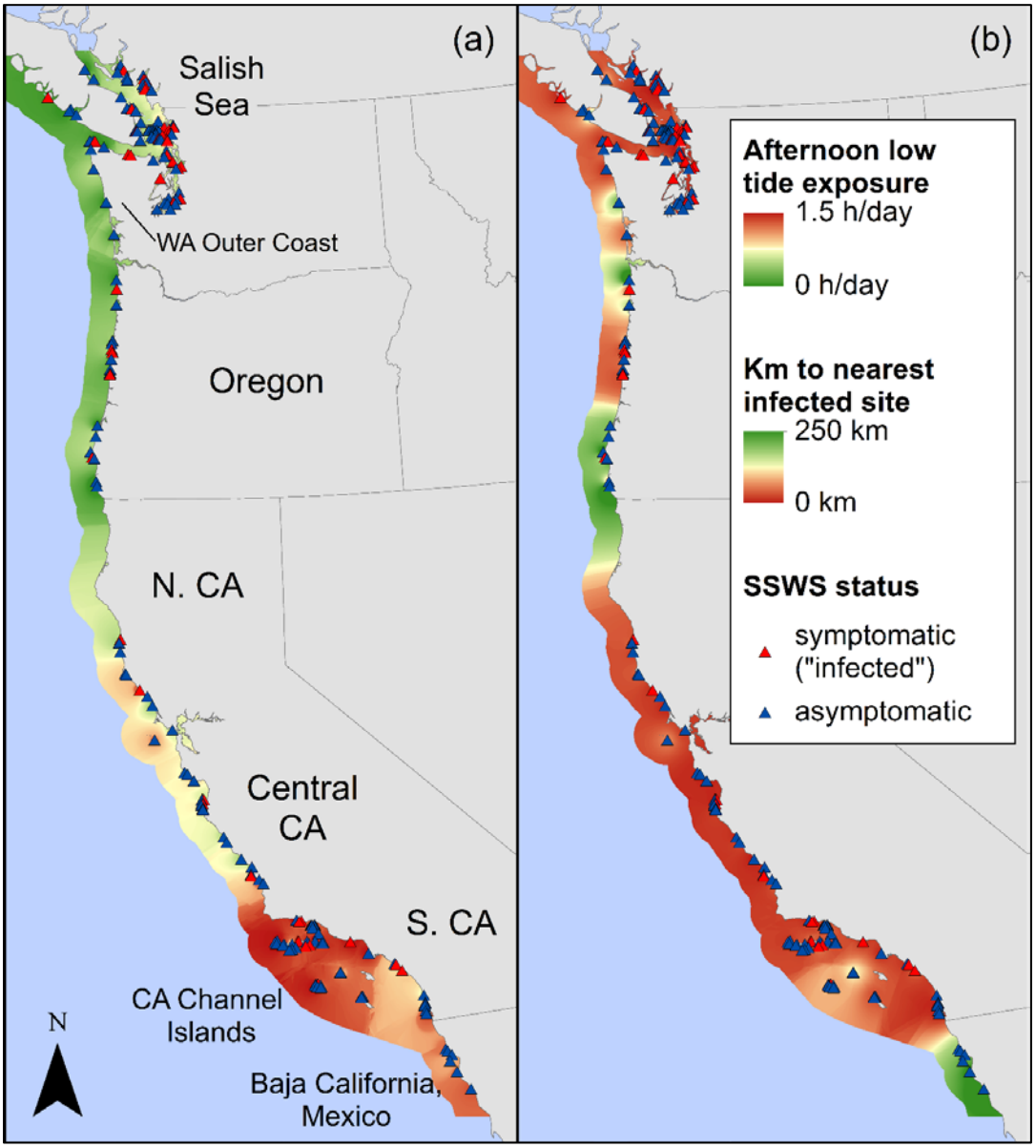

Fig. 2.1. (a) Geographic differences in mean hours of daily afternoon low tide exposure (below 0.0 m MLLW between 1200 and 1600 PST) during week(s) when sites were observed for SSWS status. **(b)** Geographic differences in mean distance (km) by water to the nearest SSWS-infected site during weeks(s) when observed for SSWS status. Each triangle represents one site (n = 284).

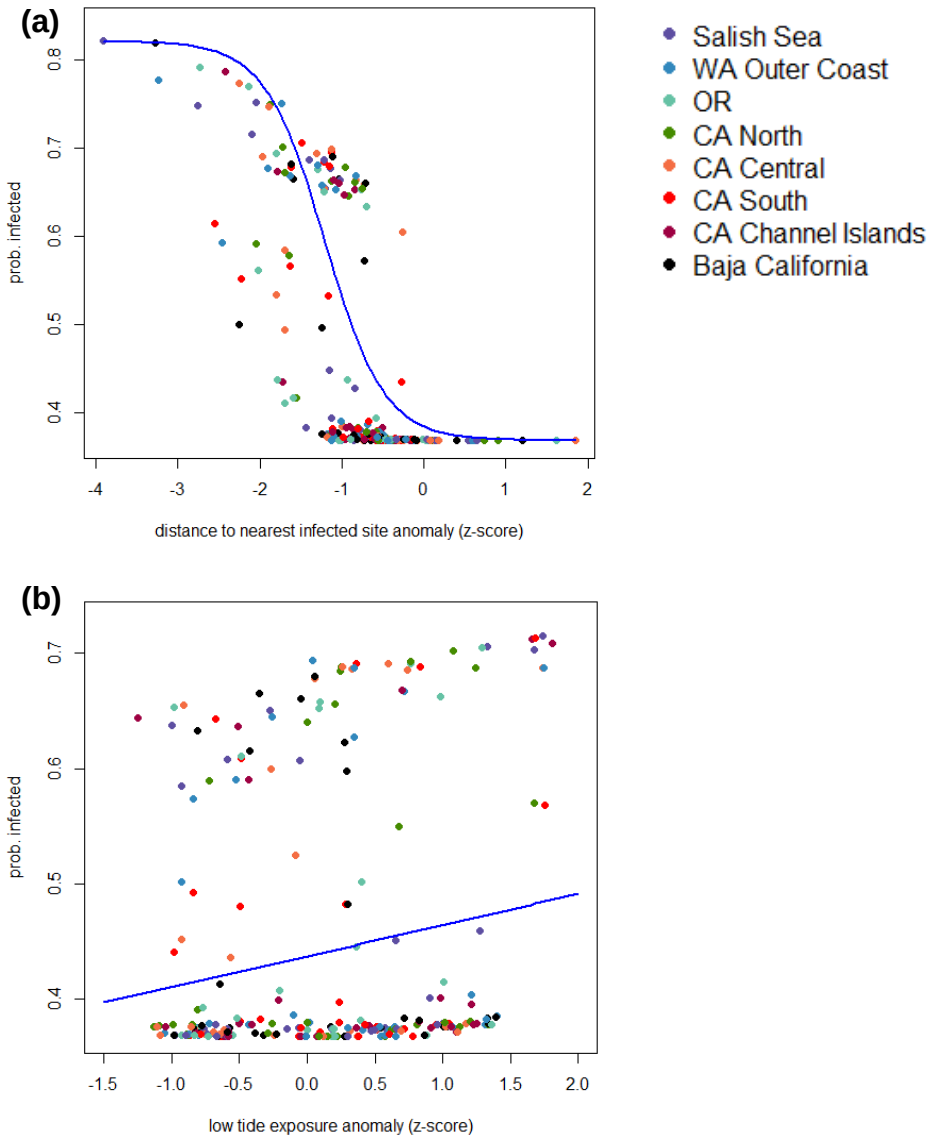

Fig. 2.2. (a) Anomaly (z-score) of distance (km) by water to the nearest SSWS-infected site and predicted probability of SSWS infection during a site's observation period. **(b)** Anomaly hours of daily afternoon low tide exposure (water level below 0.0 m MLLW between 1200 and 1600 Pacific Standard Time) and predicted probability of SSWS infection during a site's observation period. Each point represents one site (n = 284).

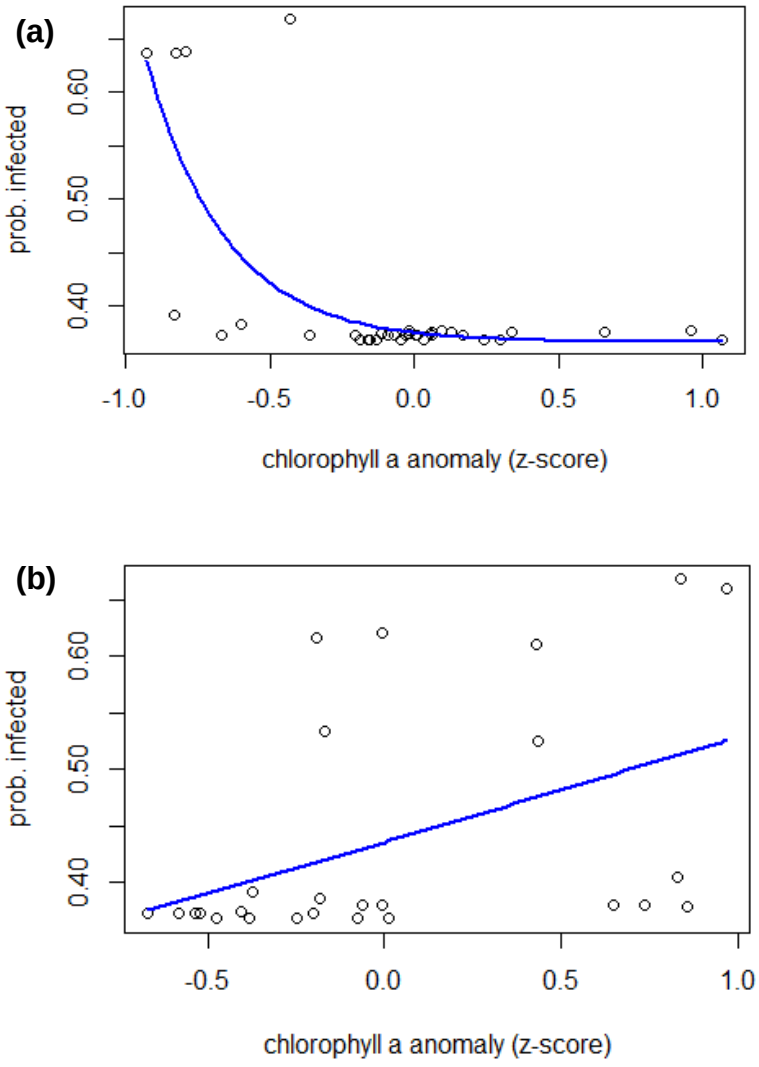

Fig. 2.3. Anomaly (z-score) of chlorophyll *a* and predicted probability of SSWS infection in the **(a)** the California Channel Islands region (n=41) and **(b)** Central California region (n = 26). Each point represents one site.

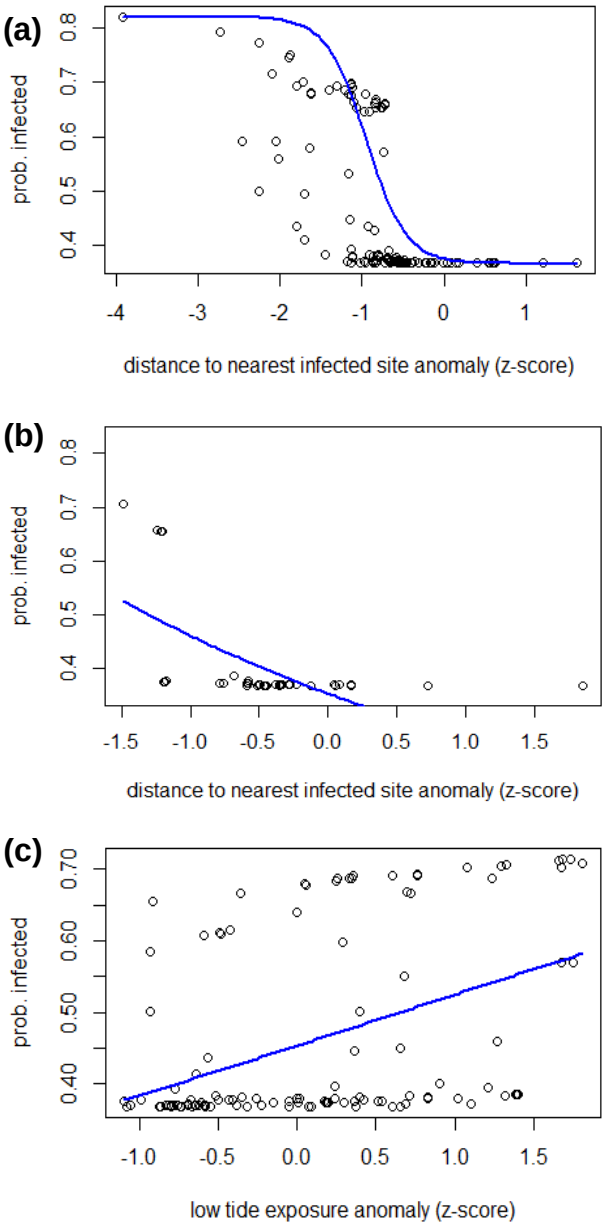

Fig. 2.4. Relationship between probability of infection and anomaly (z-score) in **(a)** distance from the nearest infected site in the Salish Sea (n = 125), **(b)** distance from the nearest infected site in the California Channel Islands (n = 41), and **(c)** low tide exposure hours in the Salish Sea (n = 125).

Chapter 3: Sea Star Wasting Syndrome impacts to intertidal communities via mass mortality of a keystone predator

Abstract

Disease shapes community composition by altering species interactions. In 2013, an outbreak of Sea Star Wasting Syndrome (SSWS) decimated populations of the keystone predator *Pisaster ochraceus* from rocky intertidal habitats on the Pacific coast of North America. Past removals of this sea star species led to expansions of the mussel bed and eventual changes in species composition on the primary substrate. We take advantage of a natural experiment to test whether the absence of keystone predation, and by extension, disease produces changes to the species composition of rocky intertidal communities. Over four years, we measured mussel bed dimensions and *Mytilus californianus* size on vertical rock walls at six rocky intertidal sites on the Central California coast. We assessed whether these changes were correlated with mussel recruitment or sea star predation pressure both pre- and post-SSWS. We also recorded species composition at regular intervals along vertical transects in and below the mussel bed. On a larger spatial scale, we assessed the relationship between mussel cover and pre-disease sea star density across 33 sites in six biogeographic regions of

the Pacific coast using data from long-term monitoring. After four years, the lower boundary of the Central California mussel beds was displaced downward 18.7 cm ± 15.8 (SD) on the rock and 11.7 cm ± 11.0 in elevation, while the upper boundary remained unchanged. Bed area increased 26% ± 17.2, but changes in bed volume varied. Downward movement of the mussel bed and total area of the mussel bed were positively correlated with average mussel recruitment but not with pre-SSWS sea star density or biomass at our six Central California focal sites. Mussel bed volume was negatively correlated with pre-SSWS sea star density but not biomass. Mussel sizes and bed depth remained similar across years, and we did not observe increases in the proportion of *M. californianus* achieving sizes conferring refuge from predation. At a larger spatial scale, changes in mussel cover were positively correlated with pre-SSWS sea star densities. Species composition within the mussel bed differed from outside of the mussel bed, but these two respective communities remained similar across years. In contrast with previous sea star removal studies, we did not observe loss of the community below the bed. Instead, this community became reduced in spatial extent while the mussel bed expanded. The magnitude of mussel bed change observed over four years suggests that on sub-decadal time scales, mussels can increase rapidly with sufficient recruitment. This natural experiment demonstrates that the intertidal community is robust to short-term changes following loss of a strongly interacting species. These results improve our ability to predict potential

changes to intertidal mussel beds in future disease outbreaks affecting keystone predators.

Introduction

Disease has the ability to restructure communities by drastically reducing populations of ecologically important species (Hughes et al. 2002, Miner et al. 2006, Smith et al. 2009). While declines of hosts themselves alter local biodiversity, modifications of species interactions have indirect and cascading effects on community composition (Wootton 1994, Menge 1995). Trophic relationships generate a plethora of indirect effects ranging from single-species behavioral modifications to multi-species trophic cascades that dramatically alter species' relative abundances and habitat structure (Paine 1966, Duggins 1980, Estes et al. 1998, Columbia et al. 2003). Disease's impact on both direct and indirect species interactions can be particularly profound when affecting keystone species, in which a species' influence on community composition is disproportionately greater than its abundance (Paine 1966, 1969b). Even if a keystone predator recovers to their pre-disease size and abundances, the community might not return to its previous state, particularly if prey body size or biomass grows beyond the predator's capacity to regulate it through consumption (Paine 1976, Hughes 1994, Ling et al. 2009). In this way, disease outbreaks can cause long-term changes in species assemblages

continuing after epidemics pass.

A combination of physical and biological factors including disturbance, competition, and predation determine community composition in rocky intertidal habitats (Paine 1966, Connell 1972a, 1978, Menge 2000). Here, tolerable physical conditions occur in a narrow band stretching vertically from completely submerged to completely dry substrate. Species interactions such as predation and competition then modify these vertical distributions (Connell 1972a). The ochre sea star, *Pisaster ochraceus,* acts as keystone predator of rocky intertidal ecosystems. They prey preferentially upon the competitively dominant California mussel *Mytilus californianus* (Landenberger 1968). By preventing competitive exclusion of many species, these sea stars maintain higher species diversity on the primary rock substrate where they are present than where they are absent (Paine 1966, 1974b). Prolonged lack of predation might lead to dominance of mussels, as these molluscs crowd out other organisms for limited space on the rocks of the mid-intertidal and low intertidal zones (Paine 1974, 1976). Many species that would not colonize bare rock can survive in the sheltered interstitial spaces of the mussel bed, giving rise to a different community of infaunal organisms as opposed to species that attach to the primary substrate (Suchanek 1986, Lohse 1993a, Lafferty and Suchanek 2016).

Multiple mechanisms regulate the position of the mussel bed and its area. Lateral mussel movement from the edges of the mussel bed can encroach on empty

space for distances under 4 cm per year. Predation pressure limits the survival of individuals smaller than refuge size below the lower tidal range limit (Paine 1976). Because *P. ochraceus* tend to venture out of the low intertidal only as far as necessary to obtain suitable prey, this creates a front of mussels at the leading edge of their tidal range that is controlled by predation pressure and seasonal desiccation risk (Paine 1976, Robles et al. 2009, Garza and Robles 2010). Movement of individual mussels much beyond this front dramatically increases risk of predation (Robles et al. 2010). A combination of encroachment (Fig. 3.1a) and recruitment (Fig. 3.1b) is required for mussels to colonize large areas of open space (Paine and Levin 1981). Without strong mussel recruitment, few new mussels settle in and along the bed, producing little change in lower limits even in the absence of keystone predators (Dayton 1971, Menge et al. 1994, Connolly and Roughgarden 1998, Hart 2010).

In fall and winter 2013, the Sea Star Wasting Syndrome (SSWS) epidemic caused mass mortalities of sea stars on the North American Pacific coast. The Central California coast was one of the first regions to experience the epidemic and one of the regions with > 95% mortality of *P. ochraceus* and other sea star species (Miner et al. 2018). Though some *P. ochraceus* populations are approaching recovery in abundance, the size structure of these post-disease populations is skewed toward smaller individuals, and biomass remains approximately < 50% of the pre-SSWS average in most regions of the coast (Moritsch and Raimondi 2018). While an influx

of *P. ochraceus* recruits arrived in the region in the years following the outbreak, juvenile and small adult sea stars prefer smaller *M. californianus* and consume less meat per feeding attempt, so predation pressure on mussels remains reduced (Feder 1956, Menge and Menge 1974, McClintock and Robnett 1986).

The SSWS outbreak provides a natural test of the generality of the paradigm that keystone predation controls species composition in rocky intertidal habitats. Furthermore, tracking what changes occur after this mass mortality improves our understanding how disease shapes communities. To determine how the absence of keystone predation by *Pisaster ochraceus* impacts rocky intertidal communities, we tracked spatial boundaries of the mussel bed, mussel sizes, and community composition for several years following the SSWS outbreak. Here we determine whether the severe decline of the keystone predator *Pisaster ochraceus* changed mussel cover and rocky intertidal community composition in the years immediately after the SSWS mass mortality by asking:

1. Does *Mytilus californianus* expand its spatial coverage and occupy lower tidal elevations?
2. Do these changes in mussel beds correlate with *M. californianus* recruitment or changes in *P. ochraceus* predation pressure?
3. Do *M. californianus* grow larger or mussel beds become deeper in the absence of *P. ochraceus*?

4. Does community composition of algae and sessile invertebrates on the primary substrate change as a result of mussel bed expansion?

Methods

Site characteristics

We selected six intertidal sites in Central California, USA (Fig. 3.2a; three in Monterey County and three in Santa Cruz County) based on previous monitoring of mussel presence and sea star populations from surveys by the Partnership for Interdisciplinary Studies for Coastal Oceans (PISCO). Because there is considerable variation in the sea star populations that existed among sites prior to the SSWS outbreak, the selected sites represent a gradient of sea star loss. At each site we selected 10 m horizontal spans of vertical rock wall with continuous mussel beds extending partially down the rock face, allowing room for potential downward expansion. Heights of rock walls between sites ranged from 1.5 m to 3.0 m. For the purposes of tracking clear limits of the mussel beds, we avoided selecting areas of excessively patchy mussels. We secured bolts in the rock to mark the locations of monitoring transects.

Pre- and post-SSWS sea star density and biomass

Using a timed search, we counted sea stars in the spring of every year from

2014 to 2017. Two researchers spent 15 minutes visually searching the 10 m span of rock wall, recording the species, health category according to a standardized symptoms severity scale (Bates et al. 2009, PISCO 2014a), and length (mm) of longest arm from the center of the oral disc to the arm tip for each *P. ochraceus* found. Although we checked crevices in the rock and interstitial spaces of the mussel bed with a flashlight, searching deep within the mussel bed was impossible without destructive sampling. Visual searches could detect individuals < 1 year old, but not recently settled individuals. We used the average height of the rock wall and the 10 m horizontal length to determine the area covered in the search and calculate sea star density. Because biomass is a proxy for predation pressure, we converted *P. ochraceus* size to estimated biomass using a log-log relationship between arm length and wet weight (Equation 3.1).

We calculated the proportion of *P. ochraceus* density and biomass ($g\text{-}m^{-2}$) at our sites compared to pre-SSWS measurements at the same site (post-SSWS level / pre-SSWS level). We used PISCO data from the most recent year before the outbreak for Davenport, Terrace, Hopkins, and Asilomar. Where PISCO data were not available (Waddell and Soberanes), we use *P. ochraceus* survey data from Hart (2010). Asilomar had pre-SSWS sea star density data but no size data, preventing estimation of biomass change (known to be non-zero) since the SSWS outbreak. However, this site had no sea stars in timed searches in 2014, 2016, and 2017, so

biomass was 0 g-m^{-2}.

Mussel recruitment

To measure *M. californianus* recruitment at each site, we deployed 4 plastic Tuffy® S.O.S. Dishwashing Pads (The Clorox Company) within the 10 m span of rock wall at each site. Tuffys were secured to the rock just below the mussel bed lower limit with a blue wall anchor, a lag bolt, and a washer. We replaced Tuffys every two months from June 2014 to June 2016. Mussels recruit to Tuffys because the mesh scrub pad structure mimics their preferred settlement substrate: a filamentous matrix of byssal threads or algal tissue (Dayton 1971, Broitman et al. 2008, Menge et al. 2009, Conway-Cranos 2010). While Tuffys do not provide an absolute measure of recruitment, they can compare relative recruitment between sites. Collected Tuffys were frozen at -80 ºC until processing. To count mussel recruits, we cut open each Tuffy and rinsed it under running water, 3 times per side, into a 250 µ sieve. Sieve contents were stored in 95% ethanol until sorting, where we separated recruits from sediment and other debris under a dissecting microscope. We counted all *Mytilus spp.* recruits < 2 mm in length from each Tuffy. *Mytilus spp.* are cryptic at this size, and species identification requires genetic testing. Previous genetic analyses of *Mytilus spp*. found in Tuffys indicated that 88 to 100% are *M. californianus,* while a mix of *M. edulis, M. trossulus,* and *M. galoprovincialis* make up the remaining

recruits in this genus (Hart 2010). We multiplied the total number of *Mytilus spp.* per Tuffy by the site-specific percentage of *M. californianus*. For sites where we did not have genetic data (Davenport, Hopkins, Asilomar), we used the nearest site with genetic data as a proxy. The number of *M. californianus* recruits per Tuffy was divided by the number of days of intertidal deployment and multiplied by 30 to calculate recruits per month.

For each site, we calculated the mean of monthly recruitment from June 2014 to March 2015 and June 2015 to March 2016. We excluded samples from < 3 months prior to sampling because recruits present during this time did not meet the 20 mm length threshold required for them to show up in mussel size surveys and would not yet be contributing to the dimensions of the mussel bed (Coe and Fox 1942).

Tracking mussel bed limits and area

We predicted that the mussel bed lower limit would move downward in the absence of predation by *P. ochraceus.* Because the SSWS epidemic began impacting Monterey Bay in fall 2013, we did not expect major changes in the mussel bed by spring of 2014. We set 2014 as our baseline year against which we compared mussel bed characteristics for all subsequent years (2015 through 2017). For every transect, we calculated the movement of the lower limit on the rock from its position in the baseline year. We also calculated movement of the upper limit from its baseline

position to identify whether the mussel bed was expanding, contracting, or merely shifting its vertical position. We used point-intercept transects to measure the distance (cm) along the rock surface from the top of the platform to the upper and lower limit of the mussel bed (*Mytilus spp.*). Transects were spaced every 0.25 m along a 10 m stretch of vertical rock wall (N = 41). *Mytilus californianus* presence or absence was recorded for every point along the transect. Points were spaced vertically 1 cm apart. We repeated mussel limit measurements and recorded mussel presence/absence every spring for four consecutive years.

Mussel beds were defined as the contiguous band of mussels that connected across ≥ 75% of the 10 m horizontal span of rock wall or touched the mussel bed at the top of the wall (Fig. 3.3a). Mussel patches were defined as clumps of mussels not in contact with any mussels in the bed (Fig. 3.3b). Patches did not contribute to overall area of the mussel bed. We estimated the area of the bed by multiplying the vertical span of the bed (meters between the upper and lower limit) on each transect by 0.25 m (the space between vertical transects) and summing the area represented by all transects at a site. We assumed that mussel cover on the transect was representative mussel cover in the 0.25m vertical swath on which it was centered.

We also calculated change in tidal elevation of the upper and lower limits of each transect to account for how the mussel bed had changed relative to water level. We measured the tidal elevations of the top and bottom of each vertical transect using

a GPS (Trimble Navigation Limited) and TerraSync version 3.21 (2008). Waddell, Davenport, and Terrace had truly vertical walls, so changes in vertical distance on the rock were very similar to changes in vertical position. Rock walls at Hopkins, Asilomar, and Soberanes had a slight angle, such that distance on the rock surface did not directly align with changes in tidal elevation. Fine-scale GPS coordinates allowed estimation of the slope of these walls and determination of vertical position for every point on the rock surface. To calculate the tidal elevations of lower limits, we subtracted the distance to the transect start from these elevation measurements (Equation 3.2).

To compare mussel bed lower boundaries at each site and year, we used a 1-sided t-test to determine whether the lower limit had moved downward significantly from the 2014 baseline position (displacement on the rock) or in tidal elevation. We used a 1-tailed t-test because we were specifically testing the hypothesis of whether mussels had moved downward, rather than moving in either direction. To determine whether tidal elevations of the upper limit had moved significantly in position or elevation, we used a 2-sided t-test, because we did not have any prior hypotheses about which direction the mussel bed's upper limit would move. A single value from each transect served as one replicate (N = 41 per site). Distance and elevation changes were square root-transformed to meet the underlying assumptions of normality.

We used multiple regression to determine whether yearly mean changes in (1) the lower limit position on the rock, (2) elevation, (3) bed area, or (4) bed volume were correlated with recruitment or raw pre-SSWS *P. ochraceus* density or biomass for the site. We included year (ordinal), mean recruitment, recruitment x year, and pre-SSWS *P. ochraceus* density in the model (N = 12). Separately, we used an alternative model that included year, mean recruitment, recruitment x year, and pre-SSWS *P. ochraceus* biomass (N = 10). All terms in the regression were fixed effects. Nonsignificant terms interaction terms were dropped from the regression. Recruitment means were natural log-transformed to meet assumptions of normality. Due to the time periods of Tuffy deployment, we limited data in the regression to 2015 and 2016 only.

Tracking mussel sizes, mussel bed depth, and mussel bed volume

To determine whether mussels were larger in the near-absence of sea star predation, we measured the girth of mussels at various tidal elevations along 11 vertical transects spaced 1 m apart along the same 10 m spans of vertical rock wall described above. We also measured depth of the mussel bed to determine if total volume of the mussel bed increased at the site. For girth measurements, we used calipers to measure the widest point of the mussel across the dorsoventral axis of the valves to the nearest millimeter. Mussels were not removed from the substrate during

measurement. For depth measurements, we inserted the depth probe on calipers into the mussel bed perpendicular to the rock face until it could go no further (MARINe 2008).

Within 25 cm of the bed's lower limit, we measured mussel girth and bed depth every 3 cm along each vertical transect. We expected that the most changes in mussel sizes would occur close to the lower limit of the bed, so we sampled more intensively in this area to be sure we could detect changes in mussel size or depth if they occurred. Outside of the zone within 25 cm of the lower limit, we did not sample as intensively. We measured girth and depth every 5 cm along each transect (Fig. 3.4). When patches of gooseneck barnacles, *Pollicipes polyermus,* were present in the mussel bed, we measured depth but not girth, resulting in more depth than girth measurements. Mussel beds typically spanned at least 25 cm vertically but were sometimes interrupted by irregular gaps, resulting in an uneven number of measurements on each transect. We recorded the position of each girth and depth measurement along the transect to assign tidal elevations to each size measurement. We repeated these measurements every spring from 2014 to 2017. We categorized each measurement according to whether it fell in the existing 2014 mussel bed or in the zone of subsequent mussel bed expansion (hereafter: "expansion zone", Fig. 3.5a,b). Mussels in patches that were disconnected from the bed (Fig. 3.3b) were excluded from size analyses. We calculated the overall volume (cm^3) of the mussel

bed in our survey area by multiplying the average depth of the bed by the area.

We converted girth measurements to length (mm) to determine the percentage of mussels at each site that were large enough (> 80 mm) to escape predation by *P. ochraceus* (Paine 1976), using a log-log length-girth relationship. The mussel girth corresponding to refuge size was 35 mm (Equation 3.3).

We used a mixed effects model to determine whether mussel girth and bed depth increased over time. We accounted for the influence of tidal elevation on mussel size by including elevation as an effect in the model. We also accounted for effects of site (categorical random effect), transect (random fixed effect), year (ordinal fixed effect), elevation (continuous fixed effect), site x year, elevation x year, and site x year x elevation. We used a separate model for mussels in the original bed and the expansion zone to assess differences in the dynamics of these two zones.

Tracking species composition of the rock surface community

To determine if species composition of vertical rock walls changed in the years since the SSWS outbreak, we used the same 11 vertical transects to record all layers (maximum 5 layers) of sessile invertebrate and algae on the primary substrate or growing as epibionts on species occupying the primary substrate. Sampling of the interstitial spaces of the mussel bed was not possible without destructive sampling, so interstitial species were excluded from this study. Nondestructive sampling, which

leaves the mussel bed intact, is a standard procedure for assessing community composition of the mussel bed (Hart 2010). Dead sessile invertebrates (mainly mussels and barnacles) were counted separately from their live counterparts because of reduced species interactions with these skeletons (e.g., they remain as a form of substrate but do not consume biotic resources). Species were identified to the lowest taxonomic level possible in the field. For coralline algae, we separated articulated and crustose forms because they promote recruitment of different algae and invertebrate species (Reed and Foster 1984). We separated the sporophyte form of *Mastocarpus spp.* from its alternative fleshy form due to the difficulty of identifying that life stage to species.

Within 25 cm above and below the mussel bed lower limit, we recorded species composition at every 1 cm. Outside of this zone, we recorded species composition every 5 cm (Fig. 3.5). Again, we sampled more intensively close to the lower edge of the mussel bed to adequately capture changes. Due to the varying heights of each transect and their individual lower limits, the number of points recorded at each site varied, but we recorded a minimum of 500 points at each site, such that one point contributed no more than 0.5 percent to overall species composition. Species composition surveys were conducted in spring 2014 and spring 2017 on the same dates as sea star surveys. Because of the short time elapsed since the start of the SSWS outbreak, we considered 2014 surveys representative of the pre-

SSWS state.

We assigned each point on the transect to an elevational zone to account for the potential influence of tidal elevation on species composition. Points within the mussel bed were categorized as “bed” or “expansion” zone as described above (Fig. 3.5). If the mussel bed contracted on a given transect between 2014 and 2017, the points between the current lower limit and the original lower limit were categorized as falling in the “contraction” zone. Points outside of the bed up to 25 cm below the lower limit of the bed for that year (or if the bed contracted, the original lower limit) fell in “zone 2”, and all points below zone 2 were considered part of “zone 3” (Fig. 3.5b,c). We pooled all sites and transects to estimate species richness by zone.

At the start of the monitoring period (spring 2014), we expected zone 2 and zone 3 to be statistically distinct communities due to the restricted elevation range of many intertidal species. As the mussel bed expanded into lower elevations, we expected new mussel infill would extirpate the original zone 2 community, and for the species composition immediately below the mussel bed to increasingly resemble the composition of zone 3 of 2014, to the point where they would become statistically indistinguishable.

We used a one-way Analysis of Similarity (ANOSIM) to assess whether there were significant differences in community composition between zone-year combinations. This was done because not all zones occurred in all years thus leaving

a two-factor model with missing combinations. For example, no expansion zone existed in 2014 by definition. Data from every transect counted as a sample for every zone, within a site-year combination. We initially used all species including *M. californianus*. We used untransformed data for all tests to reflect the actual communities under assessment. We used a Bray-Curtis similarity index to estimate relative distances between each replicate and used a cluster analysis to determine the distances between the centroids of each year-zone group.

We repeated the ANOSIM and cluster analysis excluding *M. californianus* from community composition to assess whether *M. californianus* alone drove differences between the zones and years or if other species proportions also contributed. We standardized all species proportions to total observations without *M. californianus.* This required removal of all replicates where *M. californianus* was the only species observed (N = 23). We performed a one-way pair-wise SIMPER (N = 405) on treatments that were truly significantly different to determine which species were most contributing to the differences in community composition. All species composition comparisons were performed in PRIMER 6.1.12 (PRIMER-E Ltd.).

Trends in sea star densities and mussel cover at larger spatial scales

Because our in-depth surveys were limited to a single region of the coast, we examined trends in sea star densities and mussel cover at a larger spatial scale with

PISCO's long-term intertidal monitoring data. We estimated mussel percent cover and *P. ochraceus* densities at 33 sites (Fig. 3.2b,c, Table A3.1) ranging from Southern California (33.545 ^{o}N) to Oregon (45.918 ^{o}N) and one site in British Columbia (51.905 ^{o}N). All sites had at least one pre-SSWS (before 2013) and one post-SSWS (2014 and later) survey date for both sea stars and mussels. We did not use surveys from 2013 due to the uneven timing of SSWS appearance along the Pacific coast. At each site, mussel presence or absence was recorded along 11 point-intercept transects spaced 3 m apart on sloping rock benches. Transects ran from a permanent high zone baseline down toward the water as far as the low tide would allow. Distance between points was roughly equivalent to 1/100th of the site's tidal range. Along the same transects, a thorough search for *P. ochraceus* was performed within 1 m of either side of the transect tape. Flashlights allowed inspection of crevices and rock overhangs. Density was based on the number of *P. ochraceus* found and the total area searched per site (MARINe 2008). We calculated the average *P. ochraceus* density and mussel percent cover for pre-SSWS and post-SSWS surveys separately and estimated the change in mussel cover. While biomass is a better proxy for predation pressure than density (**Chapter 1**, Moritsch and Raimondi 2018), these surveys did not record sea star size, preventing estimation of biomass.

We use regression modeling to evaluate the relationship between change in pre- and post-SSWS mussel cover and pre-SSWS sea star density from PISCO

surveys (N = 33). We selected the best-fitting relationship using the corrected Akaike Information Criterion (AICc) values. All statistical models were performed in JMP Pro 13.

Equation 3.1: Estimation of sea star biomass (Moritsch and Raimondi 2018)

$$\ln(\text{biomass g}) = 2.34723 \times \ln(\text{radius mm}) - 5.50262$$

Equation 3.2: Calculation of lower limit elevation

$$\text{lower limit elevation} = \text{transect start elevation} - \text{vertical distance to lower limit}$$

Equation 3.3: Calculation of mussel length (G. Contolini, *unpublished data*)

$$\ln(\text{girth mm}) = 0.881 \times \ln(\text{length mm}) - 0.3015$$

Results

Lower limits moved downward over time

Lower limits of the mussel bed progressed significantly downward on the rock surface at one of six sites in 2015, three sites in 2016, and four sites in 2017 (Fig. 3.6a; $p < 0.02$ for each site-year combination, square root transformation). Similarly, bed moved significantly lower in elevation at one site in 2015, two sites in 2016, and three sites in 2017 (Fig. 3.6b; $p < 0.03$ for each site-year combination, square root transformation). By 2017, mussels moved an average of 18.7 cm ± 15.8 (SD) downward on the rock surface and 11.7 cm ± 11.0 (SD) in tidal elevation. Terrace had

significant downward movement on the rock and in elevation in 2015 and 2016. The lower limit at Terrace had moved down in 2017, but due to larger variance, it was not significantly different from its initial position in 2017. Three of our six sites experienced upward movement of the mussel bed in 2015 followed by downward movement in subsequent years (Fig. 3.6).

We saw no consistent pattern in the movement of the mussel bed upper limit. The upper limit moved upward on the rock surface and in elevation at one site in 2015, downward at two sites in 2016, and downward at one site in 2017 ($p < 0.03$ for each site-year combination, square root transformation). Distances moved were far smaller than those of the lower limit. On average, upper limit movement was near zero: 0.1 cm ± 3.8 (SD) downward on the rock and 0.2 cm ± 3.4 (SD) upward in elevation by 2017. The upper limit was often aligned with the top of the rock wall where no upward movement was possible.

Over the four-year study period, area of the mussel bed increased by an average of 26.1% ± 17.2 (SD) across all sites (Fig. A3.2a). Changes in total volume of the mussel bed was more variable (Fig. A3.2b). Overall, volume increased by 28.1% ± 34.7 (SD). Volume of mussel beds at Waddell and Terrace shrank by 0.8% and 5.5%, respectively, while the other sites increased volume by up to 76%.

Recruitment, not predation pressure, associated with mussel bed expansion

Downward movement of lower limit position on the rock surface was correlated with recruitment of juvenile mussels ($p = 0.0486$, $r^2 = 0.394$) (Fig. 3.7a). We observed a nonsignificant negative trend in change in tidal elevation as recruitment increased ($p = 0.0893$, $r^2 = 0.249$) (Fig. 3.7b). Changes in mussel bed area were positively correlated with recruitment ($p = 0.0019$, $r^2 = 0.545$) (Fig. 3.7c), but changes in bed volume showed no directional trend ($p = 0.7323$, $r^2 = 0.024$) (Fig. 3.7d). density and biomass gradually increased in the Santa Cruz County sites over the study period but remained at or near zero at the Monterey County sites. While the proportion of pre-SSWS sea star density present varied considerably among sites and years, sea star biomass remained < 5% of pre-SSWS biomass, with the exception of Waddell in 2017, which had 10% of its pre-SSWS biomass (Fig. A3.3).

After accounting for recruitment in 2015 and 2016, we did not observe a correlation between raw pre-SSWS P. ochraceus densities and change in the mussel bed lower limit position (Fig. A3.4a; p = 0.7303, r2 = 0.001), change in lower limit elevation (Fig. A3.4b; p = 0.9589, r2 = 0.001), or mussel bed area (Fig. A3.4c; p = 0.6957, r2 < 0.001). We observed a negative correlation between pre-SSWS *P. ochraceus* densities and mussel bed volume (Fig. A3.4d; p = 0.0057, r2 = 0.418). We saw no correlation between raw pre-SSWS P. ochraceus biomass and change in lower limit position (Fig. A3.4e; p = 0.6897, r2 = 0.066), change in lower limit elevation

(Fig. A3.4f; p = 0.7477, r2 = 0.003), bed area (Fig. A3.4g; p = 0.7630, r2 = 0.061), or bed volume (Fig. A3.4h; p = 0.1117, r2 = 0.284).

Mussel sizes and bed depths remained similar

Within the original bed, mussel size decreased with increasing tidal elevation (Fig. A3.5a). Similarly, bed depth decreased with increasing tidal elevation (Table 3.1). In contrast, in the expansion zone, there were no consistent patterns between tidal elevation and girth or depth (Fig. A3.5b, Table 3.1). Elevation had no significant relationship with mussel size or bed depth in the expansion zone (Table 3.1). There were significant interactions between site, year, and elevation in both the bed and expansion zone (Table 3.1).

Across all sites, mean mussel sizes and bed depths did not change significantly over all four survey years (Fig. 3.8). In the original bed area, average mussel girth was 20.7 mm ± 5.0 (SD) in 2014 and 19.4 mm ± 1.6 (SD) in 2017. Average depth in the original bed was 45.1 mm ± 9.8 (SD) in 2014 and 40.8 mm ± 10.5 (SD) in 2017. Size and depth were similar in the expansion zone as well. Average girth in the expansion zone was 19.6 mm ± 1.9 (SD) and 21.5 mm ± 1.9 (SD) in 2017. Average depth in the expansion zone was 43.2 mm ± 12.6 (SD) in 2014 and 39.9 mm ± 9.4 (SD) in 2017. Size distribution of mussels in the expansion zone did not differ from those of the original bed (Fig. 3.9). The mean number of mussels

at refuge size did not increase at any site. However, mussels at refuge size decreased from 22.9% in 2014 to 1.3% in 2015 in the original bed at Waddell. In all other sites and years, > 2% of mussels were at refuge size in the original mussel bed, and > 3% of mussels were at refuge size in the expansion zone.

Species composition tracked mussel bed boundaries

We observed significant differences in species composition between zone-year combinations (ANOSIM, $p = 0.001$). When mussels were removed from species totals, clusters of groups were nearly identical to when mussels were included (Fig. A3.6; ANOSIM, $p = 0.001$). The original mussel bed zone in 2017 was most similar to the bed area in 2014, and the number of species remained roughly the same: 27 in 2014 to 25 in 2017 (Table A3.2). The composition of the 2017 expansion zone, which had 23 species, was more similar to the bed zone from either year than to other zones (Fig. 3.10a,b). Zones 2 and 3 within the same year were more similar to each other than to zone 2 or 3 from different years. The 2017 contraction zone, which had 17 species, was more similar to zones outside the bed than in the bed, though it acted as an outgroup to zones 2 and 3 (Fig 3-10a). Species richness in zones 2 and 3 combined was similar in both years: 40 in 2014 and 39 in 2017 (Table A3.2).

Considering only the data set from which cover of mussels had been removed, clustering indicated that all zone-year combinations within the main mussel area (bed,

expansion zone) formed one group, while zone-year combinations outside of it formed a separate group (contraction zone, zone 2, zone 3). Ten species and bare rock contributed to 90% of the differences between groups. *Pollicipes polymerus* and bare rock substrate contributed the most to community composition differences between these two groups (26% and 13%, respectively; Fig. 3.11, SIMPER). After *M. californianus, P. polyermus* and bare rock (uncolonized gaps in the mussel bed) were the most prevalent cover in the mussel bed. The most common cover outside the mussel bed was bare rock, *Phragmatopoma californica, Mastocarpus spp.* sporophyte, and coralline algae (both articulated and crustose) (Fig. 3.11).

Changes in mussel cover increased with pre-SSWS sea star densities on larger spatial scale

At PISCO sites, change in mussel cover was positively correlated with pre-SSWS *P. ochraceus* densities below 0.3 individuals per m^2, after which change in mussel cover approached an asymptote ($p = 0.0022$, $r^2 = 0.240$; Fig. 3.12). An asymptotic exponential curve (AICc = 220.95) better described this relationship than a linear regression (AICc = 223.92).

Discussion

Evidence and mechanisms for mussel bed expansion

Mussel beds expanded downward on the rock face and increased substantially in area during the study period. Recruitment, as opposed to the absence of predation, appeared to drive this change (Fig. 3.7a,c). Mussel beds also moved downward in tidal elevation, though the relationship with recruitment was not as pronounced (Fig. 3.6b). Change in the upper limit of the mussel bed was negligible, indicating that the bed was truly expanding instead of shifting its elevation range due to potential shifts in abiotic conditions during this period.

Mussels in the expansion zone were not significantly smaller than those in the original mussel bed (Fig. 3.8, 3.9), so it was not apparent whether these mussels were recent recruits, mussels moving down, or a combination of both. Because the bed expanded but did not get deeper, it suggests that growth and movement of existing mussels balanced the influx of recruits. If the bed expansion were driven only by adults moving down, we would likely have observed a thinning of the existing bed. Similarly, if the bed were expanding only due to recruitment, we would have observed much smaller mussels and a shallower bed in the expansion zone.

Oceanographic conditions play a large role in *M. californianus* recruitment. Upwelling regimes shape the magnitude of overall regional recruitment, while currents and site-scale processes introduce within-region variation (Booth and Brosnan 1995, Broitman et al. 2008, Menge et al. 2009). In 2014, the California Current experienced a period of abnormally low upwelling activity and large seasonal

swings in productivity, followed by El Niño conditions and warm surface waters in 2015 and 2016 (Leising et al. 2015). Abundance of mussel recruits is often correlated with phytoplankton abundance, though its relationship with El Niño conditions is not as clear (Menge et al. 2009). *M. californianus* recruitment generally increases with sea surface temperature, though the strength of this relationship is site-specific on the Central California coast even in when El Niño conditions are not present (Broitman et al. 2008).

Predation counters mussel bed expansion

Recruitment alone would not increase mussel bed area if it were counteracted by sufficient sea star predation. Relaxation of pre-SSWS predation pressure might no longer be balancing the influx of new mussels occupying space, though we did not see strong support for this explanation. We did not observe a relationship between change in the lower limit or other bed dimensions and pre-SSWS of *Pisaster ochraceus* levels, except for the negative correlation between bed volume and pre-SSWS biomass (Fig. A3.4a-h). Post-SSWS *P. ochraceus* density or biomass was most likely too uniformly low to have substantial influence on changes in the mussel bed. With one exception in 2017, sea star biomass was < 5% of its pre-SSWS levels (Fig. A3.3). It is also unlikely that compensatory predation is taking the place of *P. ochraceus* consumption in maintaining the mussel bed boundaries. The predatory

whelk *Nucella spp.* consumes mussels, but its population-level predation pressure has nonsignificant impacts on mussel bed lower limits, even in the post-SSWS absence of *P. ochraceus* (Hart 2010, Cerny-Chipman et al. 2017).

Historical predation pressure is generally thought to control mussel bed lower boundaries (Paine 1974, 1976, Hart 2010). The upper extent of *P. ochraceus* foraging is set by desiccation tolerance, creating a vertical space of minimal predation for mussels (Robles and Desharnais 2002, Robles 2013). Despite differences in pre-SSWS density and biomass spanning over one order of magnitude, we observed a negative relationship between pre-SSWS *P. ochraceus* biomass and bed volume, but we did not find a correlation with any other dimensions of the bed. As a region, the Central California coast had regained approximately 25% of its long-term pre-SSWS predation pressure by 2017, though considerable site-level variability existed within the region. Southern California remained below 10% recovery at most sites, while North Central California and Northern California began to return to near-pre-SSWS levels of density and biomass by 2017 (Moritsch and Raimondi 2018). Examining mussel beds across multiple regions revealed different patterns than those within Central California. Changes in mussel cover were positively correlated with pre-SSWS *P. ochraceus* density (Fig. 3.12). Greater variation in both mussel recruitment and sea star recovery exists between major biogeographic regions than within Central California (Broitman et al. 2008, Menge et al. 2016, Miner et al. 2018). This larger

scale variability might have contributed to the ability to detect patterns in how sea star predation shapes the mussel bed at different spatial scales. It also highlights the need for continued long-term monitoring in multiple biogeographic regions to appropriately evaluate disease consequences (Groner et al. 2016, Hughes et al. 2017).

Outcomes of predator removal vary temporally even within the same sites. Within our Central California coast study area, not all sites experienced mussel bed expansion (Fig. 3.6a). At Soberanes, the site with the largest change in mussel bed position, the mussel bed moved down the rock 34 cm over 4 years, while the mussel bed at Terrace moved down only 4 cm. In contrast, sea star removals in the early 2000's at Soberanes showed only 11 cm of downward movement after two years without *P. ochraceus*, while Terrace showed 35 cm of movement (Hart 2010). This highlights the temporal variability in the relative importance of predation pressure, recruitment, and site conditions as mechanisms for controlling mussel bed boundaries.

Abiotic contributors to mussel bed regulation

In addition to predation, abiotic context mediates the strength of keystone predation as a control of mussels (Menge 1992, 2000, Menge et al. 1994, Sanford 2002a, 2002b). Mussel survival and sea star activity are reduced by stressful physical conditions such as high air temperatures and shearing action of waves (Robles et al.

1995, Robles and Desharnais 2002, Petes et al. 2008). Even where mussels are physiologically capable of withstanding these stressors, stochastic disturbances such as storms or woody debris rip out or crush established mussel beds to open space on the rock surface for colonization (Dayton 1971, Seed and Suchanek 1976). Sand smothering can cause heavy mortality in *M. californianus.* In some locations, sand controls the lower limit of the mussel bed and prevents competitive exclusion of organisms living in the areas of sand inundation regardless of predation pressure (Littler et al. 1983). Santa Cruz County sites get inundated with sand up to the middle of mussel bed for one to two weeks at a time in winter and for periods of several weeks in summer. The study plots at our Monterey County sites do not experience sand inundation. We observed mussels continuing to persist at lower tidal elevations after repeated burial events, so it is unlikely that sand limited the mussel bed expansion here (*pers. obs.*).

Lack of change in mussel sizes and bed depths

An increase in the abundance of large, refuge-size mussels could cause loss of predator control of the mussel bed, resulting in more stable, abiotically defined boundaries rather than a dynamic equilibrium between settlement, growth, and predation (Donahue et al. 2011). Mussel growth to sizes too large for *P. ochraceus* occurred in prior sea star removal experiments in Washington, USA (Paine 1976), but

does not appear to have happened in Central California after the SSWS outbreak. The original bed and expansion zone had low proportions of refuge-size mussels over the entire observation period. This indicates that *P. ochraceus* will still be able to consume the same proportion of the mussels upon full recovery, so the mussel bed changes were not necessarily stable against future predation by 2017. The similarity of mussel sizes in the original bed and the expansion zone (Fig. 3.8, 3.9) also support the notion of short-term change that is not yet self-reinforcing against these changes persisting on longer time scales. The lack of change in mussel bed depths over the observation period could be due to negative feedbacks on mussel accumulation. Beyond location-specific threshold depths, the bed is more prone to forming unstable clumps of mussels not anchored to the substrate. These clumps are more prone to ripping off in strong waves (Pearse et al. 2010).

Community composition of mussel beds and lower intertidal communities did not shift

We observed an expansion of the mussel bed community and a reduction in space available for the community below the mussel bed. It was not surprising that the composition of the expansion zone mostly matched that of the original bed. However, because it was less similar than the original 2014 bed zone and 2017 bed zone were to one another (Fig. 3.10a), it suggests minor differences in epibiont species on mussels in the established bed compared to in the expansion zone (Table

A3.2). We observed smaller, unfouled mussels filling in gaps in the bed, overgrowing existing mussels, and growing at the lower edges of the mussel bed starting in 2015 and continuing through 2017. The low cover of epibiont growth on these mussels might contribute to the slight differences between the expansion and original bed community, where epibionts grow on top of a higher percentage of mussels. Epibiont species and other *M. californianus* recruits can establish on shell substrate quickly, though survival depends on characteristics of the shell (e.g., hardness or smoothness) and modification of abiotic conditions by surrounding epibionts (Dittman and Robles 1991, Lohse 1993b, Gutierrez et al. 2003, De Nesnera 2016).

The intertidal community changed in the expansion zone, driven by the conversion of below-bed community into mussel bed community. Given the limited area of expansion, this had the most consequences for species that live within approximately 19 cm of the lower limit. Composition of zones below the mussel bed (zones 2 and 3) were more similar within years than in the same zone across years (Fig. 3.10a). This suggests that community composition immediately below and farther below the mussel bed were highly similar and could be treated as the same community. They were not two distinct communities, which we had originally expected. Since the SSWS outbreak, this community became restricted to smaller area on the rock wall. We did not observe a displacement of a separate mid-elevation community. Within-zone vertical stratification of species still occurs, so it is possible

that if mussel bed expansion continues, these species must move down, move onto mussels, or be displaced. These results differ from other sea star removal experiments where diversity of the remaining community decreased, again highlighting the spatial and temporal variability of keystone predation's effects on the community (Paine 1974, Robles et al. 2009, Hart 2010). Many of the species that live on the primary substrate can also survive as epibionts on *M. californianus* (Table A3.2), though relative survival rates differ (Lohse 1993a). If mussels were to colonize the entire rock wall, it is likely that many species would still persist, but species richness would decline, and changes in relative abundances could still foster a different community from that of the primary substrate (Paine 1974, Menge 1983).

Implications for intertidal communities in the absence of a keystone predator

The time required for sea star recovery relative to the response time of local prey species in colonizing space will influence outcomes for the rocky intertidal community. Mussel coverage responds to local sea star predation pressure on a time scale of years, producing a lag between changes in predator populations and prey populations (Paine 1976, Menge and Blanchette 2004, Blanchette et al. 2005, Hart 2010). Five years have elapsed since the earliest observations of the SSWS outbreak. Mussel beds in Central California are already showing increased cover and expansions of their lower boundaries toward the water (Fig. 3.6), though the

proportion of mussels at refuge sizes has not increased. Similar species composition across years suggests that the lower intertidal community is robust to changes from SSWS on sub-decadal time scales, at least for sessile organisms.

Depending on how quickly sea star populations rebound, it is still possible that these changes could be reversed within a few years (Hart 2010). A longer absence of sea stars would allow mussels to further colonize space and potentially grow to a size of refuge from predation, making it a more difficult and lengthy process for sea stars to return the community to its pre-SSWS composition (Paine 1974, Robles et al. 2010). *M. californianus* might attain refuge size in ≤ 5 years under favorable conditions (Coe and Fox 1942), though at our sites that has not happened in large numbers. These results add to our knowledge on the generality of keystone predation paradigm.

This study has significant implications for how disease can indirectly shape communities. Echinoderms as a phylum might be prone to boom-bust population dynamics in part due to the way diseases impact their populations (Uthicke et al. 2009), so understanding the consequences of these mass mortalities provides insight into a common mechanism for regulation of community composition. Major die-offs of important echinoderm species, including previous outbreaks of SSWS, directly affect abundances of dominant species and have even induced shifts to alternative community states (Boyer 1987, Eckert et al. 2000). These results, combined with

long-term monitoring and modeling of conditions promoting disease outbreaks (**Chapter 2**) might help us predict the magnitude of changes to intertidal communities in future outbreaks of Sea Star Wasting Syndrome or other diseases affecting keystone species.

Tables

Table 3.1. Effects table for mixed effects model of mussel sizes and depths in the main mussel bed and expansion zone.

Term	N parameters	DF	DF Denominator	F Ratio	p-value
Girth of mussels in bed					
site	5	5	3713.4324	46.1089	< 0.0001
year	3	3	3712.2443	7.4982	< 0.0001
elevation	1	1	3713.8130	87.9511	< 0.0001
site*year*elevation	15	15	3714.9442	3.9404	< 0.0001
elevation*year	3	3	3711.7944	1.2412	0.2931
site*year	15	15	3712.1258	6.8809	< 0.0001
Depth of mussels in bed					
site	5	5	3907.5166	37.3581	< 0.0001
year	3	3	3903.6493	13.7570	< 0.0001
elevation	1	1	3904.5649	13.1779	0.0003
site*year*elevation	15	15	3905.7948	4.9559	< 0.0001
elevation*year	3	3	3903.5248	7.8577	< 0.0001
site*year	15	15	3903.6457	7.9303	< 0.0001
Girth of mussels in expansion zone					
site	5	5	922.3020	2.9926	0.0109
year	2	2	1251.7242	9.1882	0.0001
elevation	1	1	1071.9126	0.0006	0.9807
site*year*elevation	10	10	1008.8288	2.0965	0.0223
elevation*year	2	2	1238.0327	0.0430	0.9579
site*year	10	10	1270.8844	2.5506	0.0047
Depth of mussels in expansion zone					
site	5	5	1349.2662	2.4400	0.0327
year	2	2	1347.0014	1.8082	0.1644
elevation	1	1	1348.2142	0.2353	0.6277
site*year*elevation	10	10	1348.2548	2.6911	0.0029
elevation*year	2	2	1346.2626	0.0511	0.9502
site*year	10	10	1346.1558	4.2680	< 0.0001

Figures

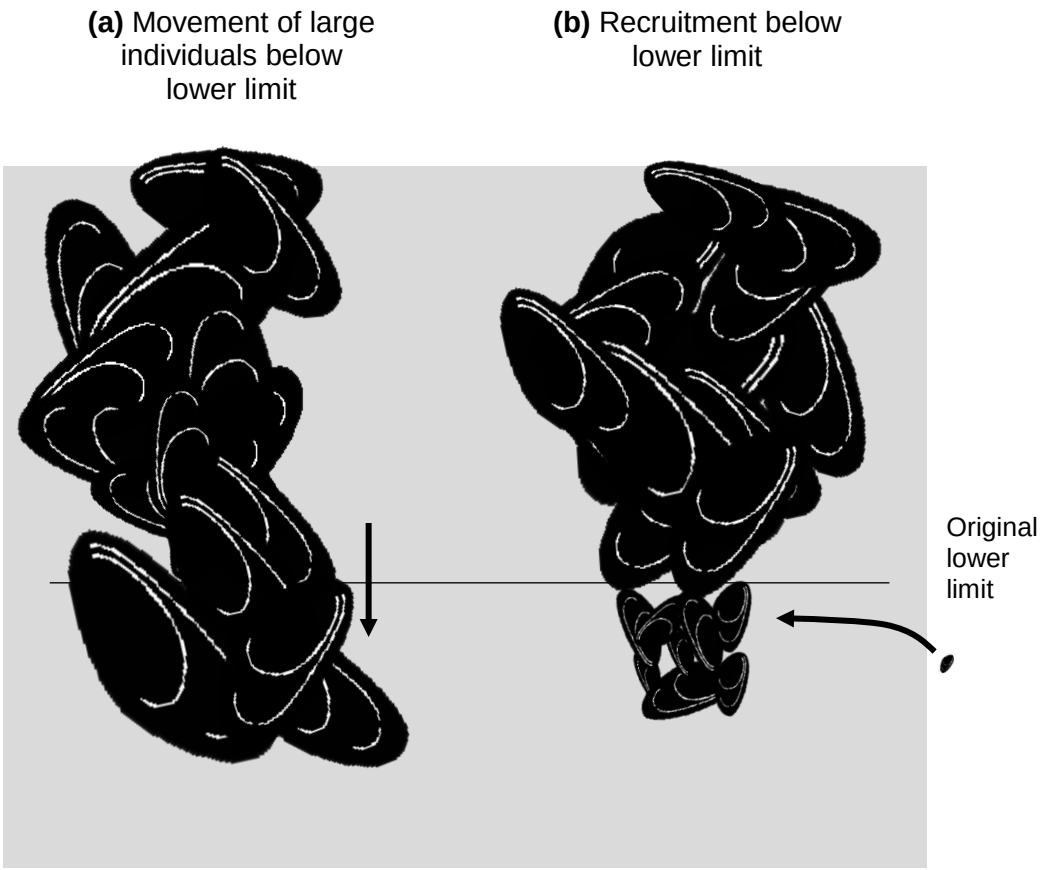

Figure 3.1 Schematic of outcomes in the mussel bed under different mechanisms of change. **(a)** When predation pressure is reduced, larger mussels can exist at lower elevations. The size distribution below the original bed would reflect what was already in the bed. **(b)** When recruitment is high, many small mussels settle in and around the mussel bed, producing a size distribution with more small individuals below the original bed.

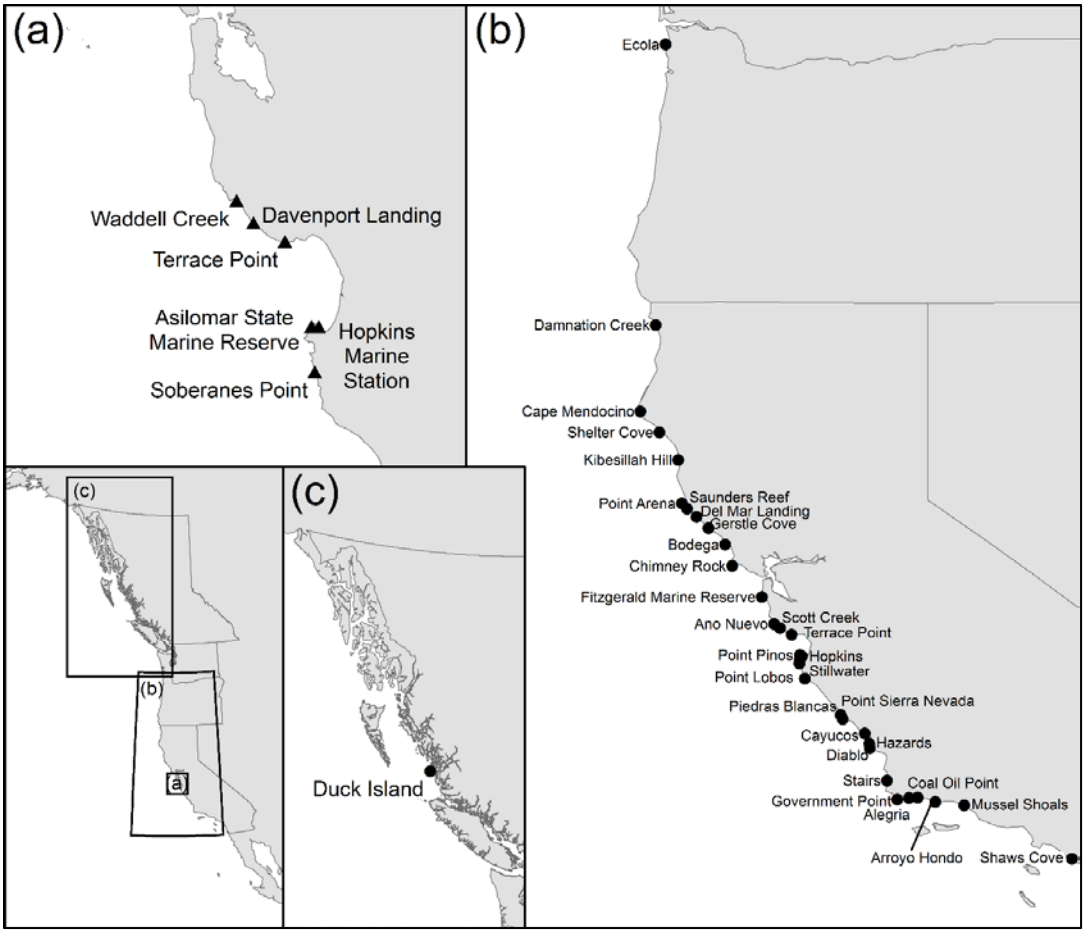

Figure 3.2 (a) Map of study area showing sites (▲) for detailed mussel bed surveys. Waddell, Davenport, and Terrace are in Santa Cruz County. Hopkins, Asilomar, and Soberanes are in Monterey County. **(b)** Map of sites (•) with sea star density and mussel percent cover sampling for California, Oregon, and **(c)** British Columbia. Inset shows corresponding extent of each panel.

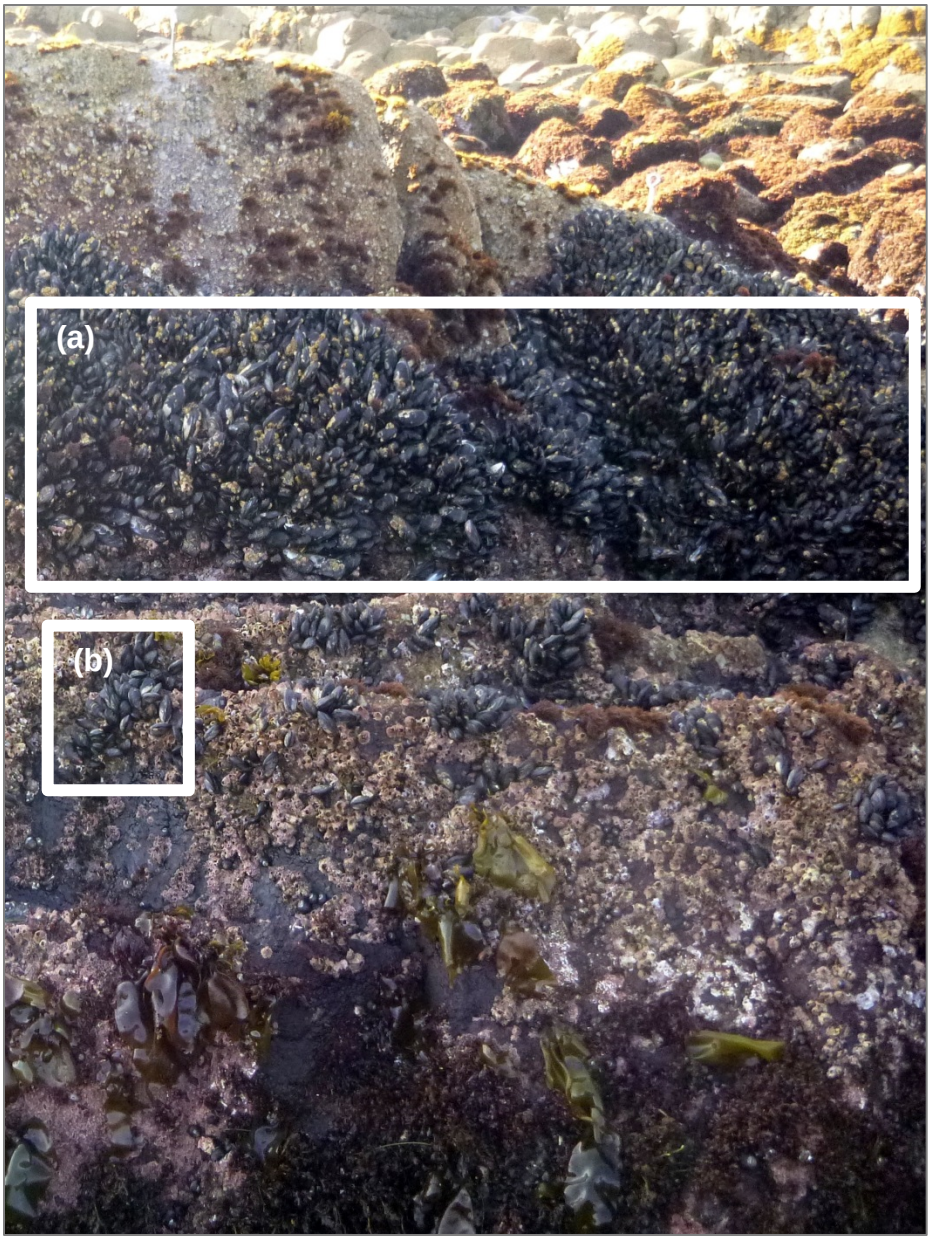

Figure 3.3 An example mussel bed and series of patches on a vertical intertidal rock wall at Hopkins Marine Station. (**a)** Mussel beds spanned continuously over the rock wall, often connecting to the mussel beds on top of the rock platform. (**b)** Mussel patches were not in contact with any mussels in the bed.

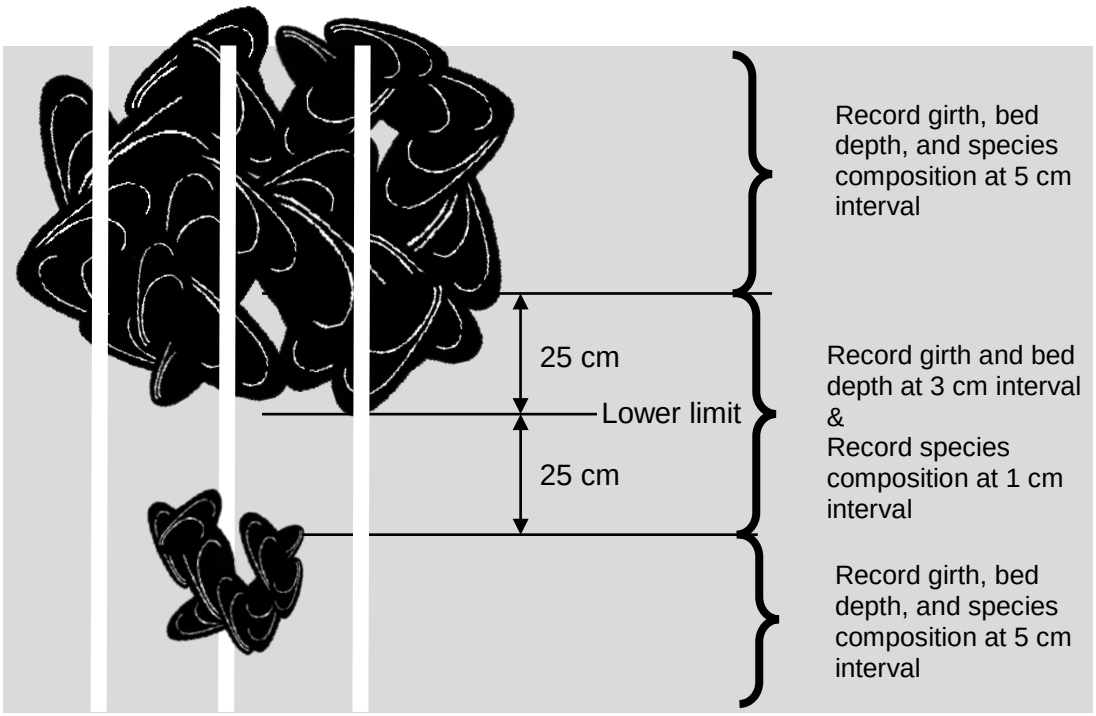

Figure 3.4. Illustration of vertical transects on a vertical rock wall showing where and how frequently mussel girth and bed depth measurements were taken. Mussel bed on top of the platform omitted from schematic for clarity.

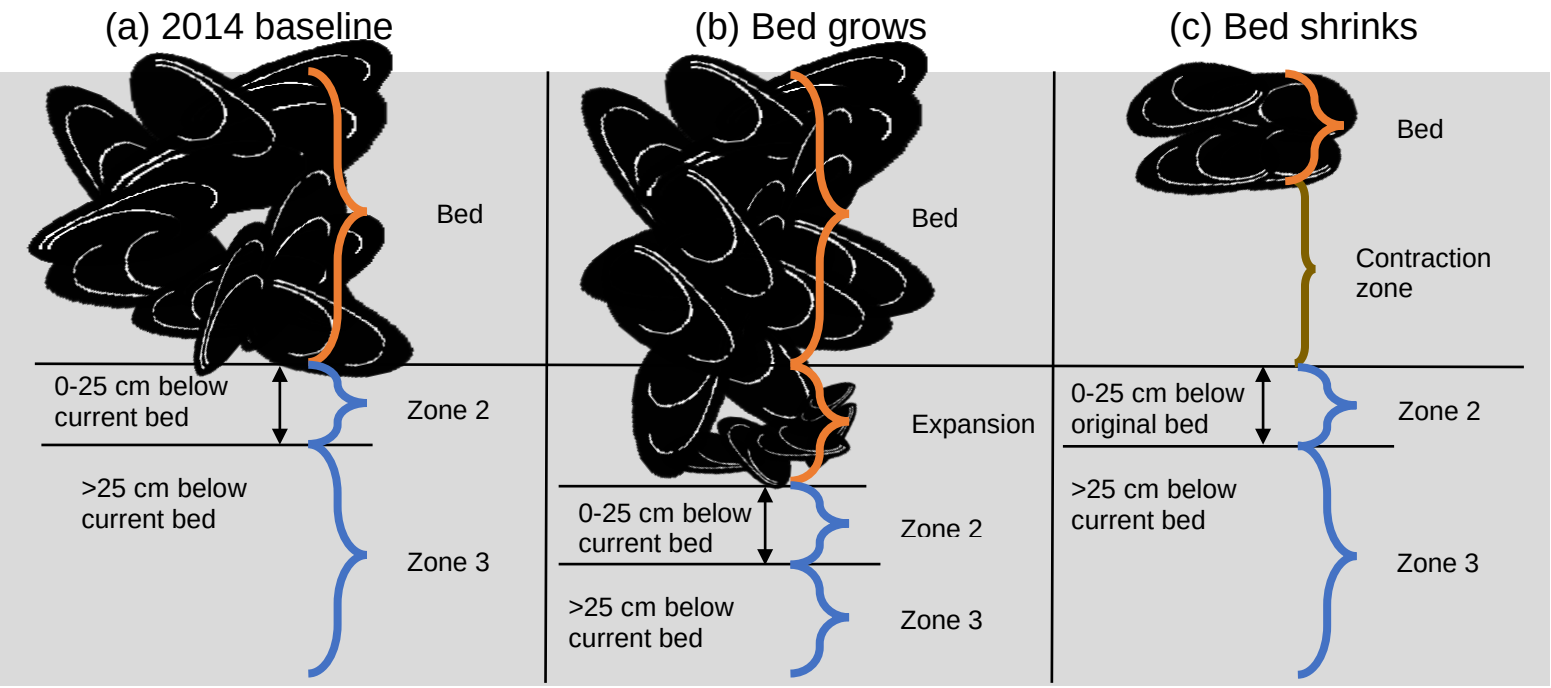

Figure 3.5. Illustration of zones used to categorize mussel sizes and species composition data. **(a)** Everything above the mussel bed lower boundary in 2014 was considered part of the original bed. Points falling 0 to 25 cm below the bed boundary were considered Zone 2, and everything >25 cm below the bed boundary was considered Zone 3. **(b)** If the bed expanded in subsequent years, points falling in the area of downward mussel bed expansion were considered the Expansion zone. Zone 2 began after the Expansion zone. **(c)** If the bed retracted upward, points falling in the area between the existing lower limit and the original lower limit were considered the Contraction zone. Zone 2 began at the end of the original bed.

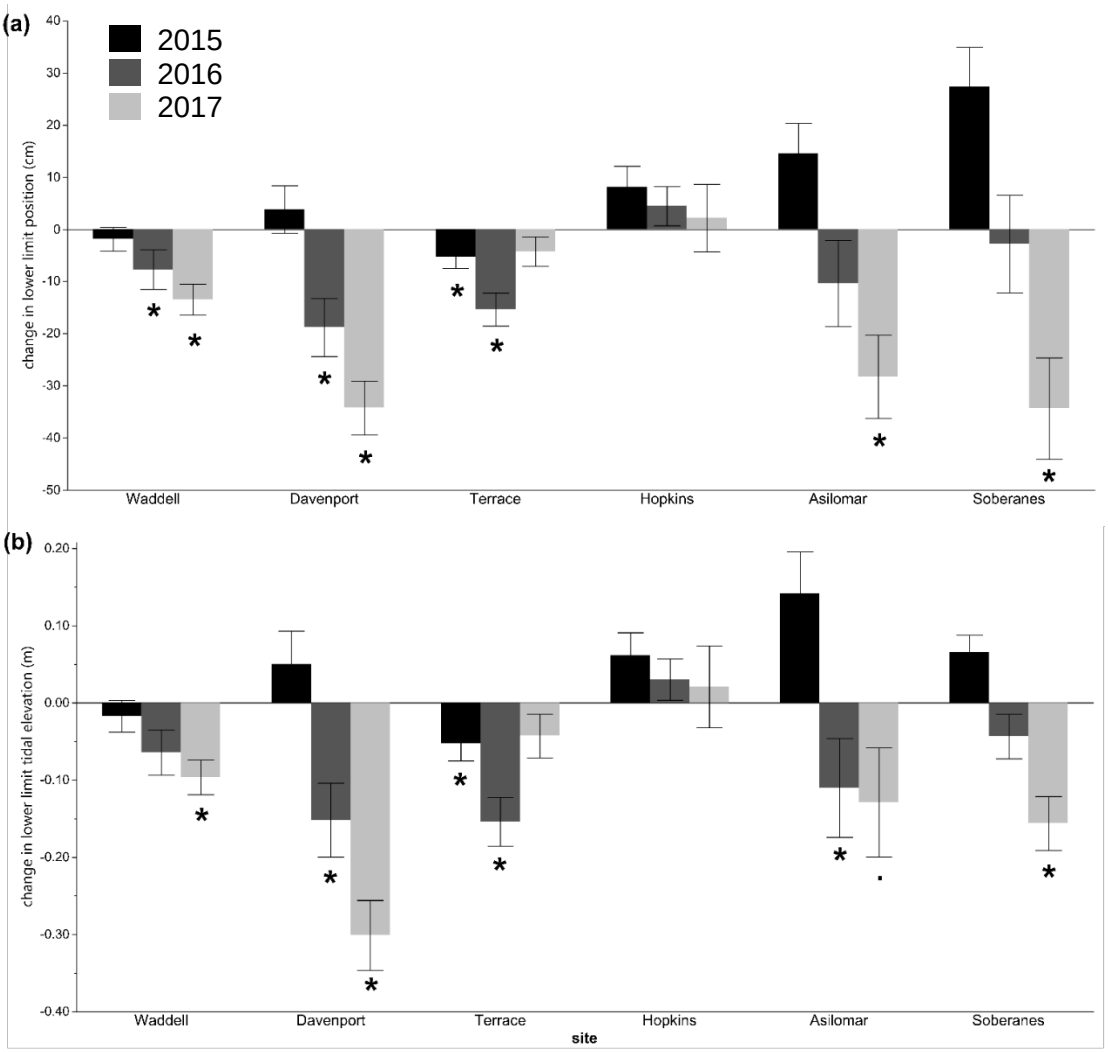

Figure 3.6. (a) Movement of the mussel bed lower limit on rock walls after the Sea Star Wasting Syndrome outbreak. Negative numbers indicate movement downward, toward the water. **(b)** Change in tidal elevation of the mussel bed lower limit. N = 11 per site per year. '*' indicates statistically lower than in 2014 (t-test, $p < 0.05$). '.' indicates marginally lower than in 2014 (t-test, $p < 0.10$). Bars indicate standard error.

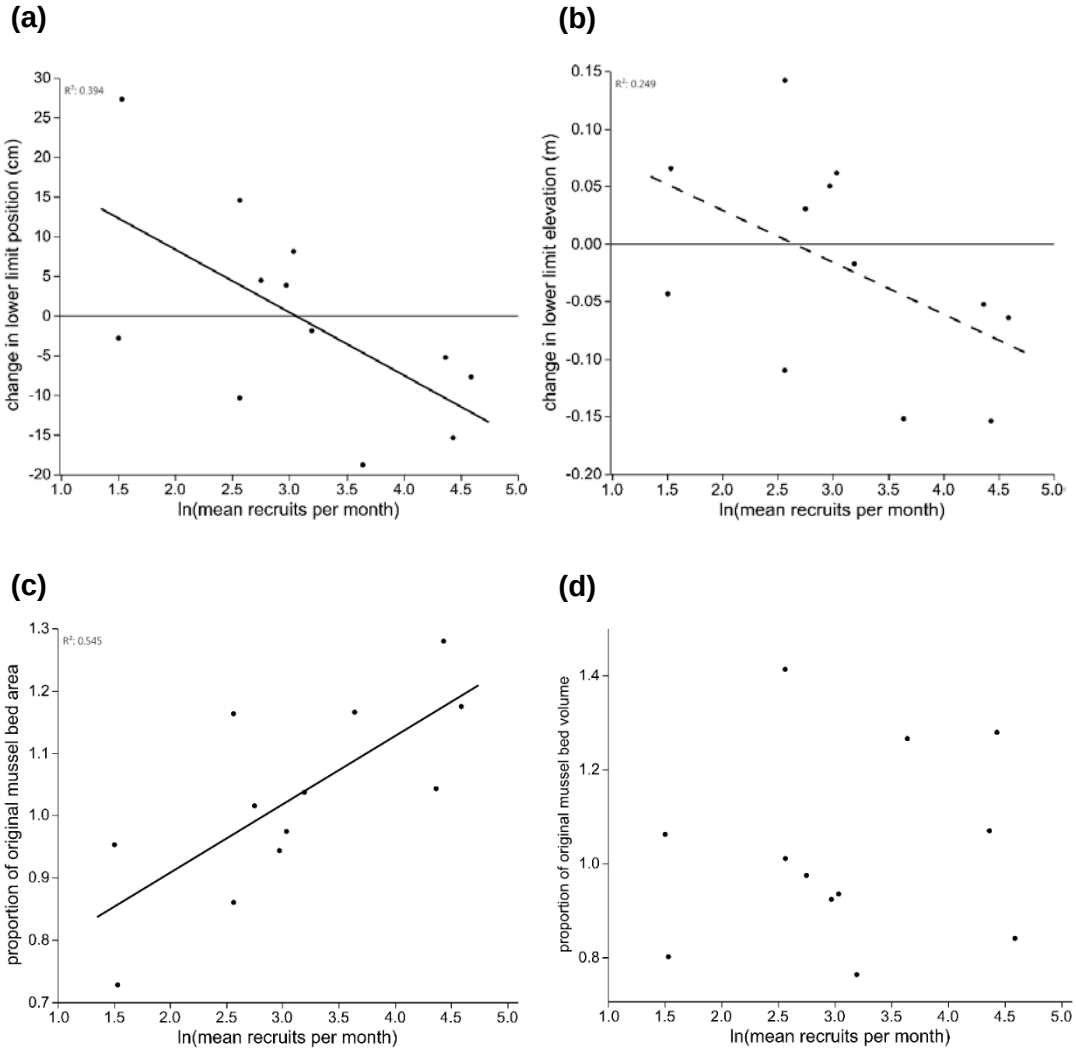

Figure 3.7. (a) Change in the position of the lower limit was negatively correlated with recruitment. Negative numbers indicate movement of the mussel bed boundary toward the water. **(b)** Changes in the elevation showed a nonsignificant negative trend with increased recruitment. Negative numbers indicate movement of the mussel bed boundary toward the water. **(c)** Mussel bed area was positively correlated with recruitment. **(d)** Mussel bed volume was not correlated with recruitment. We used recruitment data from 2015 and 2016 only. N = 12.

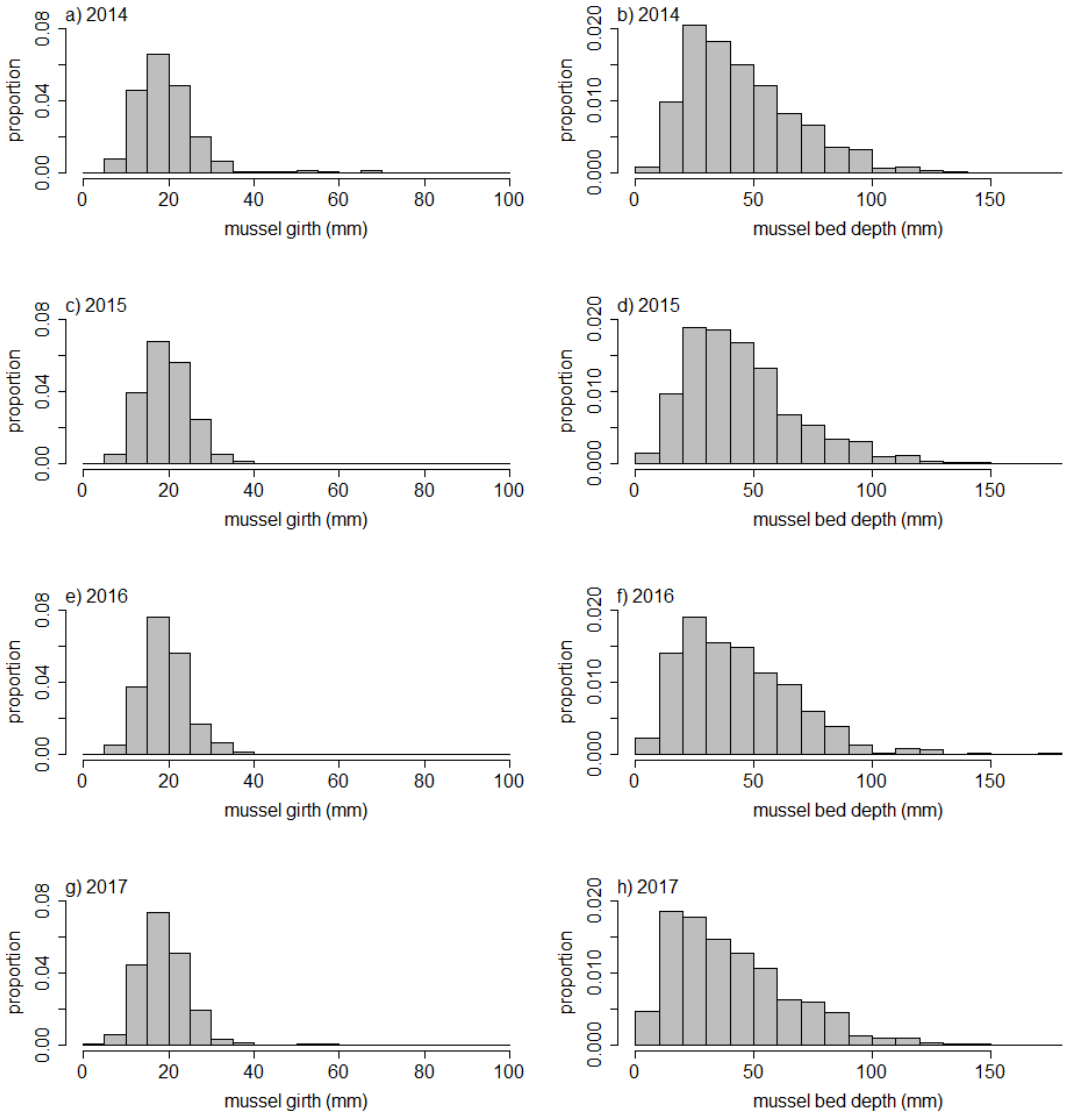

Figure 3.8. Size-frequency distributions for mussel girth **(a, c, e, g)** and mussel bed depth **(b, d, f, h)** in the location of the original 2014 mussel bed in the years following the SSWS outbreak. N ≥ 90 mussels per site per year.

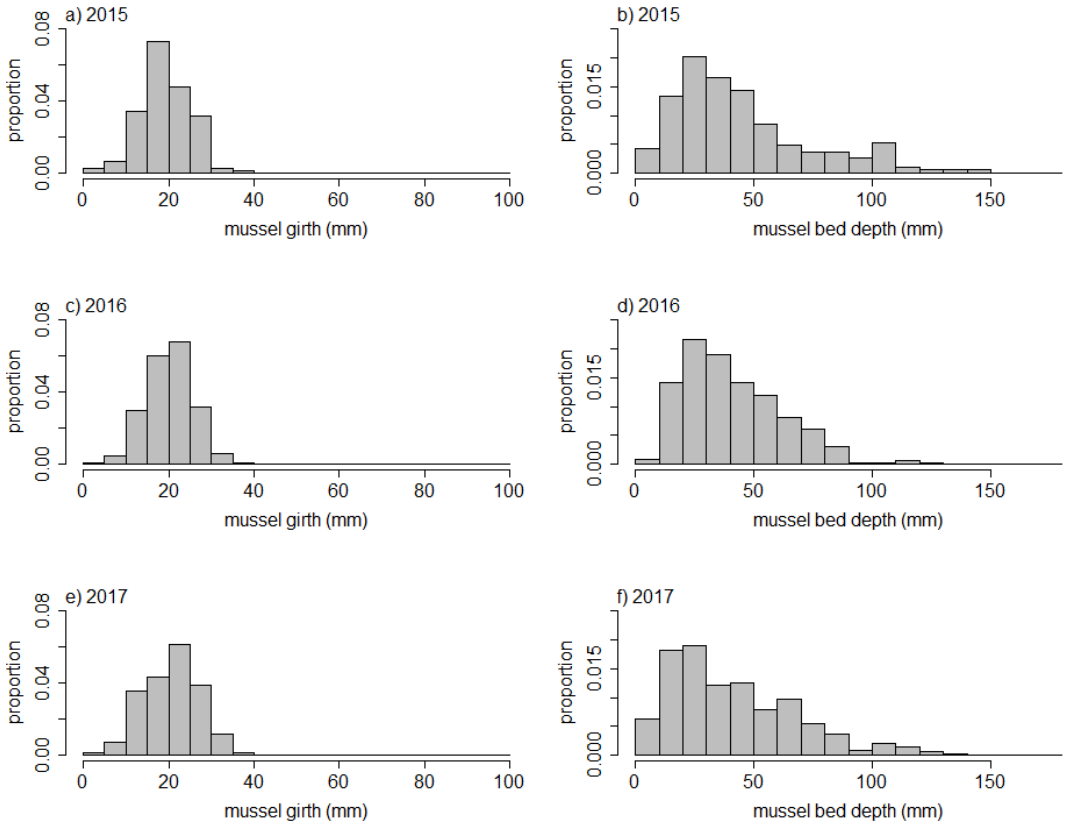

Figure 3.9. Size-frequency distributions for mussel girth **(a, c, e)** and mussel bed depth **(b, d, f)** in the new mussel bed (expansion zone) in the years following the SSWS outbreak. By definition, no expansion zone existed in 2014. $N \geq 20$ mussels per site per year.

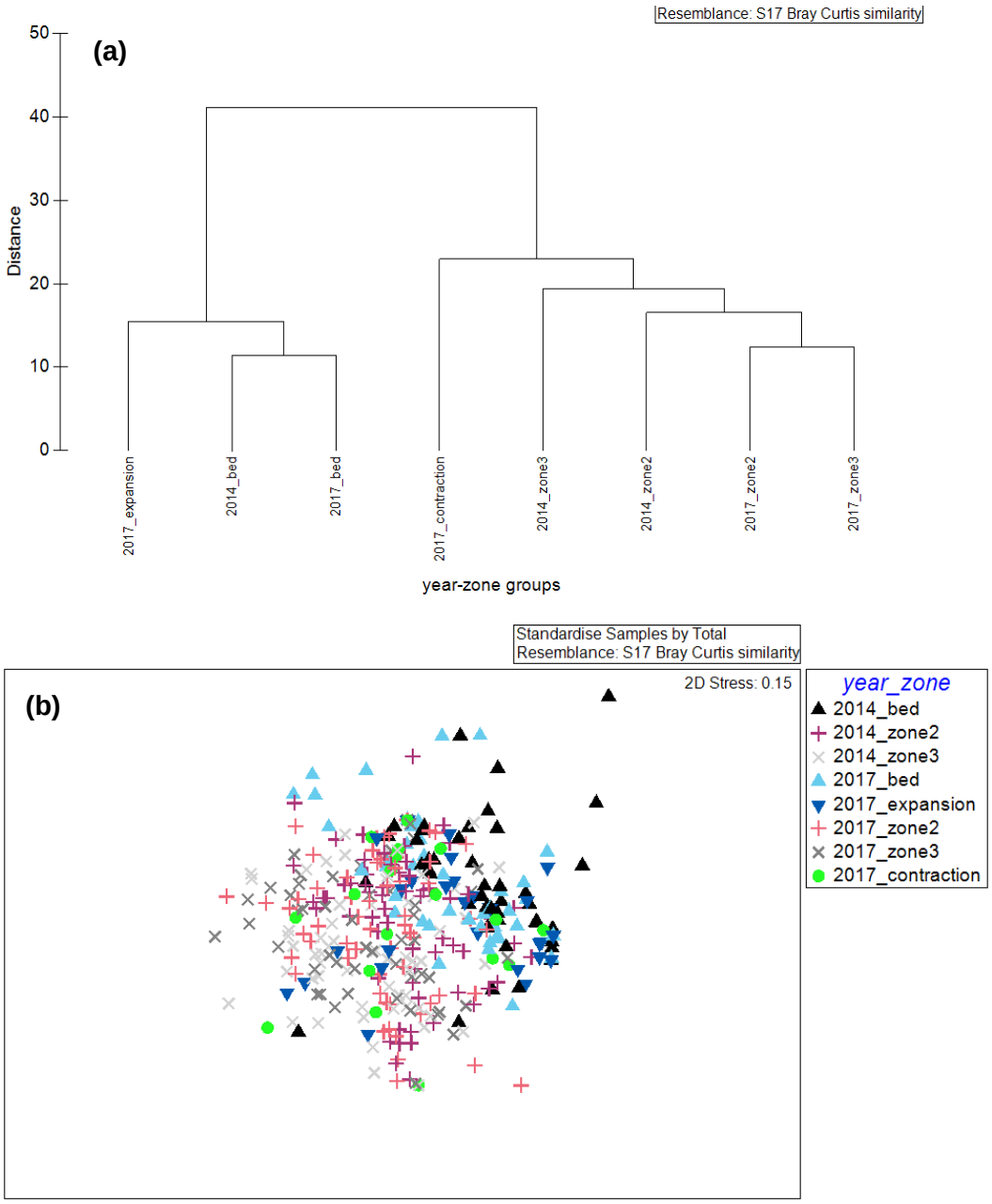

Figure 3.10. (a) Differences in community composition of intertidal zones (*Mytilus californianus* excluded) based on distance between group centroids in a Bray-Curtis similarity index. **(b)** Non-metric multidimensional scaling (NMDS) of community composition. Two samples from zone 3 fall far outside the plot boundaries and are not shown. All samples were grouped by zone and year (N = 405).

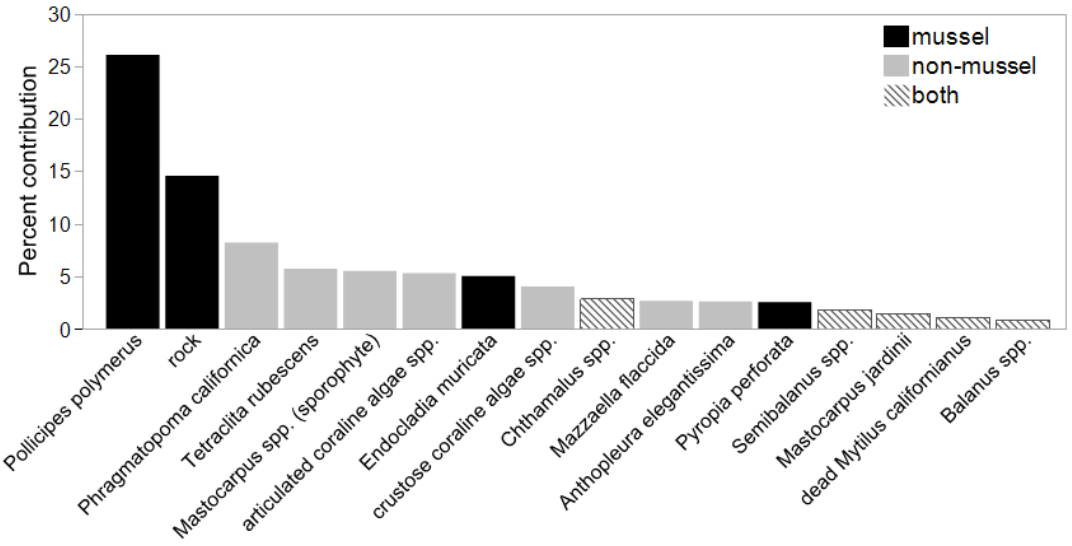

Figure 3.11. Contributions of individual species to differences between mussel bed-occupied substrate and non-bed-occupied substrate (N = 405). Data from 2014 and 2017 were pooled. Original mussel bed and expansion zone were pooled. The contraction zone, zone 2, and zone 3 were pooled. Bar shadings indicate the assemblage with which the species (or substrate type) is most commonly associated.

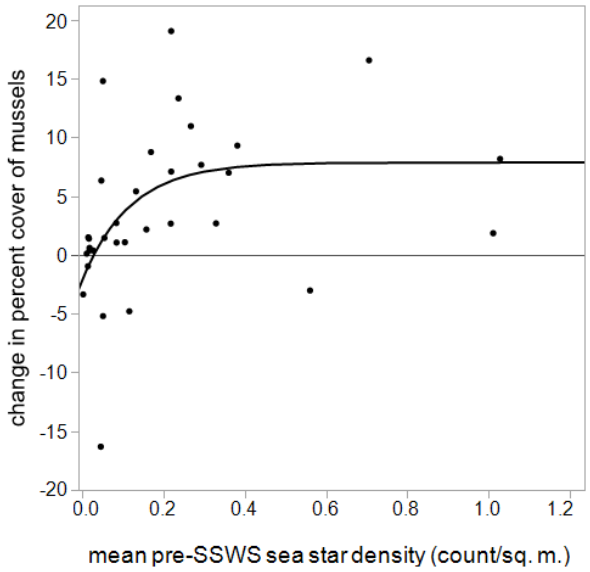

Figure 3.12. Change in mussel percent cover was positively correlated with pre-SSWS *P. ochraceus* densities (N = 33).

Synthesis

This work was motivated by an emerging need to understand the causes and consequences of the absence of a keystone predator. When the Sea Star Wasting Syndrome (SSWS) outbreak first began, the research community proposed many hypotheses for potential causes of the disease and quickly set up surveys to monitor its progression. Prior sea star exclusion experiments generated several potential outcomes ranging from small, reversible expansions in the mussel bed to extreme increases in mussel coverage with lasting shifts in intertidal biodiversity. It was unknown which scenario would result from this outbreak. To answer these questions, I addressed: (1) recovery of sea star populations and their predation pressure, (2) environmental conditions associated with the outbreak on different spatial scales, (3) responses of the intertidal community to the near-absence of keystone predation.

Key insights

My results provide insights into the causes of this epidemic, how its impact varied geographically, and how epidemics affect rocky intertidal communities. The results from **Chapter 1** show that *Pisaster ochraceus* populations are recovering in number in several regions, but the average sea star size is considerably smaller than before the outbreak, as most of the post-SSWS populations are made of recent

recruits. Biomass remains low compared to pre-SSWS levels. Because biomass is a proxy for sea star predation pressure, it suggests that sea star populations are not fulfilling their ecological role as top predator to the same degree and are not exerting the same level of control on mussel populations. The magnitude of sea star recruitment could be driving the regional differences in population and biomass recovery. Continued monitoring of sea star populations is required to determine when they return to their former numbers and predation abilities.

In **Chapter 2,** I provide evidence that probability of SSWS outbreaks is negatively associated with distance to the nearest infected site and positively associated with low tide exposure duration on a coast-wide scale. In some regions, chlorophyll *a* concentration is also positively associated with infection. This goes against the popular hypothesis that abnormally warm water temperatures caused the infections and instead suggests stressful emersion periods may be more important. Abnormally warm water temperature cannot be ruled out entirely, as experimental and small-scale field evidence suggests it increases SSWS severity and speed of onset, but on a coast-wide scale, the environmental drivers of SSWS appear complex. These findings support the idea that SSWS may be caused by multiple pathogens or a collection of region-specific stressors instead of a single pathogen. These results improve our ability to predict future SSWS outbreaks and understand potential relationships between the sea star host, the SSWS pathogen(s), and the environment.

As climate change increases stress on marine organisms, identifying conditions conducive to disease outbreaks will become critical.

In **Chapter 3,** I provide evidence that mussels, the main prey of *Pisaster ochraceus,* have expanded their coverage and moved into to lower intertidal elevations due to recruitment and adult mussel movement. At focal sites along Monterey Bay, mussel bed changes are not associated with pre-SSWS sea star density or biomass. In contrast, on a larger scale, changes in mussel cover are positively correlated with pre-SSWS density. Composition of the intertidal community below the mussel bed has not changed. My results provide a first look at potential community responses to the loss of a keystone predator. These changes so far suggest that changes to the mussel bed have not displaced lower intertidal communities and have not caused irreversible conversion to a mussel bed community. The long-term response of the community depends on length of sea star absence and degree of recovery in predation pressure (**Chapter 1**), as well as the potential for these outbreaks to reoccur (**Chapter 2**). I suggest that continued monitoring of intertidal communities is key to determining whether mussel bed changes will remain of if bed dimensions will return to their pre-SSWS state.

As a whole, these results emphasize that the potential SSWS causes, population changes, and community consequences of SSWS are not uniform across the entire coast. The severity of mortality and timing of SSWS arrival was specific to

biogeographic region, and the results from **Chapter 1** show that sea star recovery is also heterogeneous across these regions. **Chapter 2** demonstrates it is important to examine environmental conditions in each region, particularly when outbreak timing varies so dramatically. However, examining trends in potential stressors on regional scales helps discern whether a "one-size-fits-all" cause is likely. A region-by-region comparison of infection patterns also helps control for environmental heterogeneity across vast distances of coast. **Chapter 3** supports comparing changes in prey species across regions. Patterns that did not appear within my six focal sites were more evident when using tens of sites across thousands of kilometers. These results highlight the importance of studying disease on multiple spatial scales.

This work demonstrates the value of long-term monitoring at broad spatial scales to the study of disease ecology and community ecology. To evaluate the consequences of disease, it is necessary to establish some baseline against which to measure the impacts. In many epidemics, the pre-disease system is understudied, and drawing definitive conclusions is difficult. Long-term monitoring is useful for evaluating impacts of other types of ecological changes as well, including natural and anthropogenic disturbance. Without knowledge of a system's ecological history, we are limited in our abilities to interpret observed changes and to predict future changes. In an increasingly warm, acidic, polluted ocean, we need to maintain these long-term observation series if we are to adequately respond to these challenges.

This work also highlights the utility of citizen science research for capturing rapidly-emerging diseases, especially over large geographic expanses. This work would have been impossible without the observations of over one thousand citizen scientists visiting their local tidepools. For large-scale disease outbreaks, I recommend employing citizen science for documenting diseases where symptomatic individuals are easily identified. Citizen science has received criticism because most volunteers commit for short periods of time, providing low return-on-investment for time spent training them. However, in circumstances where rapid mobilization is critical and training is easy, citizen science can provide exactly what is needed. These simple, high-volume, spatially distributed observations complement long-term monitoring efforts, which employ more in-depth protocols concentrated at fewer sites. Between these two approaches, SSWS is likely the most well-documented marine disease for a noncommercial species.

In addition, citizen science provides a valuable opportunity for engaging the public in the scientific process. This benefits the science community (and society) by increasing participants' understanding how research is conducted and what questions it can answer. Participation in disease research also connects people to current challenges facing marine ecosystems. During the height of the outbreak, many citizen scientists expressed concern about the health of the ocean. They speculated on causes

of SSWS and frequently asked how they could help the sea stars. These inquiries served as a launching point for educational conversations about ocean health issues.

Future directions

In summary, this work on the ecology of SSWS contributes to our understanding of how disease shapes rocky intertidal ecosystems and improves our ability to predict the consequences of future disease outbreaks for marine communities. A better understanding of the underlying mechanisms of pathology would sharpen the search for which stressors matter and where the largest community consequences are expected. These investigations will require continued reliance on long-term monitoring and citizen scientist data.

Appendices

A.1: Supplemental Material for Chapter 1

Calculation of growth rates for *Pisaster ochraceus*

We identified clear pulses of recruits by visually examining abundances for each P. ochraceus size class over time in PISCO/MARINe's Long-Term Monitoring plots. Data are publicly available at http://www.eeb.ucsc.edu/pacificrockyintertidal/interactive-map/index.html. We used PISCO's Interactive Map and Graphing Tool to generate visualizations for the size-date-abundance data that could discern the presence of recruitment "pulses" by the presence of a large number of sea stars in small size classes relative to earlier or later years (Fig. A1). We then tracked recruitment pulse over time as the cohort matured and moved up in size classes. A recruitment pulse was not used if data gaps exceeded two years between measurements or if it was less than two years in duration. We stopped tracking cohorts when they reached the size of 90mm, at which point they were indistinguishable from existing adults.

We estimated the change in size over time to calculate growth rate for each pulse. Dates were converted to years since the start of the pulse observation, in which the first observation was considered year 0. We treated all year-size combinations as

x-y pairs. We used linear regression to fit a line to the year-size pairs in each pulse. The slope of the best fit line represented the average growth rate of the pulse (mm yr^{-1}). If a site had more than one pulse, we used a mixed regression (R 3.3.2) using points from all pulses, including pulse number as a random effect. This integrated multiple pulses into a single growth rate for each site. We recognize that growth rates fluctuate with food availability (Feder 1970), but juvenile *P. ochraceus* in both lab and field settings show approximately linear trends in growth rates (Sewell and Watson 1993, Pilkerton et al. 2016).

If a site did not have distinguishable recruitment pulses to use in growth rate calculation, we assigned the growth rates of the nearest neighboring site with a discernable recruitment pulse. We used the (Euclidean) Near function in ArcGIS 10.5 to determine nearest neighboring site.

Table A.S1. Extent of each geographic region and number of sites in each region with *Pisaster ochraceus* count and size data from PISCO/MARINe surveys used for count and biomass comparisons. Only sites with count data from the pre-SSWS period (2012 and earlier) and data from 2015 to 2017 were used in analysis. An asterisk, '*', indicates that more sites were sampled for sea stars that year but data is not yet available.

Region	2015	2016	2017	Extent of region
AK	2	2	2	Southeast Alaska panhandle
CA Central	14	13	9	Pidgeon Point to Point Conception
CA Channel Islands	4	2	0	All Channel Islands (offshore)
CA North	6	6	2	CA-OR border to Point Arena
CA North Central	7	6	7	Point Arena to Pidgeon Point
CA South	17	16	15	Point Conception to US-Mexico border (mainland)
OR	5	4	3	WA-OR border to OR-CA border
WA Olympic Coast	5	2	0	Washington open coastline (not in straits or Puget Sound)
WA Salish Sea	5	5	1	Salish Sea and San Juan Islands
Total	**68***	**57***	**41***	

Table A.S2. Number of sites used in size distribution comparisons for each region. Sample size is lower than sites used for count and biomass comparisons (Table A.S1) because size distributions could not be constructed for sites with a count of 0 *Pisaster ochraceus*.

Region	N sites 2015	N sites 2016	N sites 2017
AK	2	2	2
CA Central	11	12	6
CA Channel Islands	1	0	0
CA North	5	6	2
CA North Central	6	5	2
CA South	8	8	7
OR	5	4	3
WA Olympic Coast	5	2	0
WA Salish Sea	5	4	1
Total	**48**	**43**	**23**

Table A.S3. Individual sites sampled in each year. '1' indicates the site was sampled. A blank indicates the site was not sampled. An asterisk, '*', indicates that the site was sampled for sea stars that year but data is not yet available. We excluded sites without sampling in two consecutive years from calculation of 2015-to-2016 or 2016-to-2017 changes in count and biomass in the years without data.

Site, by region	2015	2016	2017
AK			
Pirates Cove	1	1	1
Sage Rock	1	1	1
CA Central			
Andrew Molera	1	1	1
Boat House	1	1	*
Cayucos	1	1	*
Hazards	1	1	*
Hopkins	1	1	1
Mill Creek	1	1	1
Occulto	1		
Piedras Blancas	*	*	1
Point Lobos	1	1	1
Point Piños			1
Point Sierra Nevada	1	1	*
Scott Creek	1	1	1
Shell Beach	1	1	*
Stairs	1	1	*
Stillwater	1	1	1
Terrace Point	1	1	1
CA Channel Islands			
Bird Rock	1	1	*
East Point	1	*	*
Little Harbor	1	1	*
NW Talcott	1	*	*
CA North			
Cape Mendocino	1	1	
Damnation Creek	1	1	1
Enderts	1	1	*

Table A.S3. continued

Kibesillah Hill	1	1	
Shelter Cove	1	1	
CA North Central			
Bodega	1	1	1
Bolinas Point	1	1	*
Chimney Rock			1
Del Mar Landing			1
Gerstle Cove			1
Point Arena			1
Point Bonita	1	1	*
Santa Maria Creek	1	1	*
Sea Ranch	1	1	1
Slide Ranch	1	1	*
Stornetta	1		1
CA South			
Alegria	1	1	1
Arroyo Hondo	1	1	1
Cabrillo I	1		*
Cardiff Reef	1	1	1
Carpinteria	1	1	1
Coal Oil Point	1	1	1
Crystal Cove	1	1	1
Dana Point	1	1	1
Government Point	1	1	*
Mussel Shoals	1	1	1
Old Stairs	1	1	1
Paradise Cove	1	1	1
Point Fermin	1	1	1
Scripps Reef	1	1	1
Shaws Cove	1	1	1
Treasure Island	1	1	1
White Point	1	1	1

Table A.S3. continued

OR			
Bob Creek	1	1	1
Burnt Hill	1	1	
Cape Arago	1	1	1
Ecola	1	*	*
Fogarty Creek	1	1	1
WA Olympic Coast			
Kydikabbit Point		1	*
Point Grenville	1	1	*
Point of the Arches	1	*	*
Sokol Point; Chilean Memorial	1	*	*
Starfish Point	1	*	*
Taylor Point	1	*	*
WA Salish Sea			
Hat Island East	1	1	*
Hat Island West	1	1	*
Post Point	1	1	1
Saddlebag North Cove	1	1	*
Saddlebag South East	1	1	*

Table A.S4. Reference site growth rates (mm/yr).

site	latitude	longitude	region	mean growth rate (mm/yr)	standard error of growth rate
Andrew Molera	36.281	-121.863	CA Central	4.89	1.01
Arroyo Hondo	34.473	-120.145	CA South	13.57	5.049
Bob Creek	44.245	-124.114	OR	11.81	3.035
Bodega	38.318	-123.074	CA North Central	5.53	0.813
Cape Mendocino	40.341	-124.363	CA North	11.19	2.366
Carpenteria	34.395	-119.558	CA South	18.28	5.53
Damnation Creek	41.65249	-124.128	CA North	13.03	2.29
False Klamath	41.59476	-124.106	CA North	7.46	0.793
Fogarty Creek	44.837	-124.058	OR	6.23	1.399
Hopkins	36.621	-121.907	CA Central	20	8.281
Kibesillah Hill	39.60412	-123.789	CA North	4.05	1.494
Mill Creek	35.98	-121.49	CA Central	8.45	4.017
Mussel Shoals	34.35548	-119.441	CA South	31.39	4.401
Occulto	34.881	-120.64	CA Central	5.02	2.937
Point Fermin	33.707	-118.286	CA South	18.31	7.786
Scott Creek	37.046	-122.238	CA Central	12.34	5.482
Shaw Cove	33.545	-117.8	CA South	19.5	6.353
Stairs	34.731	-120.615	CA Central	11.48	5.136
Terrace	36.949	-122.065	CA Central	15.36	3.648
White Point	33.716	-118.32	CA South	8.66	3.736

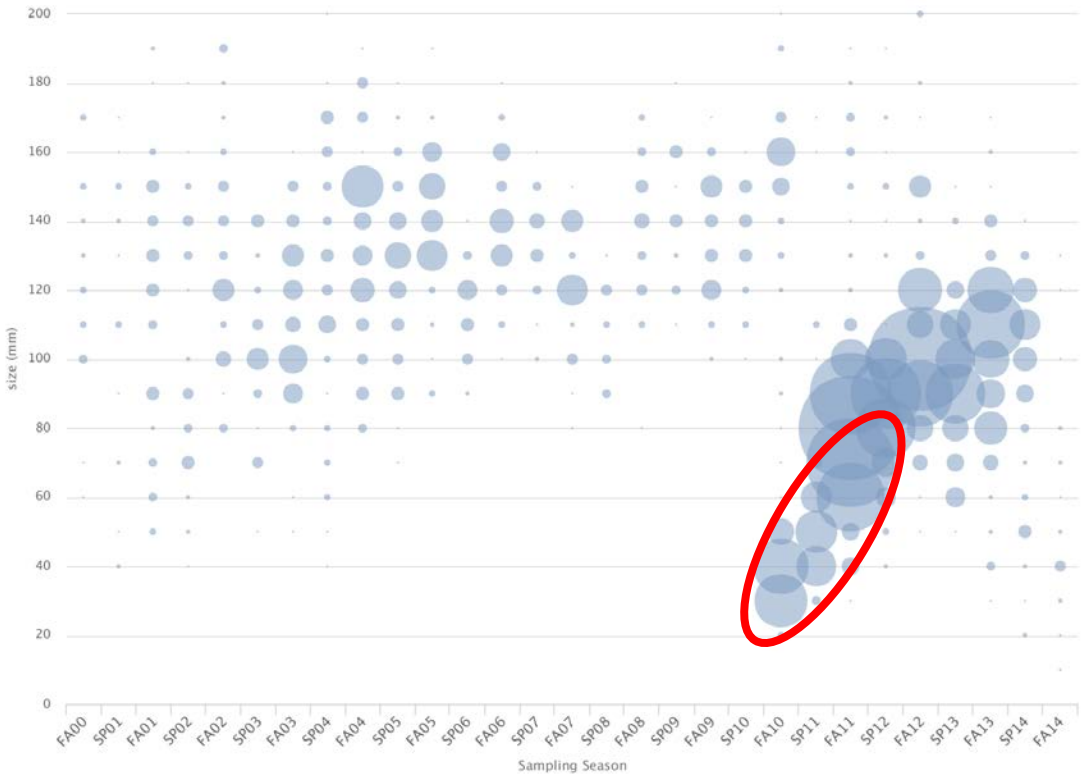

Fig A.S1. An example data visualization of *Pisaster ochraceus* abundance in different size classes over time using data from Mussel Shoals, California. Sea star size represents radius of the individual. The diameter of the circle corresponds to the number of sea stars in that size class at the given date. A recruitment pulse is circled in red. Plot courtesy of PISCO's interactive map and graphing tool at pacificrockyintertidal.org.

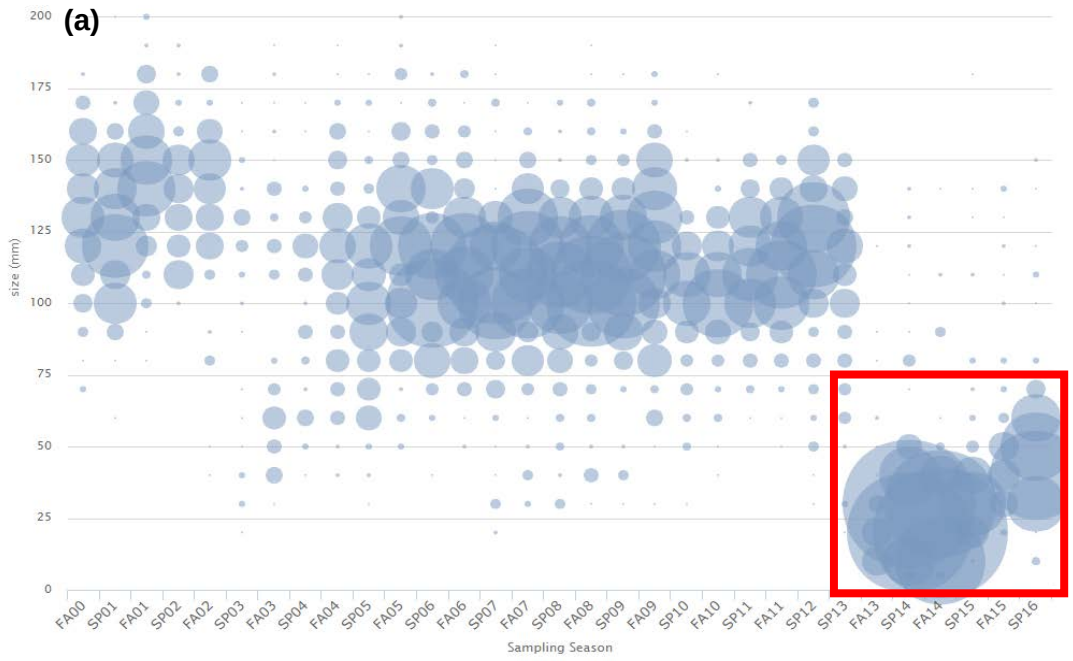

Fig A.S2. (a) Abundance of juvenile size classes of *Pisaster ochraceus* at Terrace Point in Santa Cruz, CA. This site is indicative of overall recruitment trends in the northern Monterey Bay. Sea star size represents radius of the individual. The size of the circles corresponds to the number of individuals in each size class. The area inside the red box is enlarged on the next page. **(b)** In 2014, a large number of individuals in the smallest size classes appeared, but they did not make it through to the next size classes in substantial numbers in 2015. Plots courtesy of PISCO's interactive map and graphing tool at pacificrockyintertidal.org.

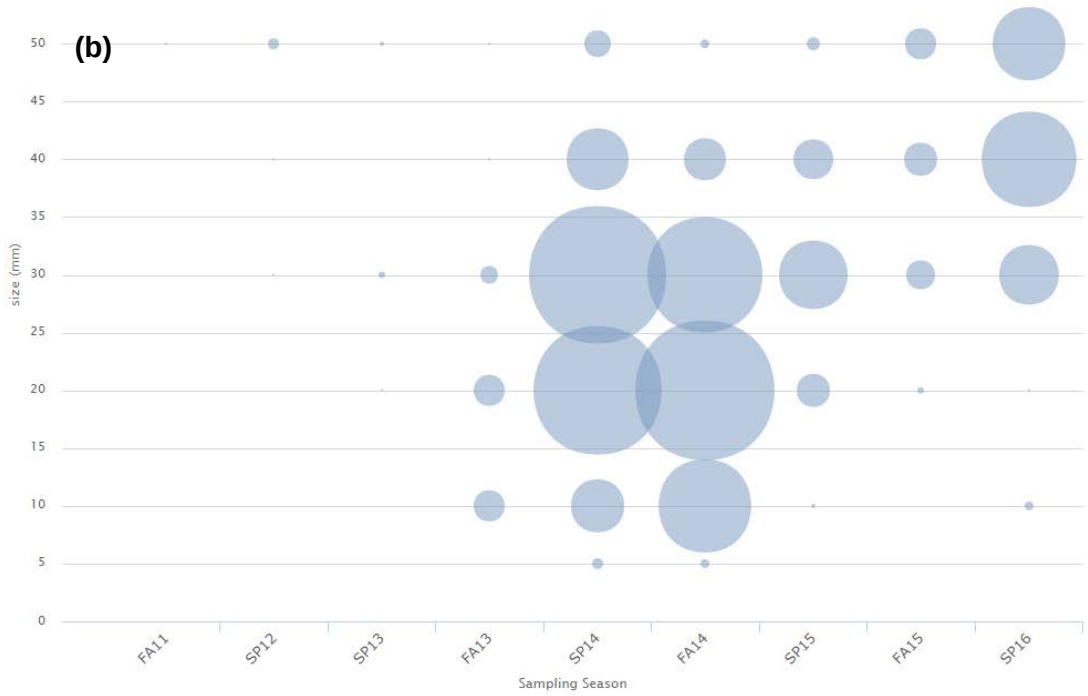

Fig A.S2. continued

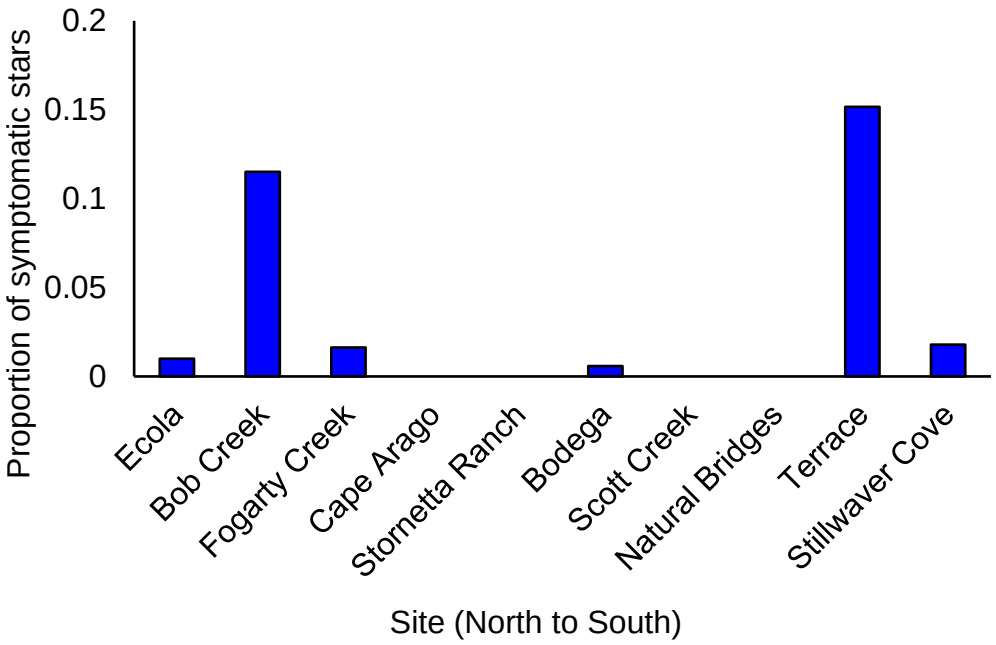

Fig A.S3. Proportion of P. ochraceus displaying Sea Star wasting Syndrome Symptoms during 2016 site surveys.

A2: Supplemental material for Chapter 2

Table A2.1. Description of geoprocessing methods, data transformations, and sources of data used in survival analysis modeling. All transformations were applied to meet assumptions of normality.

Data	Geographic Unit	Description	Source
Sea Star Wasting observations	Point	Dated observations and severities of sea star wasting syndrome on the Pacific Coast. Data were collected from PISCO/MARINe surveys, rapid response surveys, and citizen science reports. Citizen scientists submitted observations through a standardized webform: eeb.ucsc.edu/pacificrockyintertidal/data-products/sea-star-wasting/observation-log.html Distances from every point to the nearest site with SSWS present the week before the observation were calculated with the ArcGIS 10.4 Cost-Distance function, which restricted available space to 200 x 200 m cells centered over ocean water. All distances were log-transformed.	Partnership for the Interdisciplin-ary Studies of Coastal Oceans (PISCO 2014a) eeb.ucsc.edu/pacificrockyintertidal/data-products/sea-star-wasting/index.html

Intertidal *in situ* water temperature (SST)	Point	Intertidal thermistors are maintained at a suite of PISCO/MARINe sites from Point of the Arches, WA to Scripps Pier, CA to record water temperature every 15 minutes and averaged to calculate a daily mean. For intertidal sites, temperature measurements only include times when the temperature logger was submerged (i.e. temperatures recorded when the thermistor was exposed at low tide were excluded. For each week, we calculated degree heating weeks as number of degrees (^{o}C) above the 80th percentile temperature on record for that week of the year. We interpolated degree heating weeks between thermistor locations using the Inverse Distance Weighted Method in ArcGIS 10.4. Degree heating weeks were summed over a 12-week period preceding the week of observation and then square root-transformed. Interpolations from the CA Channel Islands were excluded due to lack of any temperature loggers in this region.	Partnership for the Interdisciplin-ary Studies of Coastal Oceans (PISCO) and the Multi-Agency Rocky Intertidal Network (MARINe 2008)
Tidal water level	Point	Water Level 6 Minute Verified Data were obtained for all tidal available height measurement stations on the US Pacific Coast (California, Oregon, Washington, and Alaska) from the NOAA Center for Operational Oceanographic Products and Services: opendap.co-ops.nos.noaa.gov/axis/webservices/waterlevelverifiedsixmin/index.jsp. Data interval spanned January 1, 2013 to December 31, 2013. We calculated the mean daily hours of low tide exposure (water level below 0.0 m Mean Low Low Water) between 12:00 and 16:00 Pacific Standard Time each day. Exposure hours were average by month to account for variation across multiple tidal cycles. We interpolated low tide exposure hours between stations using the Inverse Distance Weighted Method in	(NOAA Center for Operational Oceanograph-ic Products and Services 2015)

		ArcGIS 10.4. We assumed low tide exposure hours were the same as 2013 in every subsequent year. Exposure hours were square root-transformed.	
Remote sensing Chlorophyll a concentration (chl a)	0.1 degree x 0.1 degree	Chl a data for 0.1 degree, 8-day periods were obtained from NASA AQUA/MODIS ocean color data in mg/m^3. neo.sci.gsfc.nasa.gov/view.php?datasetId=MY1DMW_CHLORA&date=2015-10-01. Values were log-transformed. Missing values were then imputed using the Multivariate Normal Imputation in JMP Pro 13.	(MODIS 2014, NASA Earth Observations 2015)
Canadian population	Dissemin-ation Area	Dissemination Areas are the second smallest geographic unit recorded by the Canadian census, recording population in several thousand sub-city units of variable size. We calculated population density with the population and the area of the Dissemination Area. Distances from densely populated areas (>1,500 people per km^2) were square root-transformed.	(Statistics Canada 2011)
US population	Census Tract	Census Tracts are the standard unit for population measurement in the US, recording population in several thousand sub-city units of variable size. We calculated population density with the population and the area of the Census Tract. Distances from densely populated areas (>1,500 people per km^2) were square root-transformed.	(US Census Bureau 2010)
Mexican population	Basic Geostatist-ical Areas (AGEB)	AGEBs are the second smallest geographic unit recorded by the Mexican census, recording population in several thousand sub-city units of variable size. We calculated population density with the population and the area of the AGEB. Distances from densely populated areas (>1,500 people per km^2) were square root-transformed.	(National Institute of Statistics and Geography 2010)

Canada wastewater discharges	Point	The Canadian Ministry of the Environment requires all parties releasing pollutants or potentially polluted water to register for a Discharge Authorization. The coordinates of all Waste Discharge Authorizations registered with the Environmental Management Authorization Database for the province of British Columbia are available here: data.gov.bc.ca/dbc/catalogue/detail.page?config=dbc&P110=recorduid:176265&recorduid=176265&title=Waste%20Discharge%20Authorizations%20-%20All%20Discharges. Only discharge authorizations with a status of "Active" were incorporated. Entries with discharge type "air" were excluded from the map. We limited our analysis to discharges within coastal watersheds of British Columbia. Discharge points were grouped based on their effluent type: Wastewater Treatment (including storm water and sewage), Refinery, Aquatic (related to aquaculture or live aquatic and marine organisms), and Other. Distances to discharge points were square root-transformed.	(Ministry of the Environment 2014)
US wastewater discharges	Point	The US Environmental Protection Agency requires all parties discharging wastewater to register with the Permit Compliance System. The coordinates of all discharges in the states of California, Oregon, and Washington are available here: epa.gov/enviro/facts/pcs-icis/index.html. The coordinates of the discharge pipe location, rather than the source, were used for analysis. We limited our analysis to discharges within coastal watersheds of California, Oregon, and Washington. Discharge points were grouped based on their effluent type: Wastewater Treatment (including storm water and sewage), Industrial, Aquaculture, Refinery,	(United States Environment-al Protection Agency 2014)

		Power Plant, and Other. Distances to discharge points were square root-transformed.	
North American coastal watersheds	Area of watershed	Shapefiles of watershed boundaries, their local drainage locations, and their ultimate drainage locations were provided by the North American Atlas at a 1:10,000,000 scale.	(Natural Resources Canada et al. 2010)
Ports	Point	Port locations were represented as points. Distance-to-port calculations only considered ports within 5 km of coastal water bodies. Distances to ports were square root-transformed.	(Bureau of Transporta-tion Statistics 1998)
Marine SO_x emissions	4 km x 4 km	Model of ship emissions in the northern Pacific Ocean based on atmospheric models and shipping traffic. Distances from sites to ship emission polygons were square root-transformed.	(Corbet and Wang 2006)
Terrestrial disturbance	30 m x 30 m	The Nature Conservancy provided information on US land use through its Wind and Wildlife Landscape Assessment Tool: wind.tnc.org/#app=1db9&5362-selectedIndex=1&509c-selectedIndex=0. We measured the percent area of coastal watersheds covered by the following types of disturbance: crops, pasture, development, and total disturbance (any of the first three land use categories). For each pixel of land, TNC also provided a disturbance index of severity scaled from 0 to 1, which accounted for the type of disturbance and the impact of land use on surrounding lands. We calculated the mean disturbance index for each coastal watershed with land use data and assigned those values to all sea star observation sites within the corresponding watershed. Mean	(The Nature Conservancy and American Wind Wildlife Institute 1986)

		disturbance index and percent cover of disturbance types were square root-transformed. *Note:* In the San Juan Islands group, Washington, disturbance data was only given for San Juan Island. All other islands in the group were assumed to have similar levels of disturbance and were assigned data values for San Juan Island.	
Marine disturbance	1 km x 1 km	Marine disturbance indices developed for the Global Map of Human Impact on Marine Ecosystems were incorporated in the largest spatial extent available first from KNB knb.ecoinformatics.org/#view/doi:10.5063/F1S180FS and second from NCEAS nceas.ucsb.edu/globalmarine/ca_current_data when categories of data were not available from the first provider. Disturbance units were either a unitless magnitude or a scaled impact from 0 to 1 related to impact on a given pixel. We incorporated data from the Baja to Canada region for impacts of nutrient levels, sediment increase and decrease, ocean pollution, pesticide plumes, and fertilizer plumes by summing pixel values for each input into one composite variable ("ocean disturbance"). Values of this variable were then log transformed.	(Halpern et al. 2008, 2009)

Table A2. Comparison of model results with and without inclusion of a regional coefficient. A small reduction in AIC values of models containing the same variables was achieved when adding a coefficient for region. Baja California did not have sufficient observations to model risk of infection at a regional level.

region	AIC from regional constant + Disturbance PC1	AIC from constant + time + variable	ΔAIC without regional effect	regional effect value
Salish Sea	-238.01	-234.86	3.15	-1.032
WA Outer Coast	-28.28	-22.97	5.31	-0.966
OR	-48.36	-45.67	2.69	-0.962
CA North	-22.31	-22.17	0.14	-0.575
CA Central	-45.33	-37.71	7.62	-0.848
CA South	-51.26	-43.59	7.68	-1.326
CA Channel Islands	-83.33	-75.56	7.77	211.283
Baja California	NA	NA	NA	NA

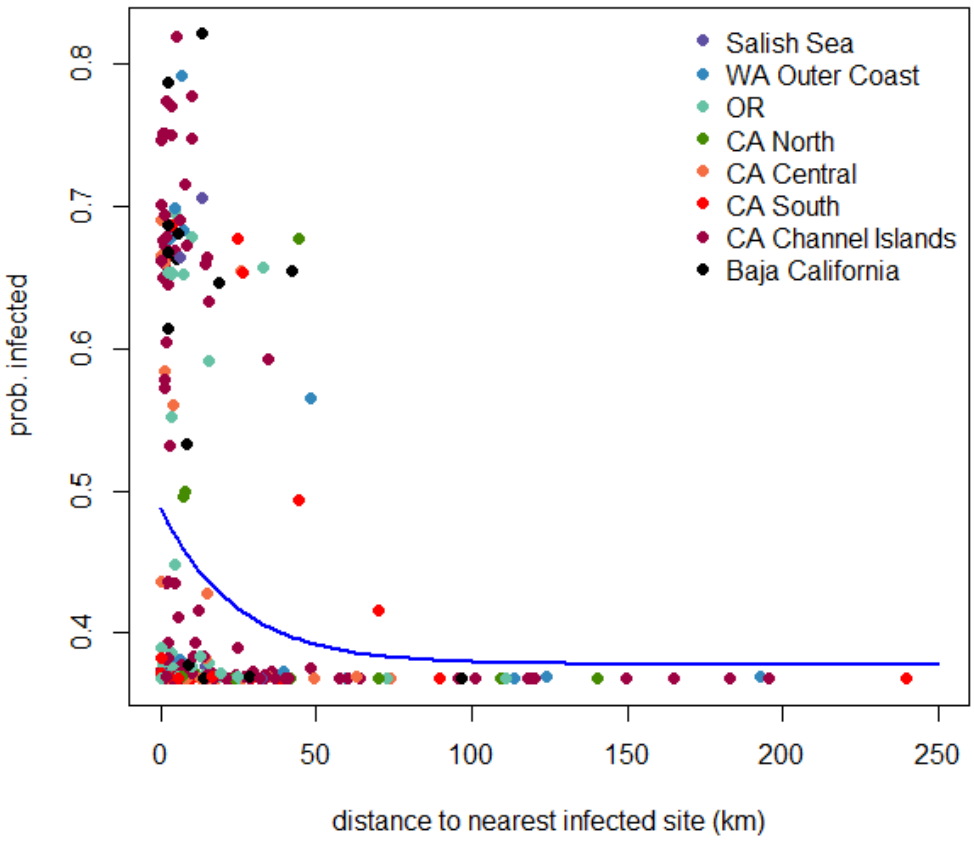

Fig. A2.1. Raw distance (km) from the nearest infected site at time of observation and predicted probability of SSWS infection.

A.3: Supplemental material for Chapter 3

Table A3.1. PISCO sites used for larger spatial scale comparisons of sea stars and mussels.

Site	Region
Duck Island	British Columbia
Ecola	Oregon
Damnation Creek	Northern California
Cape Mendocino	Northern California
Shelter Cove	Northern California
Kibesillah Hill	Northern California
Point Arena	North Central California
Saunders Reef	North Central California
Del Mar Landing	North Central California
Gerstle Cove	North Central California
Bodega	North Central California
Chimney Rock	North Central California
Fitzgerald Marine Reserve	North Central California
Año Nuevo	Central California
Scott Creek	Central California
Terrace Point	Central California
Point Pinos	Central California
Hopkins	Central California
Stillwater	Central California
Point Lobos	Central California
Andrew Molera	Central California
Point Sierra Nevada	Central California
Piedras Blancas	Central California
Cayucos	Central California
Hazards	Central California
Diablo	Central California
Stairs	Central California

Table A3.1. continued

Arroyo Hondo	Southern California
Alegria	Southern California
Government Point	Southern California
Coal Oil Point	Southern California
Mussel Shoals	Southern California
Shaw's Cove	Southern California

Table A3.2. Count of species found in each zone by year. Epibiont species are species found living on *Mytilus californianus* at least once, though they are not necessarily restricted to an epibiont lifestyle. Blank cells indicate none of that species were found.

species	Epibiont species	2014 bed	2014 zone 2	2014 zone 3	2017 bed	2017 contraction	2017 expansion	2017 zone 2	2017 zone 3
Anthopleura elegantissima	*		19	55		14	9	73	43
Anthopleura sola				3			5	7	12
Anthopleura xanthogrammica				2				29	7
Acrosiphonia spp.								1	1
Analipus spp.			27	5	14	2	6	16	2
articulated coralline algae	*	5	91	100	45	16	42	144	106
Balanus spp.	*	2	11	8	24	4	2	5	21
Callithamnion spp.	*		1	6	8			2	
Ceramium spp.				4					
Chondracanthus canaliculata		1		2				4	3
Chthamalus spp.	*	13	79	13	34	6	7	42	13
Cladophora spp.	*	1	4	1					
Codium fragile		1							
crustose coralline algae	*	4	40	68	4	31	11	86	50
Cryptopleura spp.			1						5
dead *Balanus spp.*						1	1		
dead *Mytilus californianus*		5			20	2	2		1
dead *Semibalanus spp.*					1		1		
dead *Tetraclita rubescens*					3	2			1

Table A3.2. continued

Egregia menziesii	*		2	14			9	17	24
Endocladia muricata	*	101	34	62	50		9		17
Fucus gardneri		2							
Gastroclonium spp.	*			14					8
Gelidium spp.			1	5					2
Mastocarpus jardinii	*	11	26	57	12			2	36
Mastocarpus papillatus	*			1				6	7
Mastocarpus spp. sporophyte		6	125	91	62	7	12	125	107
Mazzaella affinis	*		4	26	2			3	23
Mazzaella flaccida	*	37	48	123			4	35	40
Mazzaella leptorhynchos	*								9
Mazzaella splendens	*		26	45				33	24
Microcladia borealis	*	3	1	12				29	9
Microcladia coultouri				1					
Mytilus californianus		1641	129	84	2003	124	1424	243	142
Neorhodomella larix			1	18				9	10
Pelvitiopsis limitata	*	4			2				
Phragmatopoma californica	*	19	171	162	11	10	3	196	134
Phyllospadix spp.	*	34			2		3	1	1
Pikea robusta									4
Pollicipes polymerus	*	422	181	47	444	54	132	31	32
Polysiphonia spp.	*	2	7	1	2		1	16	2
Prionitis lanceolata				19					

Table A3.2. continued

Pyropia perforata	*	41	23	28	6		2	1	3
rock		124	269	125	205	51	143	252	128
sand				1					
Sarcodiotheca gaudichaudii				2					
Semibalanus spp.	*	19	26	2	29	5	18	25	8
Silvitia compressa	*	2			1				
Sponge (any spp.)								3	
Tetraclita rubescens	*	14	133	33	63	12	11	126	52
Ulva spp.	*	2		4	1	1		13	18
Total count		2517	1480	1252	3048	342	1857	1575	1105

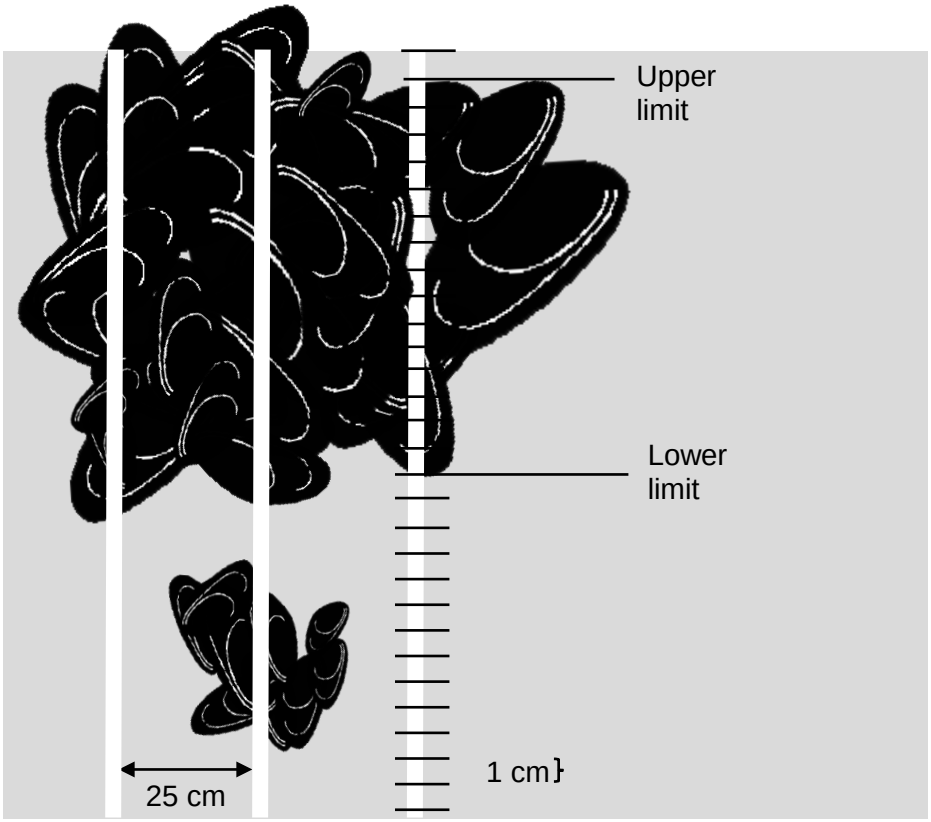

Fig A3.1. Schematic of mussel presence/absence sampling on point intercept transects. Mussel presence/absence was recorded every 1cm along the transect from the top of the rock wall to the bottom. Transects were spaced 25 cm apart horizontally across a 10 m span. Not drawn to scale.

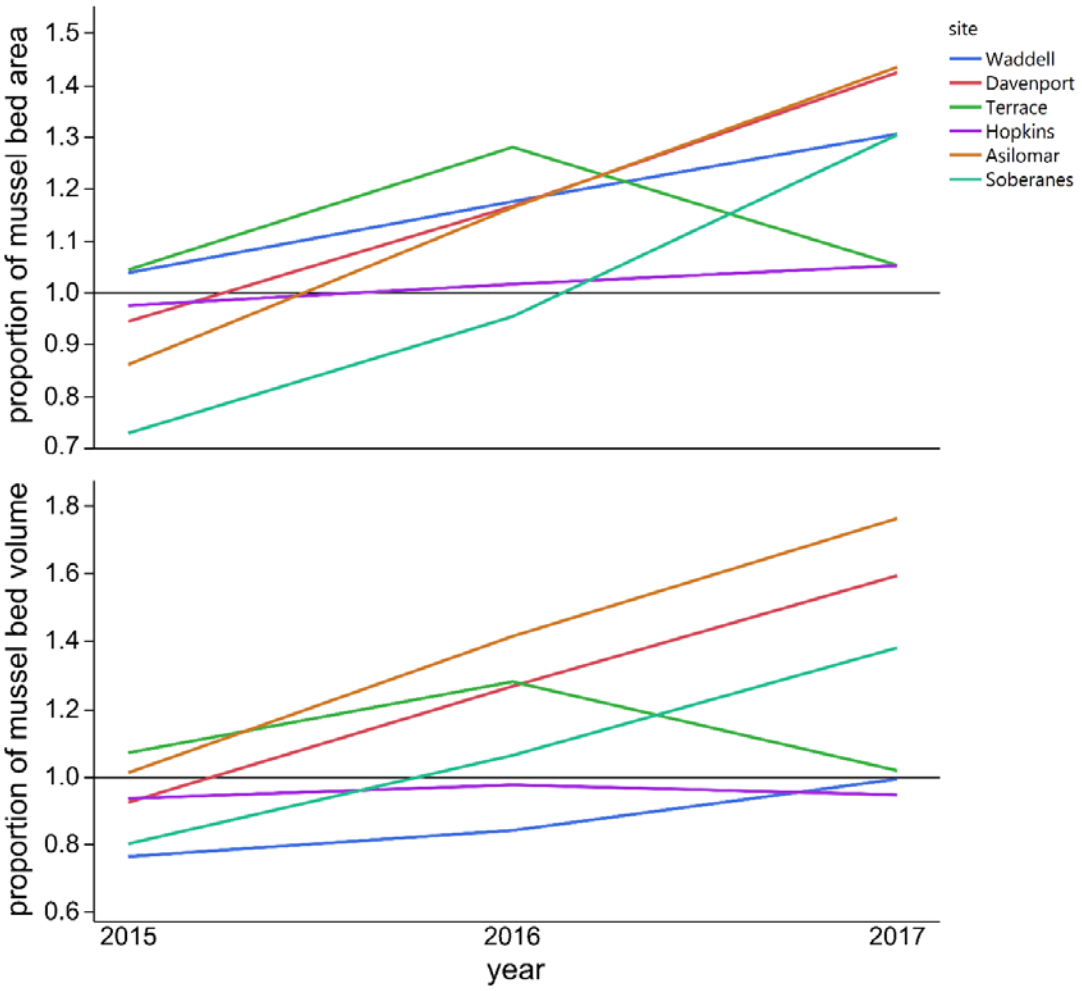

Fig A3.2. (a) Area of the mussel bed in years after SSWS outbreak, as a proportion of area of the bed in 2014. **(b)** Volume of the mussel bed in the years after SSWS outbreak, as a proportion of volume of the bed in 2014. Reference line (black) at y = 1.0 indicates parity with 2014 area or volume.

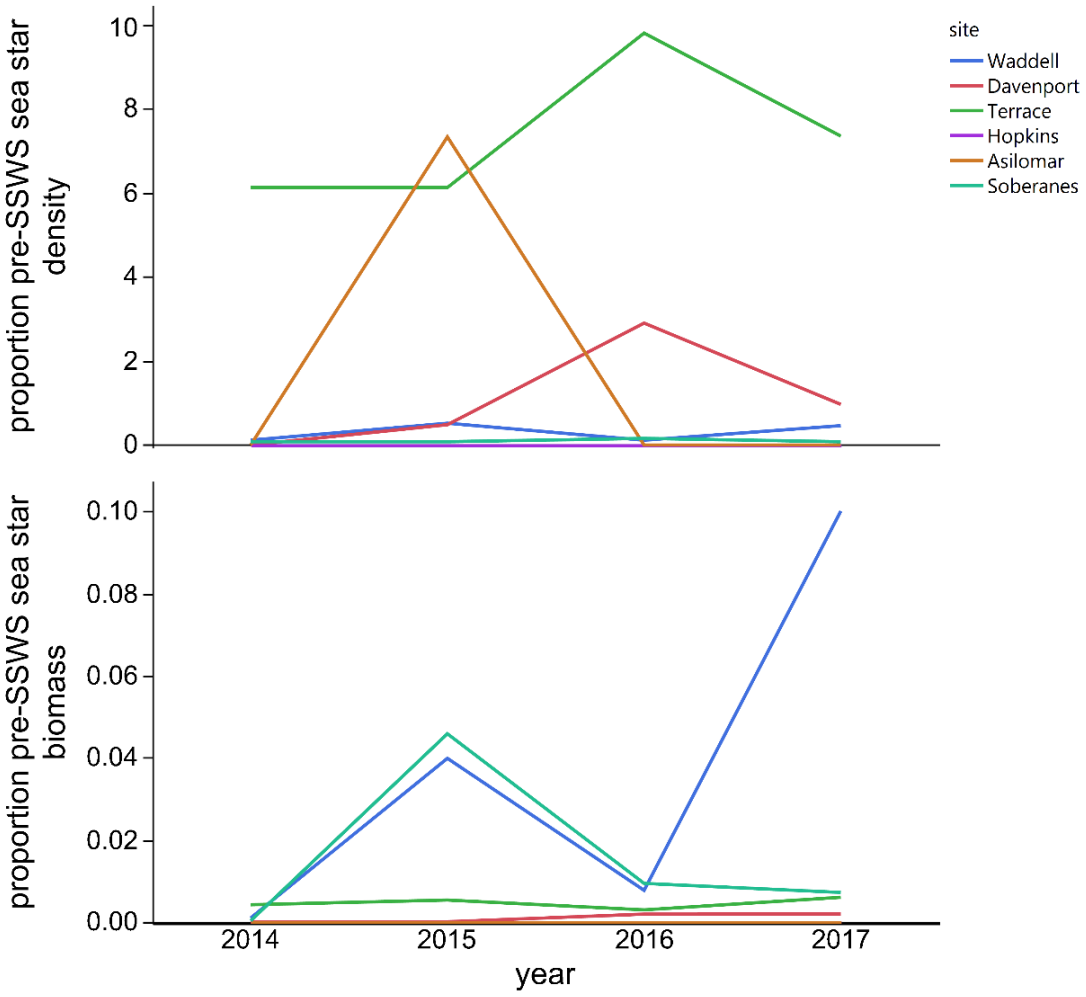

Fig A3.3. (a) Density and **(b)** biomass per square meter of *P. ochraceus* over time as a proportion of pre-SSWS estimates.

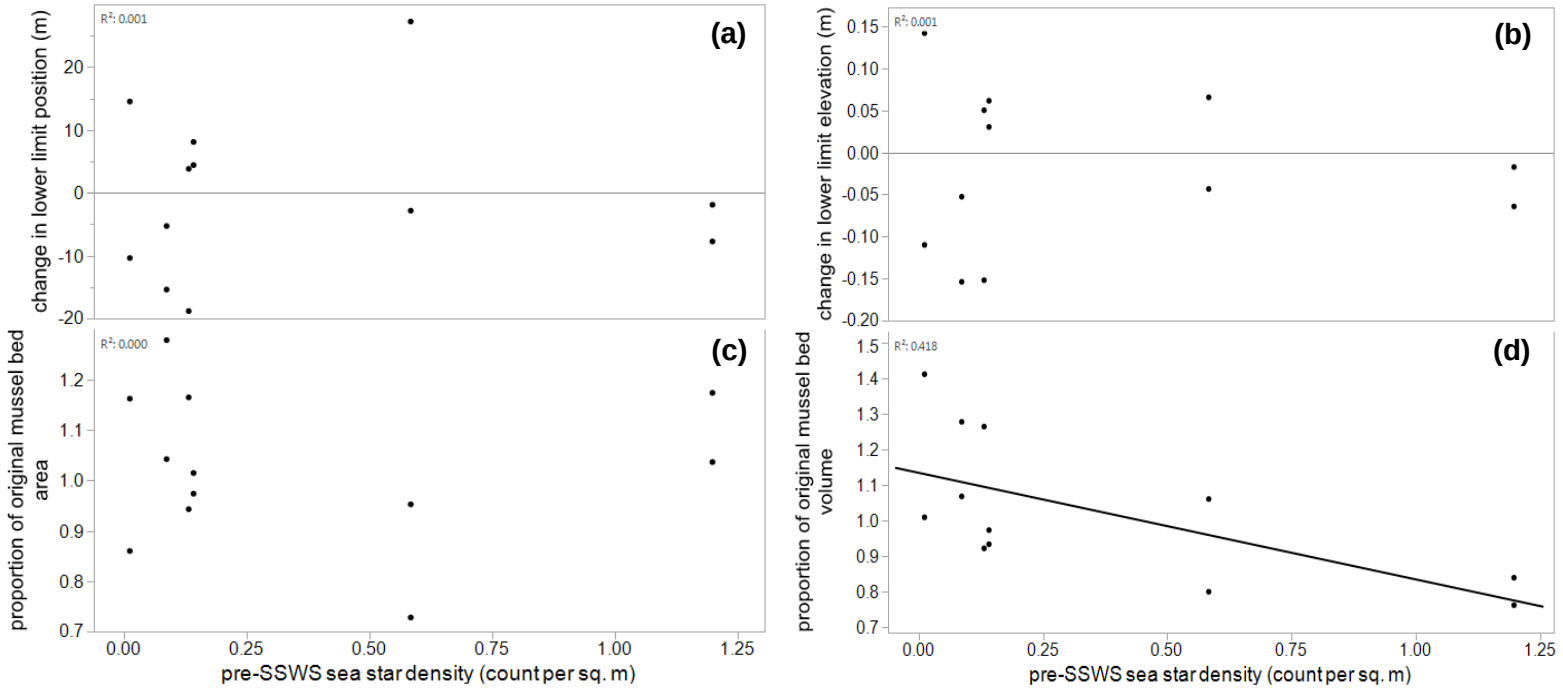

Fig A3.4. Pre-SSWS *P. ochraceus* densities were not correlated with **(a)** change in the position of the lower limit of the mussel bed, **(b)** change in the elevation of the lower limit, or **(c)** mussel bed area. **(d)** Pre-SSWS *P. ochraceus* density was negatively correlated with mussel bed volume. N=12.

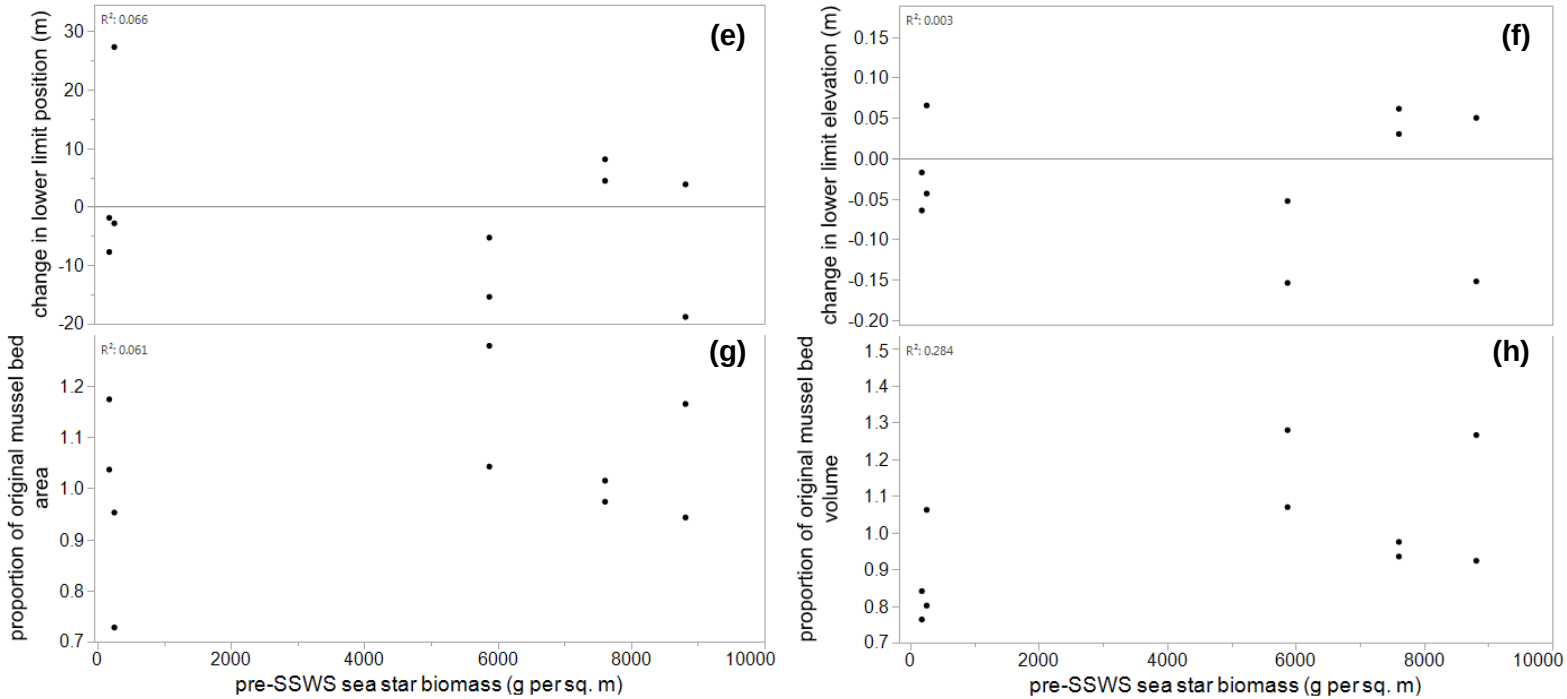

Fig. A3.4. continued Pre-SSWS biomass was not correlated with **(e)** change in position of the mussel bed, **(f)** change in the elevation of the lower limit, **(g)** mussel bed area, or **(h)** mussel bed volume. We used recruitment data from 2015 and 2016 only. N = 10.

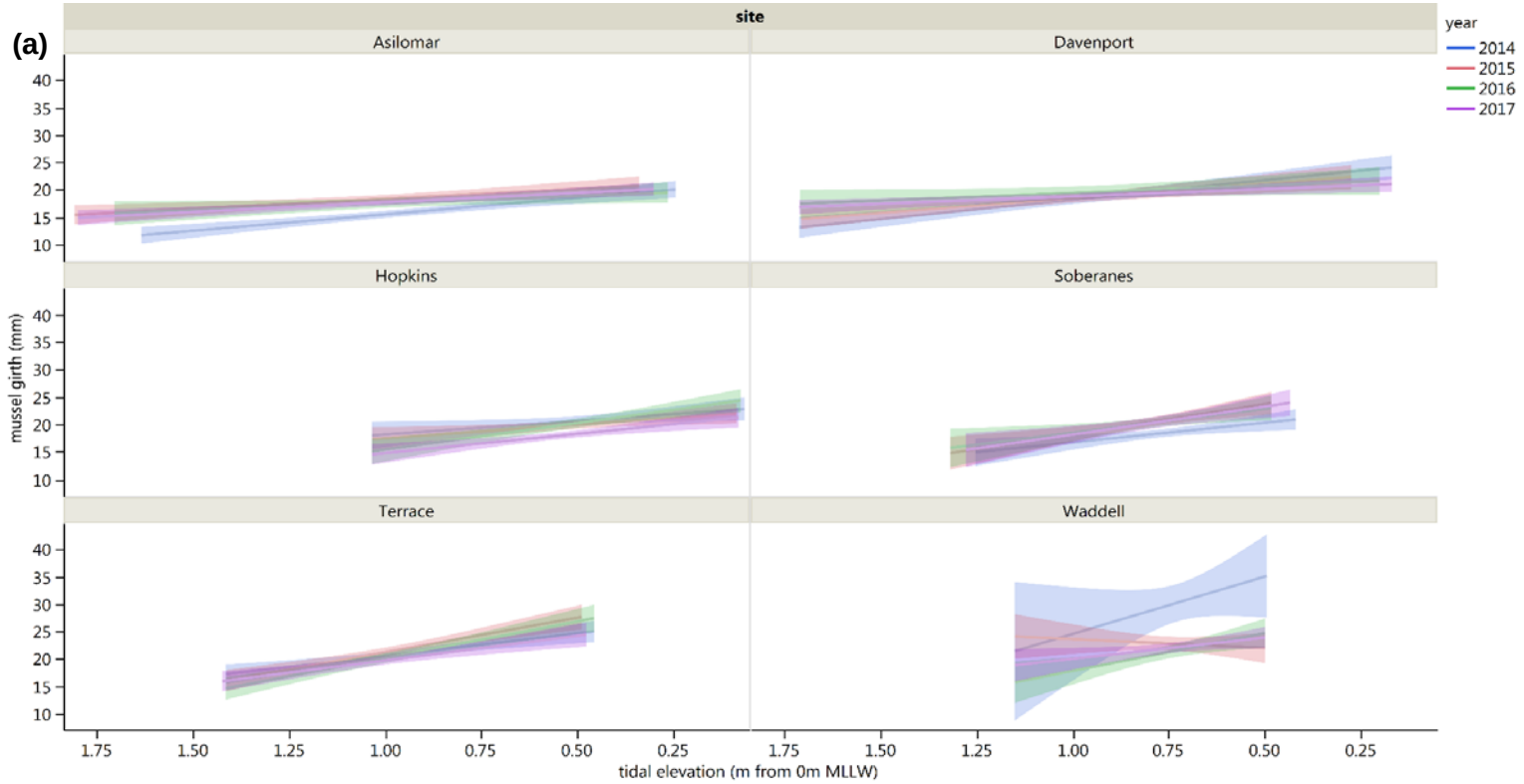

Fig A3.5. Relationship of mussel size with tidal elevation. **(a)** In the extent of the original 2014 mussel bed, mussel sizes increase at lower tidal elevations. N ≥ 90 mussels per site per year. **(b)** In the expansion zone, the relationship between mussel size and tidal elevation is site-specific. N ≥ 20 per site per year. Individual data points not shown for clarity. Note reversed x-axes.

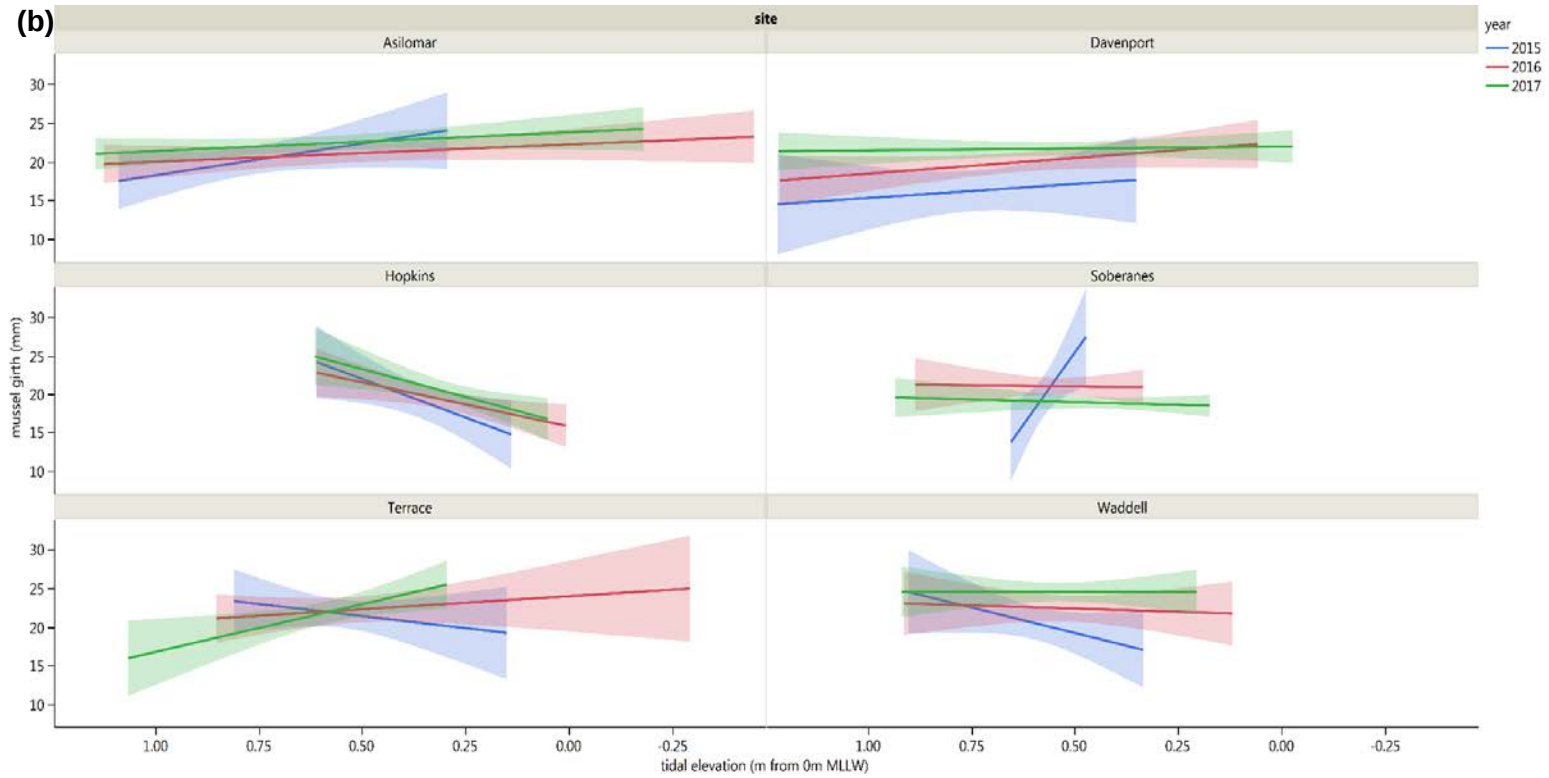

Fig A3.5. continued

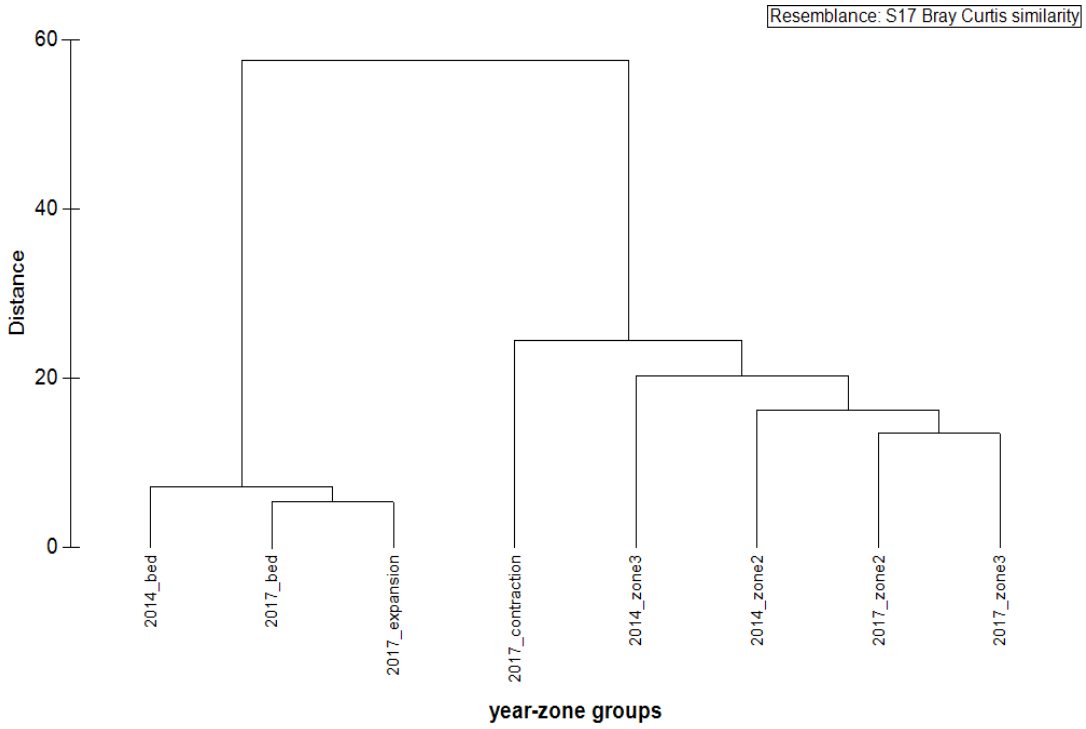

Fig A3.6. Differences in community composition (*Mytilus californianus* included) based on distance between group centroids in a Bray-Curtis similarity index.

Bibliography

Altizer, S., R. S. Ostfeld, P. T. J. Johnson, S. Kutz, and C. D. Harvell. 2013. Climate change and infectious diseases: from evidence to a predictive framework. Science 341:514–9.

Anderson, R. M., and R. M. May. 1991. A framework for discussion the popuation biology of infectious diseases. Pages 13–23 Infectious Diseases of Humans: Dynamics and Control. Oxford University Press, Oxford.

Anderson, R. S. 1987. Modulation of Nonspecific Immunity by Environmental Stressors. Page (J. A. Couch and J. W. Fournie, Eds.) Pathobiology of Marine and Estuarine Organisms. CRC Press, Boca Raton, FL.

Baker-Austin, C., J. a. Trinanes, N. G. H. Taylor, R. Hartnell, A. Siitonen, and J. Martinez-Urtaza. 2012. Emerging *Vibrio* risk at high latitudes in response to ocean warming. Nature Climate Change 3:73–77.

Bascompte, J., and P. Jordano. 2007. Mutualistic Networks: The Architecture of Biodiversity. Annual Review of Ecology, Evolution, and Systematics 38:567–593.

Bates, A. E., B. J. Hilton, and C. D. G. Harley. 2009. Effects of temperature, season and locality on wasting disease in the keystone predatory sea star *Pisaster ochraceus*. Diseases of Aquatic Organisms 86:245–251.

Bellwood, D. R., A. S. Hoey, and T. P. Hughes. 2012. Human activity selectively impacts the ecosystem roles of parrotfishes on coral reefs. Proceedings of the Royal Society B: Biological Sciences 279:1621–1629.

Bird, D. F., and J. Kalff. 1984. Empirical Relationships between Bacterial Abundance and Chlorophyll Concentration in Fresh and Marine Waters. Canadian Journal of Fisheries and Aquatic Sciences 41:1015–1023.

Blanchette, C. A., D. V Richards, J. M. Engle, B. R. Broitman, and S. D. Gaines. 2005. Regime shifts, community change and population booms of keystone predators at the Channel Islands. Proceedings of the California Islands Symposium 6:1–10.

Booth, D. J., and D. M. Brosnan. 1995. The role of recruitment dynamics in rocky shore and coral reef fish communities. Advances in Ecological Research 26: 309–385.

Bourne, D. G., M. Garren, T. M. Work, E. Rosenberg, G. W. Smith, and C. D. Harvell. 2009. Microbial disease and the coral holobiont. Trends in Microbiology 17:554–562.

Boyer, E. H. 1987. The natural disappearance of a top carnivore and its impact on an intertidal invertebrate community: the interplay of temperature and predation on community structure. University of Arizona. PhD Thesis. Department of Ecology and Evolutionary Biology.

Boyett, H. V., D. G. Bourne, and B. L. Willis. 2007. Elevated temperature and light enhance progression and spread of black band disease on staghorn corals of the Great Barrier Reef. Marine Biology 151:1711–1720.

Brodeur, R. D. 1991. Ontogenetic variations in the type and size of prey consumed by juvenile coho, *Oncorhynchus kisutch*, and chinook, *O. tshawytscha*, salmon. Environmental Biology of Fishes 30:303–315.

Broitman, B. R., C. A. Blanchette, B. A. Menge, J. Lubchenco, C. Krenz, M. Foley, P. T. Raimondi, D. Lohse, and S. D. Gaines. 2008. Spatial and Temporal Patterns of Invertebrate Recruitment Along the West Coast of the United States. Ecological Monographs 78:403–421.

Bruno, J. F., E. R. Selig, K. S. Casey, C. A. Page, B. L. Willis, C. D. Harvell, H. Sweatman, and A. M. Melendy. 2007. Thermal stress and coral cover as drivers of coral disease outbreaks. PLoS Biology 5:1220–1227.

Bucci, C., M. Francoeur, J. Mcgreal, R. Smolowitz, V. Zazueta-novoa, G. M. Wessel, and M. Gomez-chiarri. 2017. Sea Star Wasting Disease in *Asterias forbesi* along the Atlantic Coast of North America. PLoS ONE 12:e0188523.

Bureau of Transportation Statistics. 1998. North American Transportation Atlas Data (NORTAD). Research and Innovative Technology Administration, U.S. Department of Transportation:1.

Burge, C. A, C. Mark Eakin, C. S. Friedman, B. Froelich, P. K. Hershberger, E. E. Hofmann, L. E. Petes, K. C. Prager, E. Weil, B. L. Willis, S. E. Ford, and C. D. Harvell. 2014. Climate change influences on marine infectious diseases:

implications for management and society. Annual Review of Marine Science 6:249–77.

Caldwell, J. M., S. F. Heron, C. Mark Eakin, and M. J. Donahue. 2016. Satellite SST-based coral disease outbreak predictions for the Hawaiian Archipelago. Remote Sensing 8:93–107.

Center for Coastal Monitoring, and National Ocean Service. 2014. Mussel Watch Contaminant Monitoring. https://products.coastalscience.noaa.gov/collections/ltmonitoring/nsandt/data2.aspx. Accessed 1 January 2016.

Cerny-Chipman, E. B., J. M. Sullivan, and B. A. Menge. 2017. Whelk predators exhibit limited population responses and community effects following disease-driven declines of the keystone predator *Pisaster ochraceus*. Marine Ecology Progress Series 570:15–28.

Chen, C., T. Epp, and E. Jenkins. 2012. Predicting Weekly Variation of *Culex tarsalis* (Diptera: Culicidae) West Nile Virus Infection in a Newly Endemic Region, the Canadian Prairies. Journal of Medical Entomology 45:1144–1153.

Clemente, S., J. Lorenzo-Morales, J. C. Mendoza, C. López, C. Sangil, F. Alves, M. Kaufmann, and J. C. Hernández. 2014. Sea urchin *Diadema africanum* mass mortality in the subtropical eastern Atlantic: Role of waterborne bacteria in a warming ocean. Marine Ecology Progress Series 506:1–14.

Coe, W., and D. Fox. 1942. Biology of the California sea mussel (Mytilus californianus). Journal of Experimental Zoology 90:1–30.

Columbia, B., F. Centre, L. M. Dill, M. R. Heithaus, and C. J. Walters. 2003. Behaviorally mediated indirect interactions in marine communities and their conservation implications. Ecology 84:1151–1157.

Connell, J. 1972a. Community interactions on marine rocky intertidal shores. Annual Review of Ecology and Systematics 3:169–192.

Connell, J. 1978. Diversity in tropical rain forests and coral reefs. Science 199:1302–1310.

Connell, J. H. J. 1972b. Community Interactions on Marine Rocky Shores. Annual Review of Ecology and Systematics 3:169–192.

Connolly, S. R., and J. Roughgarden. 1998. A latitudinal gradient in northeast Pacific intertidal community structure: evidence for an oceanographically based synthesis of marine community theory. The American Naturalistaturalist 151:311–326.

Conway-Cranos, L. L. 2010. Recovery dynamics in rocky intertidal communities: Patterns, mechanisms and simulations. University of California, Santa Cruz.

Corbet, J., and C. Wang. 2006. North American Commercial Marine Vessel Emissions Inventory. Commission for Environmental Cooperation in North America.

Cox, D. R. 1972. Models and Life-Tables Regression. Journal of the Royal Statistical Society. Series B (Methodological) 34:187–220.

Crichton, N. 2002. Cox Proportional Hazards Model. Journal of Clinical Nursing 11:723.

Dayton, P. 1971. Competition, disturbance, and community organization: the provision and subsequent utilization of space in a rocky intertidal community. Ecological Monographs 41:351–389.

DelSesto, C. J. 2015. Assessing the Pathogenic Cause of Sea Star Wasting Disease in *Asterias forbesi* along the East Coast of the United States. University of Rhode Island. Masters thesis. Department of Biological and Environmental Sciences.

Dittman, D., and C. D. Robles. 1991. Effect of algal epiphytes on the mussel *Mytilus californianu*s. Ecology 72:286–296.

Donahue, M. J., R. A. Desharnais, C. D. Robles, and P. Arriola. 2011. Mussel Bed Boundaries as Dynamic Equilibria: Thresholds, Phase Shifts, and Alternative States. Ther American Naturalist 178:612–625.

Duggins, D. 1980. Kelp Beds and Sea Otters: An Experimental Approach. Ecology 61:447–453.

Dungan, M. L., T. E. Miller, and D. a Thomson. 1982. Catastrophic decline of a top carnivore in the Gulf of California rocky intertidal zone. Science 216:989–991.

Eckert, G. L., J. M. Engle, and D. J. Kushner. 2000. Sea star disease and population declines at the Channel Islands. Proceedings of the Fifth California Islands Symposium, US Minerals Management Service 5:390–393.

Eisenlord, M. E., M. L. Groner, R. M. Yoshioka, J. Elliott, J. Maynard, S. Fradkin, M. Turner, K. Pyne, N. Rivlin, R. van Hooidonk, and C. D. Harvell. 2016. Ochre star mortality during the 2014 wasting disease epizootic: role of population size structure and temperature. Philosophical Transactions of the Royal Society of London B: Biological Sciences 371.

Estes, J. A., N. S. Smith, and J. F. Palmisano. 1978. Sea Otter Predation and Community Organization in the Western Aleutian Islands, Alaska. Ecology 59:822–833.

Estes, J. A., M. T. Tinker, T. M. Williams, and D. F. Doak. 1998. Killer Whale Predation on Sea Otters Linking Oceanic and Nearshore Ecosystems. Science 282:473–476.

Feder, H. M. 1956. Natural history studies on the starfish *Pisaster ochraceus* (Brandt, 1835) in Monterey Bay area. Stanford University.

Feder, H. M. 1959. The Food of the Starfish, *Pisaster Ochraceus* Along the California Coast. Ecology 40:721–724.

Feder, H. M. 1970. Growth and predation by the ochre sea star, *Pisaster ochraceus* (Brandt), in Monterey Bay, California. Ophelia 8:165–185.

Ferrer, R. P., E. T. Lunsford, C. M. Candido, M. L. Strawn, and K. M. Pierce. 2015. Saxitoxin and the Ochre Sea Star: Molecule of Keystone Significance and a Classic Keystone Species. Integrative and Comparative Biology 55:533–542.

Fly, E. K., C. J. Monaco, S. Pincebourde, and A. Tullis. 2012. The influence of intertidal location and temperature on the metabolic cost of emersion in *Pisaster ochraceus*. Journal of Experimental Marine Biology and Ecology 422–423:20–28.

Fouchet, D., J. Le Pendu, J. S. Guitton, M. Guiserix, S. Marchandeau, and D. Pontier. 2009. Evolution of microparasites in spatially and genetically structured host populations: The example of RHDV infecting rabbits. Journal of Theoretical Biology 257:212–227.

Friedman, C. S., N. Wight, L. M. Crosson, G. R. VanBlaricom, and K. D. Lafferty. 2014. Reduced disease in black abalone following mass mortality: Phage therapy and natural selection. Frontiers in Microbiology 5:1–10.

Froeschke, G., and S. Von der Heyden. 2014. A review of molecular approaches for

investigating patterns of coevolution in marine host-parasite relationships. Pages 209–252 *in* D. Rollinson, editor. Advances in Parasitology. Elsevier Science, Oxford, UK.

Frontana-Uribe, S., J. de la Rosa-Vélez, L. Enríquez-Paredes, L. B. Ladah, and L. Sanvicente-Añorve. 2008. Lack of genetic evidence for the subspeciation of *Pisaster ochraceus* (Echinodermata: Asteroidea) in the north-eastern Pacific Ocean. Journal of the Marine Biological Association of the UK 88:395–400.

Fuess, L. E., M. E. Eisenlord, C. J. Closek, A. M. Tracy, R. Mauntz, S. Gignoux-Wolfsohn, M. M. Moritsch, R. Yoshioka, C. A. Burge, C. D. Harvell, C. S. Friedman, I. Hewson, P. K. Hershberger, and S. B. Roberts. 2015. Up in Arms: Immune and Nervous System Response to Sea Star Wasting Disease. Plos One 10:e0133053.

Gálvez, R., M. A. Descalzo, I. Guerrero, G. Miró, and R. Molina. 2011. Mapping the current distribution and predicted spread of the leishmaniosis sand fly vector in the Madrid region (Spain) based on environmental variables and expected climate change. Vector-Borne and Zoonotic Diseases 11:799–806.

Garza, C., and C. D. Robles. 2010. Effects of brackish water incursions and diel phasing of tides on vertical excursions of the keystone predator *Pisaster ochraceus*. Marine Biology 157:673–682.

George, S. B. 1999. Egg quality, larval growth and phenotypic plasticity in a forcipulate seastar. Journal of Experimental Marine Biology and Ecology 237:203–224.

Gibble, C. M., M. B. Peacock, and R. M. Kudela. 2016. Evidence of freshwater algal toxins in marine shellfish: Implications for human and aquatic health. Harmful Algae 59:59–66.

Groner, M. L., C. a. Burge, C. S. Couch, C. J. S. Kim, G. F. Siegmund, S. Singhal, S. C. Smoot, A. Jarrell, J. K. Gaydos, C. D. Harvell, and S. Wyllie-Echeverria. 2014. Host demography influences the prevalence and severity of eelgrass wasting disease. Diseases of Aquatic Organisms 108:165–175.

Groner, M. L., J. Maynard, R. Breyta, R. B. Carnegie, A. Dobson, C. S. Friedman, B. Froelich, M. Garren, M. D. Gulland, S. F. Heron, R. T. Noble, C. W. Revie, E. Weil, S. Wyllie-, J. D. Shields, and C. D. Harvell. 2016. Managing marine disease emergencies in an era of rapid change. Philosophical Transactions of the

Royal Society of London B: Biological Sciences 371:20150364.

Gudenkauf, B. M., and I. Hewson. 2015. Metatranscriptomic Analysis of *Pycnopodia helianthoides* (Asteroidea) Affected by Sea Star Wasting Disease. PloS one 10:e0128150.

Gutierrez, J. L., C. G. Jones, D. L. Strayer, and O. O. Iribarne. 2003. Mollusks as ecosystem engineers: the role of shell production in aquatic habitats. Oikos 101:79–90.

Halpern, B. S., C. V. Kappel, K. A. Selkoe, F. Micheli, C. M. Ebert, C. Kontgis, C. M. Crain, R. G. Martone, C. Shearer, and S. J. Teck. 2009. Mapping cumulative human impacts to California Current marine ecosystems. Conservation Letters 2:138–148.

Halpern, B. S., S. Walbridge, K. A. Selkoe, C. V. Kappel, F. Micheli, C. D'Agrosa, J. F. Bruno, K. S. Casey, C. Ebert, H. E. Fox, R. Fujita, D. Heinemann, H. S. Lenihan, E. M. P. Madin, M. T. Perry, E. R. Selig, M. Spalding, R. Steneck, and R. Watson. 2008. A Global Map of Human Impact on Marine Ecosystems. Science 319:948–953.

Hamilton, S. L., and J. E. Caselle. 2015. Exploitation and recovery of a sea urchin predator has implications for the resilience of southern California kelp forests. Proceedings of the Royal Society of London. Series B, Biological Sciences 282:20141817.

Harley, C. D. G., M. S. Pankey, J. P. Wares, R. K. Grosberg, and M. J. Wonham. 2006. Color Polymorphism and Genetic Structure in the Sea Star *Pisaster ochraceus.* Biological Bulletin 211:248–262.

Hart, D. M. 2010. Generality and consequences of keystone predation in rocky intertidal habitats of Central California. University of California, Santa Cruz. PhD Thesis. Department of Ecology and Evolutionary Biology.

Harvell, C. D., K. Kim, J. M. Burkholder, R. P. Colwell, D. J. Grimes, E. E. Hofmann, E. K. Lipp, A. D. M. E. Osterhaus, R. M. Overstreet, J. W. Porter, G. W. Smith, and G. R. Vasta. 1999. Emerging Marine Diseases--Climate Links and Anthropogenic Factors. Science 285:1505–1510.

Hatcher, M. J., J. T. A. Dick, and A. M. Dunn. 2006. How parasites affect interactions between competitors and predators.

Heisey, D. 2009a. Chapter 1: Survival and Hazard Functions – S(t) and h(t). Pages 1–19 A primer of wildlife event time analysis using WinBUGS. Madison, WI.

Heisey, D. 2009b. Chapter 2: Basic Estimation of S(t) and h(t). Pages 1–20 A primer of wildlife event time analysis using WinBUGS. United States Geological Survey, Madison, WI.

Hewson, I., K. S. I. Bistolas, E. M. Quijano Cardé, J. B. Button, P. J. Foster, J. M. Flanzenbaum, J. Kocian, and C. K. Lewis. 2018. Investigating the Complex Association Between Viral Ecology, Environment, and Northeast Pacific Sea Star Wasting. Frontiers in Marine Science 5:00077.

Hewson, I., J. B. Button, B. M. Gudenkauf, B. Miner, A. L. Newton, J. K. Gaydos, J. Wynne, C. L. Groves, G. Hendler, M. Murray, S. Fradkin, M. Breitbart, E. Fahsbender, K. D. Lafferty, a M. Kilpatrick, C. M. Miner, P. Raimondi, L. Lahner, C. S. Friedman, S. Daniels, M. Haulena, J. Marliave, C. a Burge, M. E. Eisenlord, and C. D. Harvell. 2014. Densovirus associated with sea-star wasting disease and mass mortality. Proceedings of the National Academy of Sciences 111:17278–17283.

Hughes, B. B., R. Beas-Luna, A. K. Barner, K. Brewitt, D. R. Brumbaugh, E. B. Cerny-Chipman, S. L. Close, K. E. Coblentz, K. L. De Nesnera, S. T. Drobnitch, J. D. Figurski, B. Focht, M. Friedman, J. Freiwald, K. K. Heady, W. N. Heady, A. Hettinger, A. Johnson, K. A. Karr, B. Mahoney, M. M. Moritsch, A. M. K. Osterback, J. Reimer, J. Robinson, T. Rohrer, J. M. Rose, M. Sabal, L. M. Segui, C. Shen, J. Sullivan, R. Zuercher, P. T. Raimondi, B. A. Menge, K. Grorud-Colvert, M. Novak, and M. H. Carr. 2017. Long-Term studies contribute disproportionately to ecology and policy. BioScience 67:271–278.

Hughes, J., L. Deegan, and J. Wyda. 2002. The effects of eelgrass habitat loss on estuarine fish communities of southern New England. Estuaries 25:235–249.

Hughes, T. P. 1994. Catastrophes, Phase Shifts, and Large-Scale Degradation of a Caribbean Coral Reef. Science 265:1547–1551.

Jellett, J. F., and R. E. Scheibling. 1988. Effect of Temperature and Prey Availability on Growth of Paramoeba invadens in Monoxenic Culture. Applied and environmental microbiology 54:1848–1854.

Jousimo, J., A. J. M. Tack, O. Ovaskainen, T. Mononen, H. Susi, C. Tollenaere, and A.-L. Laine. 2014. Ecological and evolutionary effects of fragmentation on

infectious disease dynamics. Science 344:1289–93.

Jurgens, L. J., L. Rogers-Bennett, P. T. Raimondi, L. M. Schiebelhut, M. N. Dawson, R. K. Grosberg, and B. Gaylord. 2015. Patterns of mass mortality among rocky shore invertebrates across 100 km of northeastern Pacific coastline. PLoS ONE 10:1–21.

Keesing, F., R. D. Holt, and R. S. Ostfeld. 2006. Effects of species diversity on disease risk. Ecology Letters 9:485–498.

Keever, C. C., J. Sunday, J. B. Puritz, J. A. Addison, R. J. Toonen, R. K. Grosberg, and M. W. Hart. 2009. Discordant distribution of populations and genetic variation in a sea star with high dispersal potential. Evolution 63:3214–3227.

Kilpatrick, A. M., M. A. Meola, R. M. Moudy, and L. D. Kramer. 2008. Temperature, viral genetics, and the transmission of West Nile virus by *Culex pipiens* mosquitoes. PLoS Pathogens 4:e1000092.

Kohl, W. T., T. I. Mcclure, and B. G. Miner. 2016. Decreased Temperature Facilitates Short- Term Sea Star Wasting Disease Survival in the Keystone Intertidal Sea Star *Pisaster ochraceus*. PLoS ONE 11:e0153670.

Kroeker, K. J., J. M. Rose, C. A. Blanchette, F. P. Chavez, B. Helmuth, M. Hill, G. E. Hofmann, M. A. McManus, B. M. Menge, K. J. Nielsen, P. T. Raimondi, A. D. Russell, and L. Washburn. 2016. Interacting environmental mosaics drive geographic variation in mussel performance and predation vulnerability. Ecology Letters 19:771–779.

Kumar, D., and B. Klefsjo. 1994. Proportional hazards model: a review. Reliability Engineering and System Safety 44:177–188.

Lafferty, K. D., and A. M. Kuris. 1999. How environmental stress affects the impacts of parasites. Limnology and Oceanography 44:925–931.

Lafferty, K. D., and T. H. Suchanek. 2016. Revisiting Paine's 1966 Sea Star Removal Experiment, the Most-Cited Empirical Article in the *American Naturalist*. The American Naturalist 188:000–000.

Lamb, J. B., A. S. Wenger, M. J. Devlin, D. M. Ceccarelli, D. H. Williamson, and B. L. Willis. 2016. Reserves as tools for alleviating impacts of marine disease. Philosophical Transactions of the Royal Society of London B: Biological Sciences 371:20150210.

Lamb, J. B., B. L. Willis, E. A. Fiorenza, C. S. Couch, R. Howard, D. N. Rader, J. D. True, L. A. Kelly, A. Ahmad, J. Jompa, and C. D. Harvell. 2018. Plastic waste associated with disease on coral reefs. Science 359:460–462.

Landenberger, D. E. 1968. Studies on Selective Feeding in the Pacific Starfish *Pisaster* in Southern California. Ecology 49:1062–1075.

Leighton, B., J. Boom, C. Bouland, E. Hartwick, and M. Smith. 1991. Castration and mortality in *Pisaster ochraceus* parasitized by *Orchitophyra stellarum* (Ciliophora). Diseases of Aquatic Organisms 10:71–73.

Leising, A. W., I. Schroeder, S. Bograd, J. Abell, R. Durazo, G. Caxiola-Castro, E. Bjorkstedt, J. Field, K. Sakuma, R. Robertson, R. Goericke, W. Peterson, R. Brodeur, C. Barcelo, T. Auth, E. Daly, R. Suryan, A. Gladics, J. Porquez, S. McClatchie, E. Weber, W. Watson, J. Santora, W. Sydeman, S. Melin, F. Chavez, R. Golightly, S. Schneider, J. Fisher, C. Morgan, R. Bradley, and P. Warybok. 2015. State of the California Current 2014-15: Impacts of the warm-water "Blob." CalCOFI Report 56:31–68.

Lessios, H. A. 1988. Mass Mortality of Diadema Antillarum in the Caribbean: What Have We Learned? Annual Review of Ecology and Systematics 19:371–393.

Ling, S. D., C. R. Johnson, S. D. Frusher, and K. R. Ridgway. 2009. Overfishing reduces resilience of kelp beds to climate-driven catastrophic phase shift. Proceedings of the National Academy of Sciences 106:22341–22345.

Littler, M., D. Martz, and D. Littler. 1983. Effects of recurrent sand deposition on rocky intertidal organisms: importance of substrate heterogeneity in a fluctuating environment. Marine Ecology Progress Series 11:129–139.

Lohse, D. P. 1993a. The importance of secondary substratum intertidal community in a rocky intertidal community. Journal of Experimental Marine Biology and Ecology 166:1–17.

Lohse, D. P. 1993b. The effects of substratum type on the population dynamics of three common intertidal animals. Journal of Experimental Marine Biology and Ecology 173:133–154.

MARINe. 2008. Unified Monitoring Protocols for the Multi-Agency Rocky Intertidal Network Unified Monitoring Protocols for the Multi-Agency Rocky Intertidal Network:1–84.

MARINe. 2013. Unprecedented Sea Star Mass Mortality along the West Coast of North America due to Wasting Syndrome. Press Release:1–3.

Mauzey, K., C. Birkeland, and P. Dayton. 1968. Feeding behavior of asteroids and escape responses of their prey in the Puget Sound region. Ecology 49:603–619.

McClintock, J. B., and T. J. Robnett. 1986. Size Selective Predation by the Asteroid *Pisaster ochraceus* on the Bivalve *Mytilus californianus*: A Cost-Benefit Analysis. Marine Ecology 7:321–332.

Meentemeyer, R., D. Rizzo, W. Mark, and E. Lotz. 2004. Mapping the risk of establishment and spread of sudden oak death in California. Forest Ecology and Management 200:195–214.

Menge, B. A. 1983. Components of predation intensity in the low zone of the New England rocky intertidal region. Oecologia 58:141–155.

Menge, B. A. 1995. Indirect Effects in Marine Rocky Intertidal Interaction Webs: Patterns and Importance. Ecological Monographs 65:21–74.

Menge, B. A. 2000. Top-down and bottom-up community regulation in marine rocky intertidal habitats. Journal of Experimental Marine Biology and Ecology 250:257–289.

Menge, B. A., E. L. Berlow, C. A. Blanchette, S. A. Navarrete, and B. Yamada. 1994. The Keystone Species Concept: Variation in Interaction Strength in a Rocky Intertidal Habitat. Ecological Monographs 64:249–286.

Menge, B. A., E. B. Cerny-chipman, A. Johnson, J. Sullivan, S. Gravem, and F. Chan. 2016. Sea Star Wasting Disease in the Keystone Predator Pisaster ochraceus in Oregon : Insights into Differential Population Impacts, Recovery, Predation Rate, and Temperature Effects from Long-Term Research. PLoS ONE 11:e0153994.

Menge, B. A., F. Chan, K. J. Nielsen, E. Di Lorenzo, and J. Lubchenco. 2009. Climatic variation alters supply-side ecology: Impact of climate patterns on phytoplankton and mussel recruitment. Ecological Monographs 79:379–395.

Menge, B. A. 1992. Community Regulation : Under What Conditions Are Bottom-Up Factors Important on Rocky Shores? Ecology 73:755–765.

Menge, B., and C. Blanchette. 2004. Species interaction strength: testing model

predictions along an upwelling gradient. Ecological Monographs 74:663–684.

Menge, J. L., and B. A. Menge. 1974. Role of resource allocation, aggression and spatial heterogeneity in coexistence of two competing intertidal starfish. Ecological Monographs 44:189–209.

Miller, M. A., R. M. Kudela, A. Mekebri, D. Crane, S. C. Oates, M. T. Tinker, M. Staedler, W. A. Miller, S. Toy-Choutka, C. Dominik, D. Hardin, G. Langlois, M. Murray, K. Ward, and D. A. Jessup. 2010. Evidence for a novel marine harmful algal bloom: Cyanotoxin (microcystin) transfer from land to sea otters. PLoS ONE 5:e12576.

Miner, C. M., J. M. Altstatt, P. T. Raimondi, and T. E. Minchinton. 2006. Recruitment failure and shifts in community structure following mass mortality limit recovery prospects of black abalone. Marine Ecology Progress Series 327:107–117.

Miner, C. M., J. L. Burnaford, R. F. Ambrose, L. Antrim, H. Bohlmann, C. A. Blanchette, J. M. Engle, S. C. Fradkin, R. N. Gaddam, C. D. G. Harley, B. G. Miner, S. N. Murray, J. R. Smith, S. G. Whitaker, and P. T. Raimondi. 2018. Large-scale impacts of sea star wasting disease (SSWD) on intertidal sea stars and implications for recovery. PLoS ONE 13:e0192870.

Ministry of the Environment. 2014. Waste Discharge Authorizations - All Discharges. Government of Canada.

MODIS. 2014. Ocean Color Chlorophyll Reprocessing 2014.0. http://neo.sci.gsfc.nasa.gov/view.php?datasetId=MY1DMW_CHLORA&date=2015-10-01. Accessed 1 January 2016.

Monaco, C. J., D. S. Wethey, S. Gulledge, and B. Helmuth. 2015. Shore-level size gradients and thermal refuge use in the predatory sea star *Pisaster ochraceus*: the role of environmental stressors. Marine Ecology Progress Series 539:191–205.

Monaco, C. J., D. S. Wethey, and B. Helmuth. 2014. A Dynamic Energy Budget (DEB) model for the keystone predator Pisaster ochraceus. PloS one 9:e104658.

Monaco, C. J., D. S. Wethey, and B. Helmuth. 2016. Thermal sensitivity and the role of behavior in driving an intertidal predator-prey interaction. Ecological Monographs 86:429–447.

Montecino, D., M. E. Eisenlord, M. Turner, C. D. Harvell, R. Yoshioka, C. V

Pattengill-Semmens, and J. K. Gaydos. 2016. Devastating transboundary impacts of Sea Star Wasting Disease on subtidal asteroids. PLoS ONE 11:e0163190.

Moritsch, M. M., and P. Raimondi. 2018. Reduction and recovery of keystone predation pressure after disease-related mass mortality. Ecology and Evolution 8:3952–3964.

Multi-Agency Rocky Intertidal Network (MARINe). 2014. *Pisaster ochraceus* symptoms guide. University of California Santa Cruz. https://www.eeb.ucsc.edu/pacificrockyintertidal/data-products/sea-star-wasting/#id-guides. Accessed 12 July 2017.

Mydlarz, L. D., L. E. Jones, and C. D. Harvell. 2006. Innate immunity, environmental drivers, and disease ecology of marine and freshwater invertebrates. Annual Review of Ecology, Evolution, and Systematics 37:251–288.

NASA Earth Observations. 2015. CHLOROPHYLL CONCENTRATION (8 DAY - AQUA/MODIS). http://neo.sci.gsfc.nasa.gov/view.php?datasetId=MY1DMW_CHLORA&date=2015-10-01. Accessed 1 January 2016.

National Institute of Statistics and Geography. 2010. Census of Population and Housing 2010.

Natural Resources Canada, National Institute of Statistics and Geography, and US Geological Survey. 2010. North American Atlas - Basin Watersheds.

de Nesnera, K. 2016. Linking ecology, restoration science, and litigation policy to guide management of rocky intertidal habitats affected by oil spills. University of California, Santa Cruz. PhD Thesis. Department of Ecology and Evolutionary Biology.

de Nesnera, K. L. 2016. Stress, ontogeny, and movement determine the relative importance of facilitation for juvenile mussels. Ecology 97:2199–2205.

NOAA Center for Operational Oceanographic Products and Services. 2015. Parameters Description.

Ohman, M. D., N. Mantua, J. Keister, M. Garcia-reyes, and S. Mcclatchie. 2016. ENSO impacts on ecosystem indicators in the California Current System. US Clivar Variations 15:8–15.

Paine, R. 1974. Intertidal community structure: experimental studies on the relationship between a dominant competitor and its principal predator. Oceologia 15:93–120.

Paine, R. T. 1966. Food Web Complexity and Species Diversity. The American Naturalist 100:65–75.

Paine, R. T. 1969a. A Note on Trophic Complexity and Community Stability. The American Naturalist 103:91–93.

Paine, R. T. 1969b. The Pisaster-Tegula interaction: prey patches, predator food preference, and intertidal community structure. Ecology 50:950–961.

Paine, R. T. 1976. Size-Limited Predation: An Observational and Experimental Approach with the Mytilus-Pisaster Interaction. Ecology 57:858–873.

Paine, R. T., and S. a Levin. 1981. Intertidal Landscapes : Disturbance and the Dynamics of Pattern. Ecological Monographs 51:145–178.

Pankey, M. S., and J. P. Wares. 2009. Overdominant maintenance of diversity in the sea star Pisaster ochraceus. Journal of Evolutionary Biology 22:80–7.

Peacock, M. B., C. M. Gibble, D. B. Senn, J. E. Cloern, and R. M. Kudela. 2018. Blurred lines: Multiple freshwater and marine algal toxins at the land-sea interface of San Francisco Bay, California. Harmful Algae 73:138–147.

Pearse, J., J. McClintock, K. Vicknair, and H. M. Feder. 2010. Long-term population changes in sea stars at three contrasting sites. Pages 633–640 *in* L. G. Harris, S. A. Botteger, C. W. Walker, and M. P. Lesser, editors. Echinoderms: Durham. Taylor & Francis Group, London.

Petes, L. E., M. E. Mouchka, R. H. Milston-Clements, T. S. Momoda, and B. A. Menge. 2008. Effects of environmental stress on intertidal mussels and their sea star predators. Oecologia 156:671–680.

Pfister, C. A., R. T. Paine, and J. T. Wootton. 2016. The iconic keystone predator has a pathogen. Frontiers in Ecology and the Environment 14:285–286.

Phillips, N. E. 2007. A spatial gradient in the potential reproductive output of the sea mussel *Mytilus californianus*. Marine Biology 151:1543–1550.

Piccinali, R. V, P. L. Marcet, F. Noireau, U. Kitron, R. E. Gürtler, and E. M. Dotson.

2009. Molecular population genetics and phylogeography of the Chagas disease vector *Triatoma infestans* in South America. Journal of Medical Entomology 46:796–809.

Pilkerton, A., J. Apple, C. Kohnert, H. Bohlmann, and N. Burnett. 2016. Investigating Patterns in the Growth Dynamics of Pacific Northwest Sea Stars, *E. troschelii* and *P. ochraceus.* Proceedings of the Pacific Estuarine Resesarch Society, 39th Annual Meeting. Brackendale, B.C.

PISCO. 2014a. Sea Star Wasting Disease. University of California Santa Cruz. http://www.eeb.ucsc.edu/pacificrockyintertidal/data-products/sea-star-wasting/index.html. Accessed 11 July 2018.

PISCO. 2014b. Intertidal Sea Star Protocol. Santa Cruz, CA.

Ponton, F., F. Ot, T. Lef, P. M. Guerin, C. Lebarbenchon, D. Duneau, D. G. Biron, F. Ponton, F. Ot, T. Lef, P. M. Guerin, C. Lebarben-, D. Duneau, and D. G. Biron. 2011. Water-seeking behavior in worm-infected crickets and reversibility of parasitic manipulation. Behavioral Ecology 22:392–400.

Powell, E. N., J. D. Gauthier, E. A. Wilson, A. Nelson, R. R. Fay, and J. M. Brooks. 1992. Oyster Disease and Climate Change. Are Yearly Changes in Perkinsus marinus Parasitism in Oysters (*Crassostrea virginica*) Controlled by Climatic Cycles in the Gulf of Mexico? Marine Ecology 13:243–270.

R Core Team. 2017. R: A language and environment for statistical computing. R foundation for statistical computing. R Foundation for Statistical Computing, Vienna, Austria.

Raimondi, P. T., C. M. Wilson, R. F. Ambrose, J. M. Engle, and T. E. Minchinton. 2002. Continued declines of black abalone along the coast of California: are mass mortalities related to El Niño events ? Marine Ecology Progress Series 242:143–152.

Reed, D. C., and M. S. Foster. 1984. The Effects of Canopy Shadings on Algal Recruitment and Growth in a Giant Kelp Forest. Ecology 65:937–948.

Remily, E. R., and L. L. Richardson. 2006. Ecological physiology of a coral pathogen and the coral reef environment. Microbial Ecology 51:345–352.

Rice, D. W., C. P. Seltenrich, R. B. Spies, and M. L. Keller. 1993. Seasonal and annual distribution of organic contaminants in marine sediments from Elkhorn

slough, moss landing harbor and nearshore Monterey Bay, California. Environmental Pollution 82:79–91.

Robles, C. D. 2013. Chapter 16: *Pisaster ochraceus*. In Starfish: The biology and ecology of the Asteroidea. J. M. Lawrence (ed.) John Hopkins University Press. Pages 161–174 *in* J. M. Lawrence, editor. Starfish: The biology and ecology of the Asteroidea. John Hopkins University Press, Baltimore, OH.

Robles, C. D., and R. Desharnais. 2002. History and current development of a paradigm of predation in rocky intertidal communities. Ecology 83:1521–1536.

Robles, C. D., R. A. Desharnais, C. Garza, M. J. Donahue, A. Martinez, A. Desharnais, and J. Donahue. 2009. Complex Equilibria in the Maintenance of Boundaries: Experiments with Mussel Beds. Ecology 90:985–995.

Robles, C. D., C. Garza, R. A. Desharnais, and M. J. Donahue. 2010. Landscape patterns in boundary intensity: A case study of mussel beds. Landscape Ecology 25:745–759.

Robles, C. D., R. Sherwood-Stephens, and M. Alvarado. 1995. Responses of a Key Intertidal Predator to Varying Recruitment of Its Prey. Ecology 76:565–579.

Rockwood, L. L. 2006. Host-Parasite Interactions. Page Introduction to Population Ecology. Blackwell Publishing, Malden, MA.

Rogers, D. J., and S. E. Randolph. 2003. Studying the global distribution of infectious diseases using GIS and RS. Nature Reviews Microbiology 1:231–237.

Rogers, T. L., H. K. Schultz, and J. K. Elliott. 2018. Size-dependent interference competition between two sea star species demographically affected by wasting disease. Marine Ecology Progress Series 589:167–177.

Sanford, E. 2002a. Water temperature, predation, and the neglected role of physiological rate effects in rocky intertidal communities. Integrative and Comparative Biology 42:881–891.

Sanford, E. 2002b. The feeding, growth, and energetics of two rocky intertidal predators (*Pisaster ochraceus* and *Nucella canaliculata*) under water temperatures simulating episodic upwelling. Journal of Experimental Marine Biology and Ecology 273:199–218.

Sato, T., T. Egusa, K. Fukushima, T. Oda, N. Ohte, N. Tokuchi, K. Wanatabe, M.

Kanaiwa, I. Murakami, and K. Lafferty. 2012. Nematomorph parasites indirectly alter the food web and ecosystem function of streams through behavioural manipulation of their cricket hosts. Ecology Letters 15:786–793.

Schade, F. M., L. Shama, and K. Wegner. 2014. Impact of thermal stress on evolutionary trajectories of pathogen resistance in three-spined stickleback (*Gasterosteus aculeatus*). BMC Evolutionary Biology 14:164.

Scheibling, R. E. 1994. Molluscan Grazing and Macroalgal Zonation on a Rocky Intertidal Platform At Perth, Western-Australia. Australian Journal of Ecology 19:141–149.

Scheibling, R. E., and J.-S. Lauzon-Guay. 2010. Killer storms: North Atlantic hurricanes and disease outbreaks in sea urchins. Limnology and Oceanography 55:2331–2338.

Scheibling, R. E., and R. L. Stephenson. 1984. Mass mortality of *Strongylocentrotus droebachiensis* (Echinodermata: Echinoidea) off Nova Scotia, Canada. Marine Biology 78:153–164.

Schiebelhut, L. M., J. B. Puritz, and M. N. Dawson. 2018. Decimation by sea star wasting disease and rapid genetic change in a keystone species, *Pisaster ochraceus*. Proceedings of the National Academy of Sciences PNAS Lates:1–6.

Schulien, J. A., M. B. Peacock, K. Hayashi, P. Raimondi, and R. M. Kudela. 2017. Phytoplankton and microbial abundance and bloom dynamics in the upwelling shadow of Monterey Bay, California, from 2006 to 2013. Marine Ecology Progress Series 572:43–56.

Seed, R., and T. H. Suchanek. 1976. Population and community ecology of Mytilus. Pages 87–156 *in* B. L. Bayne, editor. Marine mussels: their ecology and physiology. Cambridge University Press, Cambridge, UK.

Selakovic, S., P. C. de Ruiter, and H. Heesterbeek. 2014. Infectious disease agents mediate interaction in food webs and ecosystems. Proceeding of the Royal Society B 281:20132709.

Sewell, M., and J. Watson. 1993. A “source” for asteroid larvae?: recruitment of Pisaster Pycnopodia helianthoides and Dermasterias imbricata in Nootka Sound, British Columbia. Marine Biology 117:387–398.

Sindermann, C. J. 1993. Interactions of Pollutants and Disease in Marine Fish and

Shellfish. Pages 451–482 *in* J. Couch and J. Fournie, editors. Pathobiology of Marine and Estuarine Organisms. CRC Press, Ann Arbor, MI.

Smith, J. R., and S. N. Murray. 2005. The effects of experimental bait collection and trampling on a *Mytilus californianus* mussel bed in southern California. Marine Biology 147:699–706.

Smith, K. F., M. D. Behrens, and D. F. Sax. 2009. Local scale effects of disease on biodiversity. EcoHealth 6:287–95.

Smith, K. F., D. F. Sax, and K. D. Lafferty. 2006. Evidence for the role of infectious disease in species extinction and endangerment. Conservation Biology 20:1349–1357.

Snieszko, S. F. 1974. The effects of environmental stress on outbreaks of infectious diseases of fishes. Journal of Fish Biology 6:197–208.

Snow, M., N. Bain, J. Black, V. Taupin, C. O. Cunningham, J. A. King, H. F. Skall, and R. S. Raynard. 2004. Genetic population structure of marine viral haemorrhagic septicaemia virus (VHSV). Diseases of Aquatic Organisms 61:11–21.

Sousa, W. P. 1984. Intertidal Mosaics : Patch Size , Propagule Availability , and Spatially Variable Patterns of Succession. Ecology 65:1918–1935.

Staehli, A., R. Schaerer, K. Hoelzle, and G. Ribi. 2009. Temperature induced disease in the starfish *Astropecten jonstoni.* Marine Biodiversity Records 2:1–5.

Statistics Canada. 2011. Boundary Files, 2011 Census. Government of Canada.

Stickle, W. B., D. W. Foltz, M. Katoh, and H. L. Nguyen. 1992. Genetic structure and mode of reproduction in five species of sea stars (Echinodermata: Asteroidea) from the Alaskan coast. Canadian Journal of Zoology 70:1723–1728.

Strathmann, R. 1978. Length of pelagic period in echinoderms with feeding larvae from the Northeast Pacific.

Suchanek, T. 1986. Mussels and their role in structuring rocky shore communities. Pages 70–96 *in* P. G. Moore and R. Seed, editors. Ecology of Rocky Coasts. Columbia University Press, New York.

Suchanek, T. H. 1994. Temperate coastal marine communities: biodiversty and

threats. American Zoologist 34:100–114.

The Nature Conservancy, and American Wind Wildlife Institute. 1986. Wind and Wildlife Landscape Assesssment Tool.

Thompson, J. 2005. The Conceptual Framework: The Geographic Mosaic Theory of Coevolution. Pages 97–135. The Geographic Mosaic Theory of Coevolution. University of Chicago Press, Chicago.

Thompson, R. C., T. P. Crowe, and S. J. Hawkins. 2002. Rocky intertidal communities: past environmental changes, present status and predictions for the next 25 years. Environmental Conservation 29:168–191.

United States Environmental Protection Agency. 2014. Permit Compliance System - Integrated Compliance Information System Overview. Government of the United States of America.

US Census Bureau. 2010. 2010 Census Data Product Descriptions. Government of the United States of America.

Uthicke, S., B. Schaffelke, and M. Byrne. 2009. A boom-bust phylum? Ecological and evolutionary consequences of density variations in echinoderms. Ecological Monographs 79:3–24.

Vezzulli, L., M. Previati, C. Pruzzo, A. Marchese, D. G. Bourne, and C. Cerrano. 2010. *Vibrio* infections triggering mass mortality events in a warming Mediterranean Sea. Environmental Microbiology 12:2007–2019.

Ward, J. R., and K. D. Lafferty. 2004. The elusive baseline of marine disease: Are diseases in ocean ecosystems increasing? PLoS Biology 2:542–547.

Wares, J., and L. Schiebelhut. 2015. What doesn’t kill them makes them stronger: An association between elongation factor 1-α overdominance in the sea star *Pisaster ochraceus* and "sea star wasting disease”. PeerJ 4:e1464v2.

De Wit, P., L. Rogers-Bennett, R. M. Kudela, and S. R. Palumbi. 2014. Forensic genomics as a novel tool for identifying the causes of mass mortality events. Nature Communications 5:3652.

Wood, C. L., J. E. Byers, K. L. Cottingham, I. Altman, M. J. Donahue, and A. M. H. Blakeslee. 2007. Parasites alter community structure. Proceedings of the National Academy of Sciences 104:9335–9339.

Wood, C. L., and K. D. Lafferty. 2013. Biodiversity and disease: A synthesis of ecological perspectives on Lyme disease transmission. Trends in Ecology and Evolution 28:239–247.

Wootton, T. 1994. Predicting Direct and Indirect Effects: An Integrated Approach Using Experiments and Path Analysis. Ecology 75:151–165.